Supporting information

N-Amino-7-Azaindole as *N,N'*- Bidentate Directing Group: Ruthenium-Catalyzed Oxidative Annulation of *N*-(7-Azaindole) Benzamides with Alkynes *via* C-H Bond Activation

Prateep Singh Sagara,† Prem Felix Siril,† Ponneri Chandrababu Ravikumar ‡

† School of Basic Sciences, Indian Institute of Technology Mandi, Mandi, Himachal Pradesh-175005, India.

‡ School of Chemical Sciences, National Institute of Science Education and Research (NISER) Bhubaneswar, Jatani Campus, Dt: Khurda, Odisha 752050, India. E-mail: pcr@niser.ac.in

Table of Contents

1. Optimization of Reaction Conditions.....S3

2. Mechanistic Studies.....S4

3. Copies of ^{1}H & ^{13}C NMR Data …..…….....S8

4. X-ray Crystallographic Analysis….....S53

Table S1. Optimization of Reaction Conditions:

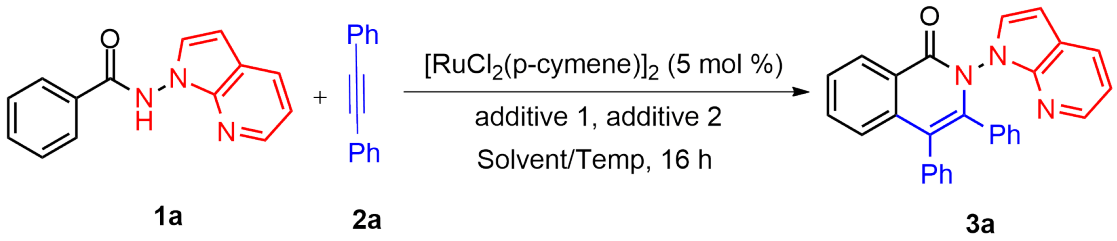

1a **2a** **3a**

Entry	Additive 1	Additive 2	Solvent/Temp (°C)	Yield [b](%)
1	-	NaOAc	MeOH/100	30
2	PivOH	CsOAc	MeOH/120	30
3	MesCOOH	KOAc	H_2O /100	50
4	MesCOOH	KOAc	TFE/100	60
5	MesCOOH	$Cu(OAc)_2.H_2O$	TFE/100	65
6	MesCOOH	KOAc	PEG-400/100	15
7	MesCOOH	KOAc	DCE/120	45
8	-	CsOAc	DCE/120	40
9	$AgSbF_6$	-	DCE/120	25
10	-	$Cu(OAc)_2.H_2O$	DCE/120	50
11[c]	$AgSbF_6$	$Cu(OAc)_2.H_2O$	DCE/120	28
12[d]	$AgSbF_6$	$Cu(OAc)_2.H_2O$	DCE/120	34
13[e]	$AgSbF_6$	$Cu(OAc)_2.H_2O$	DCE/120	42
14[f]	$AgSbF_6$	$Cu(OAc)_2.H_2O$	DCE/120	60
15[g]	**$AgSbF_6$**	**$Cu(OAc)_2.H_2O$**	**DCE/120**	**85**
16[h]	-	-	DCE/120	trace

Reaction conditions: [a] 1a (0.5 mmol), 2a (1.2 equiv), $[Ru(p\text{-cymene})Cl_2]_2$ (5.0 mol %), Additive 1 (10 mol %), Additive 2 (2.0 equiv), solvent (3.0 mL), 100 – 120 °C, 16h. [b] Isolated Yield. [c] $Cu(OAc)_2.H_2O$ (10 mol %), [d] $Cu(OAc)_2.H_2O$ (30 mol %), [e] $Cu(OAc)_2.H_2O$ (50 mol %), [f] $Cu(OAc)_2.H_2O$ (100 mol %), [g] $Cu(OAc)_2.H_2O$ (200 mol %), [h] without additives.

2. Mechanistic Studies:

Scheme S1. Deuterium labeling experiments:

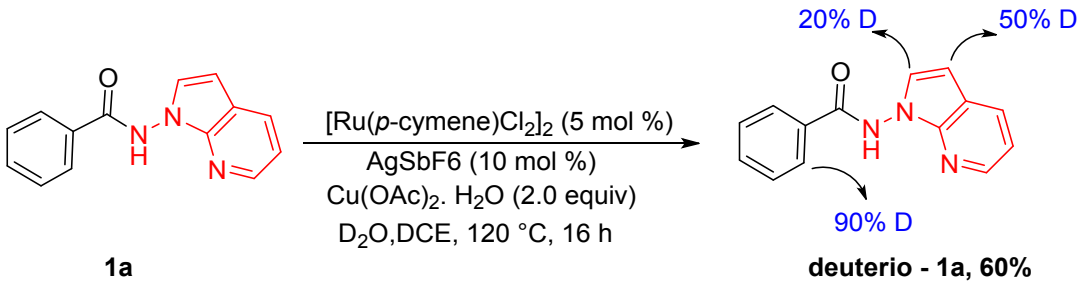

A 15 mL screw cap vial was equipped with magnetic stir bar and charged with starting compound 1a (0.21 mmol, 50 mg), [Ru(p-cymene)Cl_2]$_2$ (5 mol %), $AgSbF_6$ (10 mol %), Cu(OAc)$_2$. H_2O (2.0 equiv), D_2O (1.0 mL) and DCE (1.0 mL). The vessel was heated at 120 °C for 16h, and cooled down to room temperature. Later, the reaction mixture was diluted with 10 mL of dichloromethane and filtered through a Celite pad. The filtered solution was concentrated under reduced pressure. Then, the residue was purified by column chromatography with EtOAc/Hexane as eluent. The H/D exchange was calculated by ^{1}H NMR.

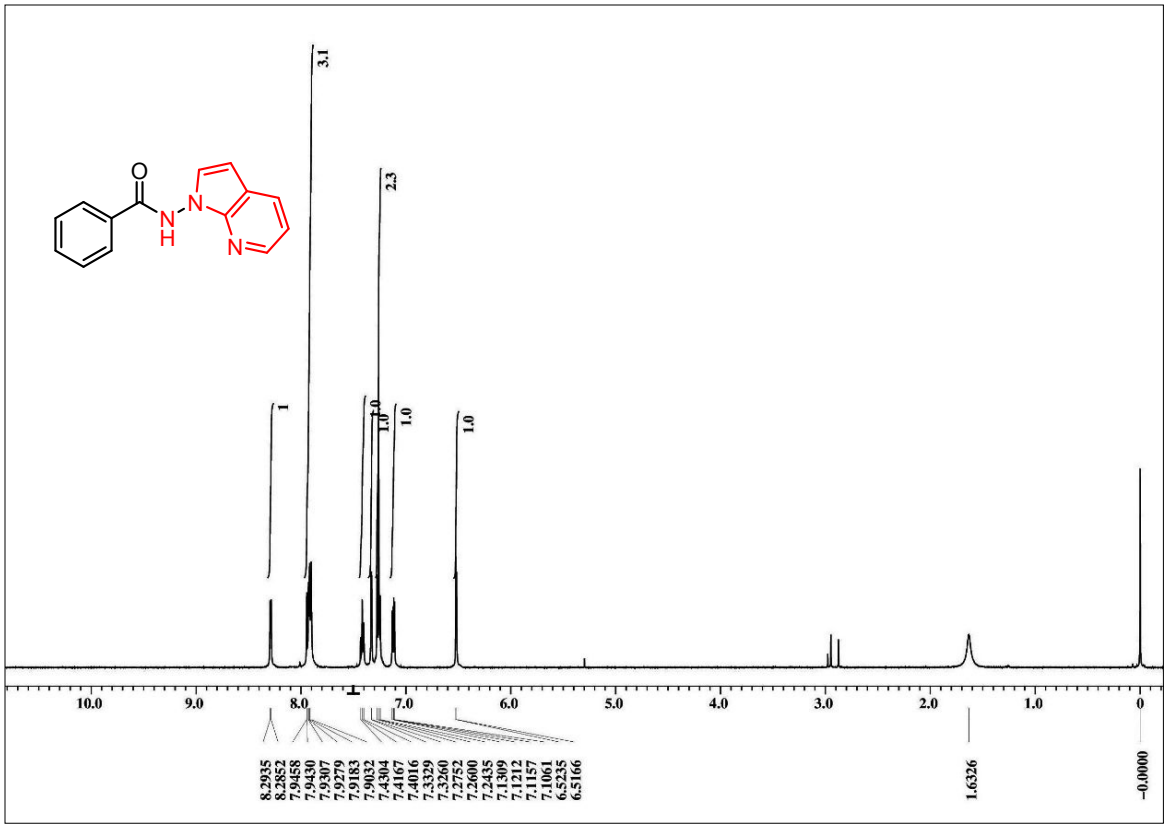
3.1
2.3
1
1.0
1.0
1.0
10.0
9.0
8.0
7.0
6.0
5.0
4.0
3.0
2.0
1.0
0
8.2935
8.2852
7.9458
7.9430
7.9307
7.9279
7.9183
7.9032
7.4304
7.4167
7.4016
7.3329
7.3260
7.2752
7.2600
7.2435
7.1309
7.1212
7.1157
7.1061
6.5235
6.5166
1.6326
-0.0000

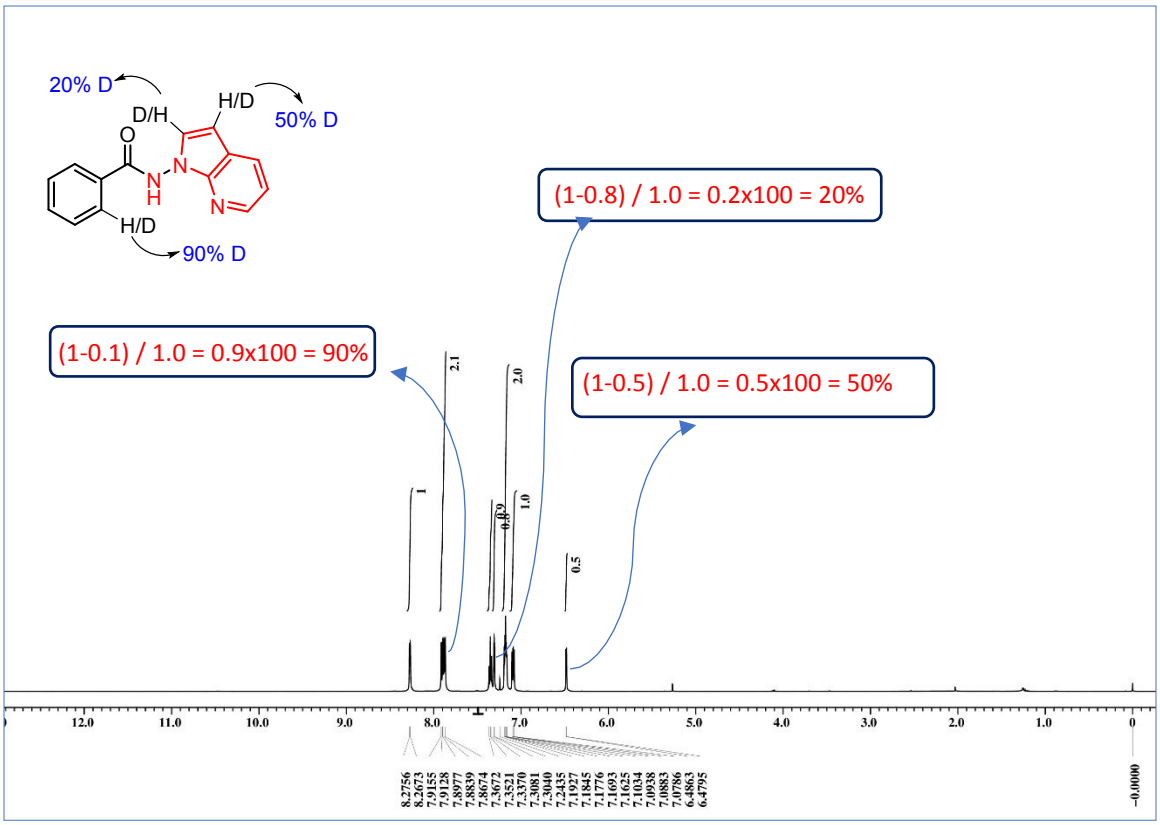
20% D
D/H
H/D
50% D
H/D
90% D
(1-0.8) / 1.0 = 0.2x100 = 20%
(1-0.1) / 1.0 = 0.9x100 = 90%
(1-0.5) / 1.0 = 0.5x100 = 50%
2.1
2.0
1
0.9
1.0
0.5
12.0
11.0
10.0
9.0
8.0
7.0
6.0
5.0
4.0
3.0
2.0
1.0
0
8.2756
8.2673
7.9155
7.9128
7.8977
7.8839
7.8674
7.3672
7.3521
7.3370
7.3081
7.3040
7.2435
7.1927
7.1845
7.1776
7.1693
7.1625
7.1034
7.0938
7.0883
7.0786
6.4863
6.4795
-0.0000

Scheme S2. Intermolecular competition KIE for the reaction

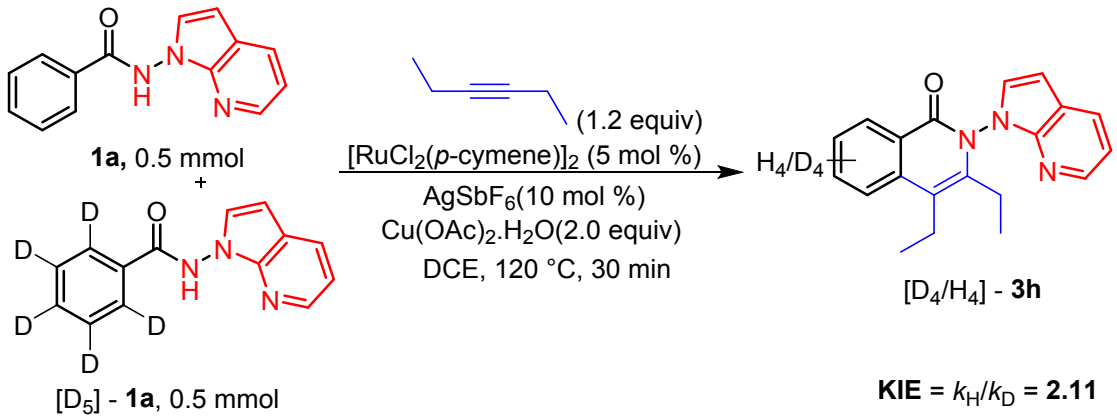

A 15 mL screw cap vial was equipped with magnetic stir bar and charged with starting compound 1a (0.5 mmol, 50 mg), [D_5]-1a (0.5 mmol), 3-hexyne (1.2 mmol), [Ru(p-cymene)Cl_2]$_2$ (5 mol %), $AgSbF_6$ (10 mol %), $Cu(OAc)_2$. H_2O (2.0 equiv), and DCE (3.0 mL). The reaction mixture was stirred at 120 °C for 16h, and cooled down to room temperature. Later, the reaction mixture was diluted with 15 mL of dichloromethane and filtered through a Celite pad. The filtered solution was concentrated under reduced pressure. Then, the residue was purified by column chromatography with EtOAc/Hexane as eluent to afford the desired product [D_4/H_4]-3h. The crude ^{1}H NMR spectram of the mixture [D_4/H_4]-3h, revealed the different integration related to the hydrogen resonances, the kinetic isotopic calculated to be $k_H/k_D \approx 2.11$.

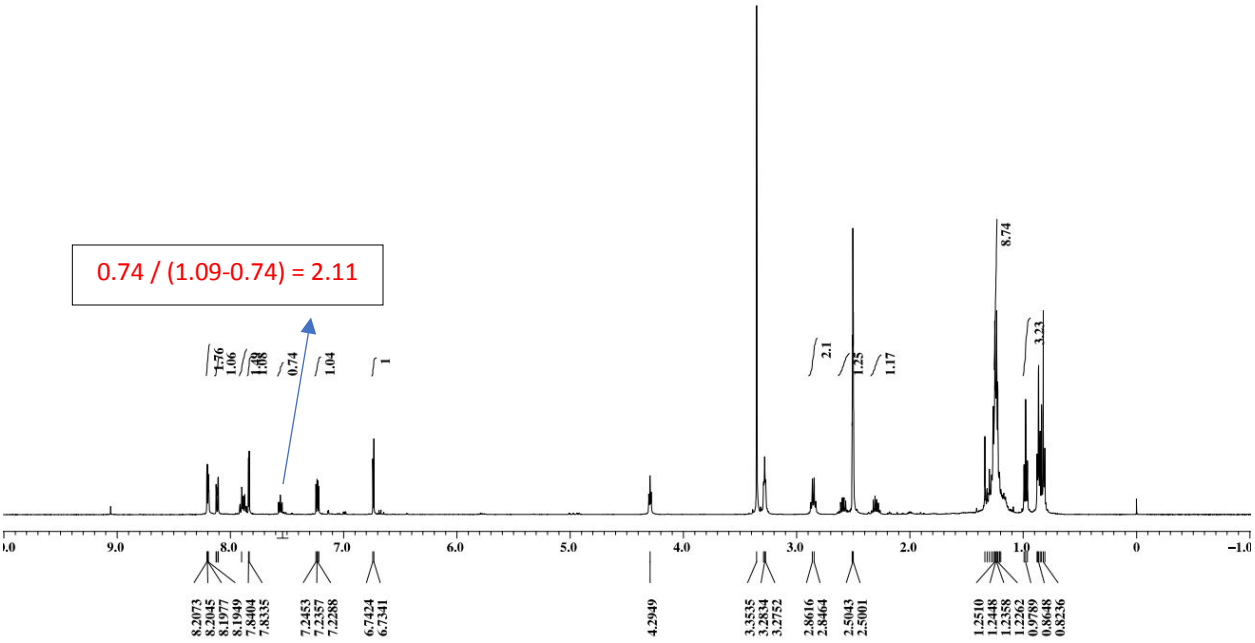
0.74 / (1.09-0.74) = 2.11
8.74
3.23
2.1
1.25
1.17
1.04
0.74
1

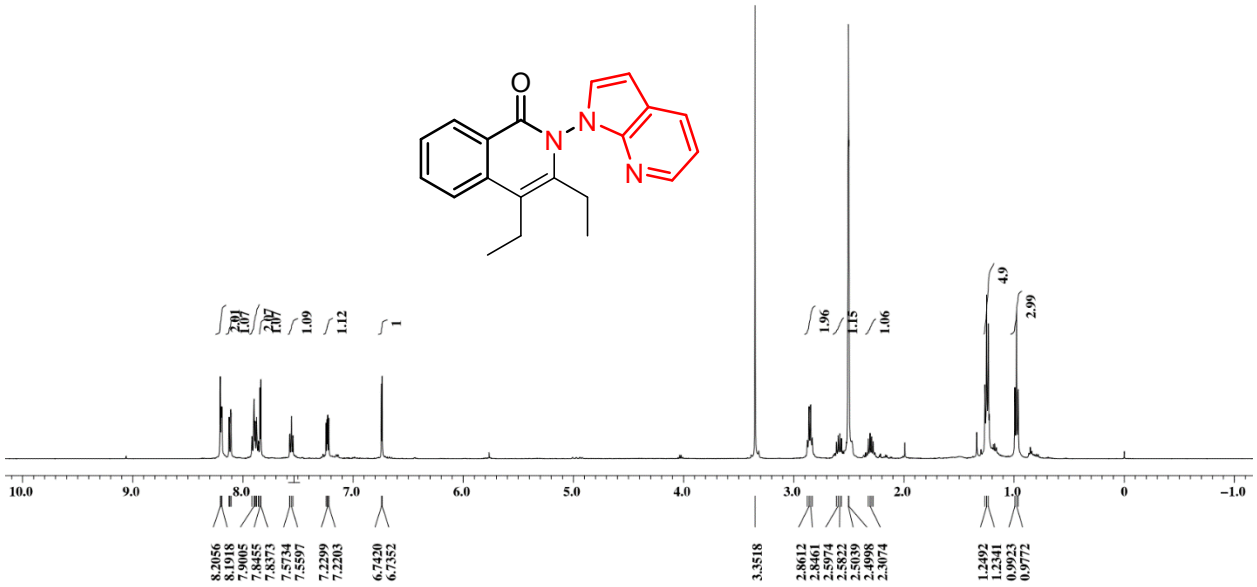
O
N
N
4.9
2.99
1.96
1.15
1.06
1.09
1.12
1

3. Copies of ^{1}H & ^{13}C NMR Data:

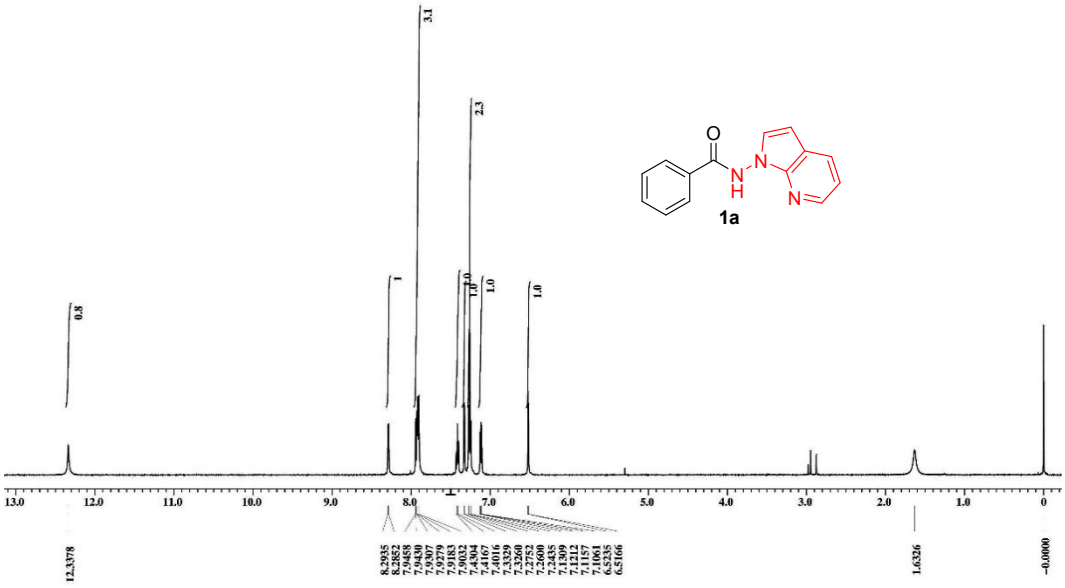

Fig. S1. ^{1}H NMR spectrum of **1a** (500 MHz, $CDCl_3$)

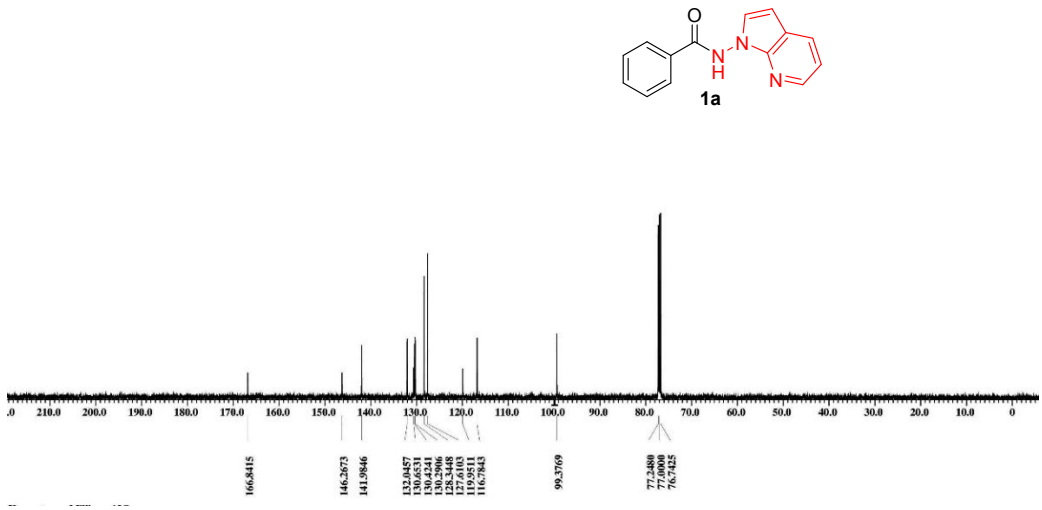

Fig. S2. ^{13}C NMR spectrum of **1a** (125 MHz, $CDCl_3$)

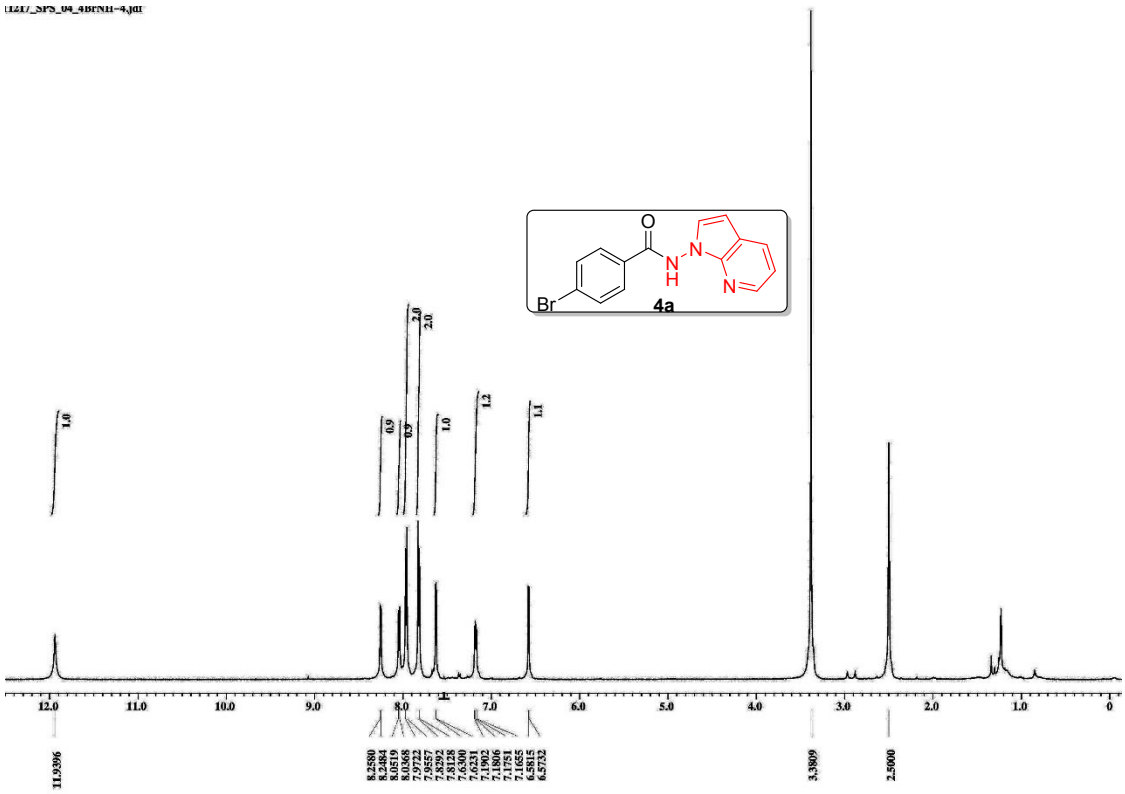

Fig. S3. ^{1}H NMR spectrum of **4a** (500 MHz, DMSO-d_6)

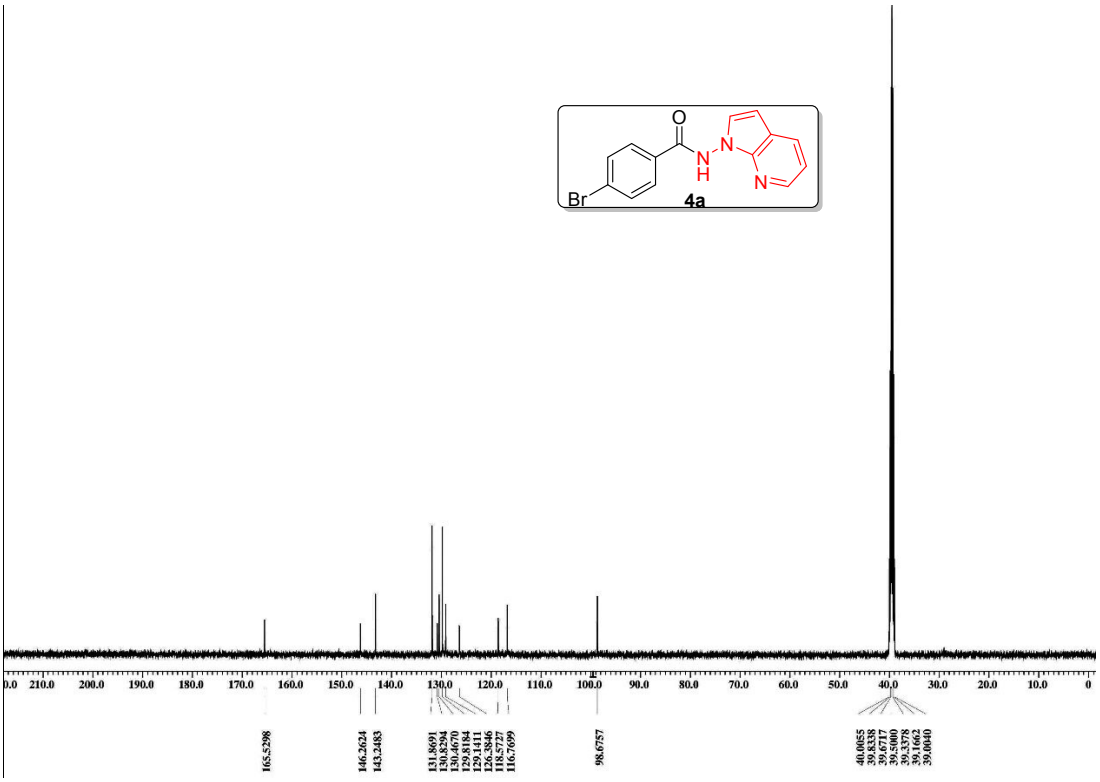

Fig. S4. ^{13}C NMR spectrum of **4a** (125 MHz, DMSO-d_6)

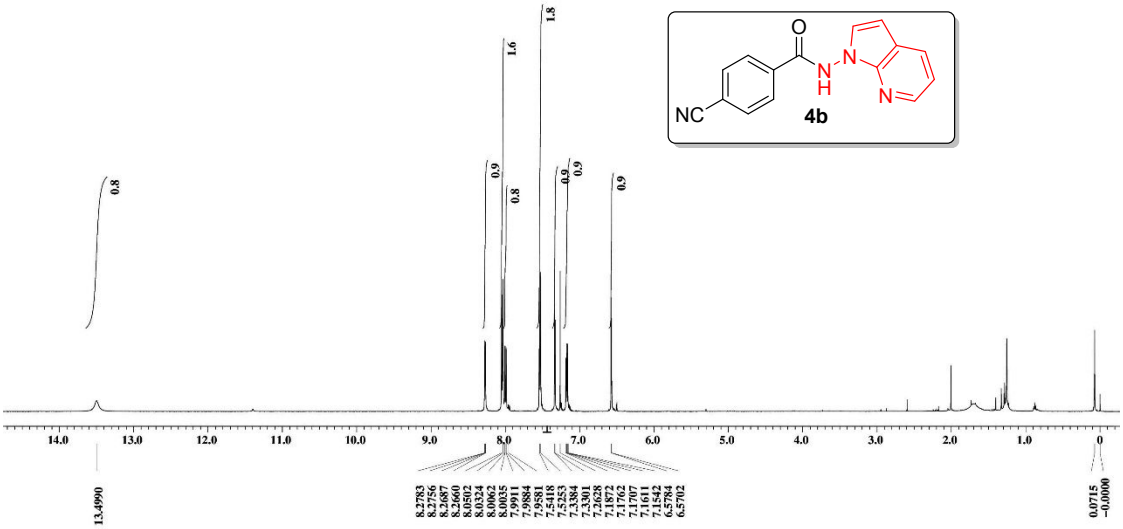

Fig. S5. ^{1}H NMR spectrum of **4b** (500 MHz, $CDCl_3$)

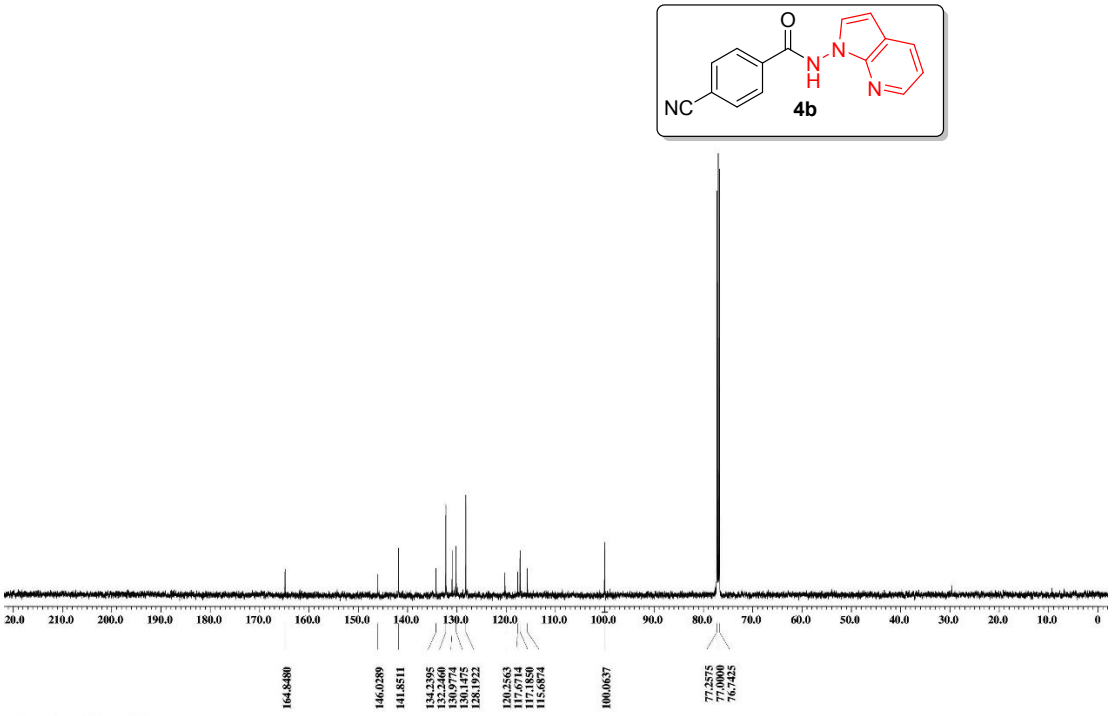

Fig. S6. ^{13}C NMR spectrum of **4b** (125 MHz, $CDCl_3$)

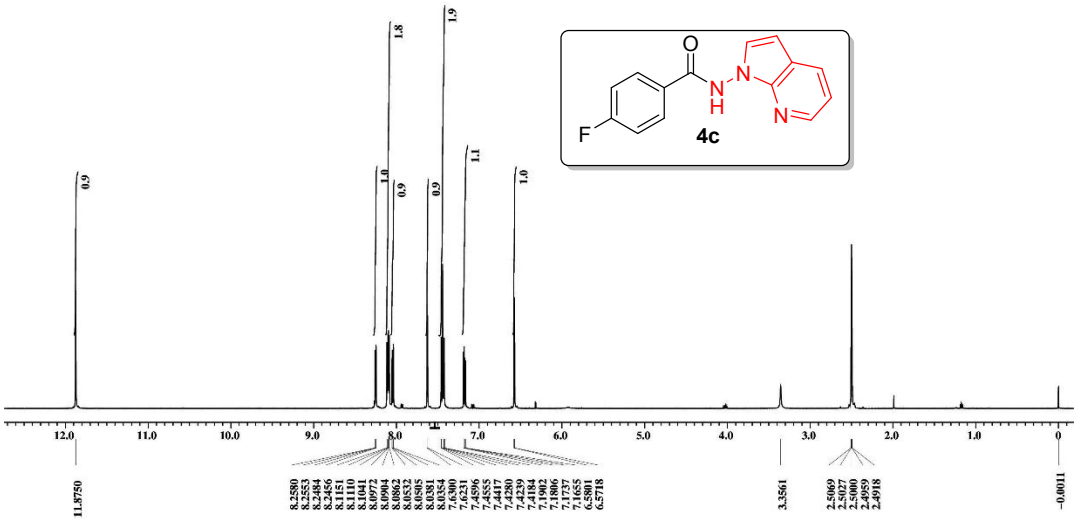

Fig. S7. ^{1}H NMR spectrum of **4c** (500 MHz, DMSO-d_6)

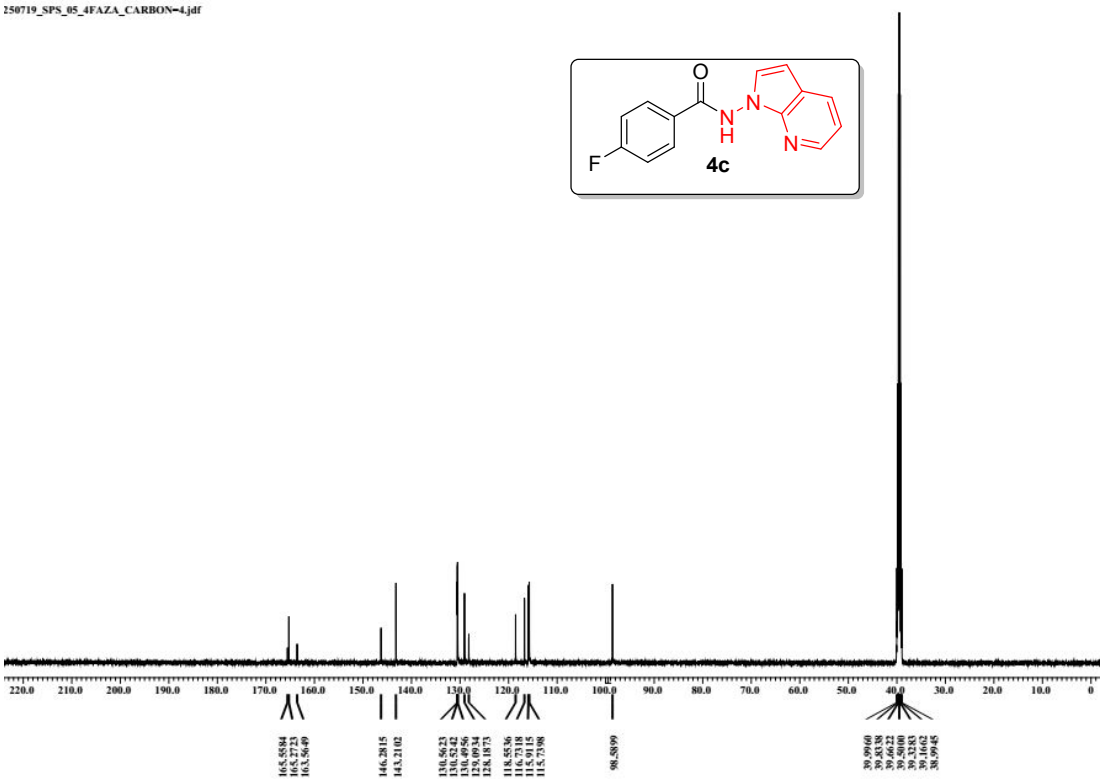

Fig. S8. ^{1}H NMR spectrum of **4c** (125 MHz, DMSO-d_6)

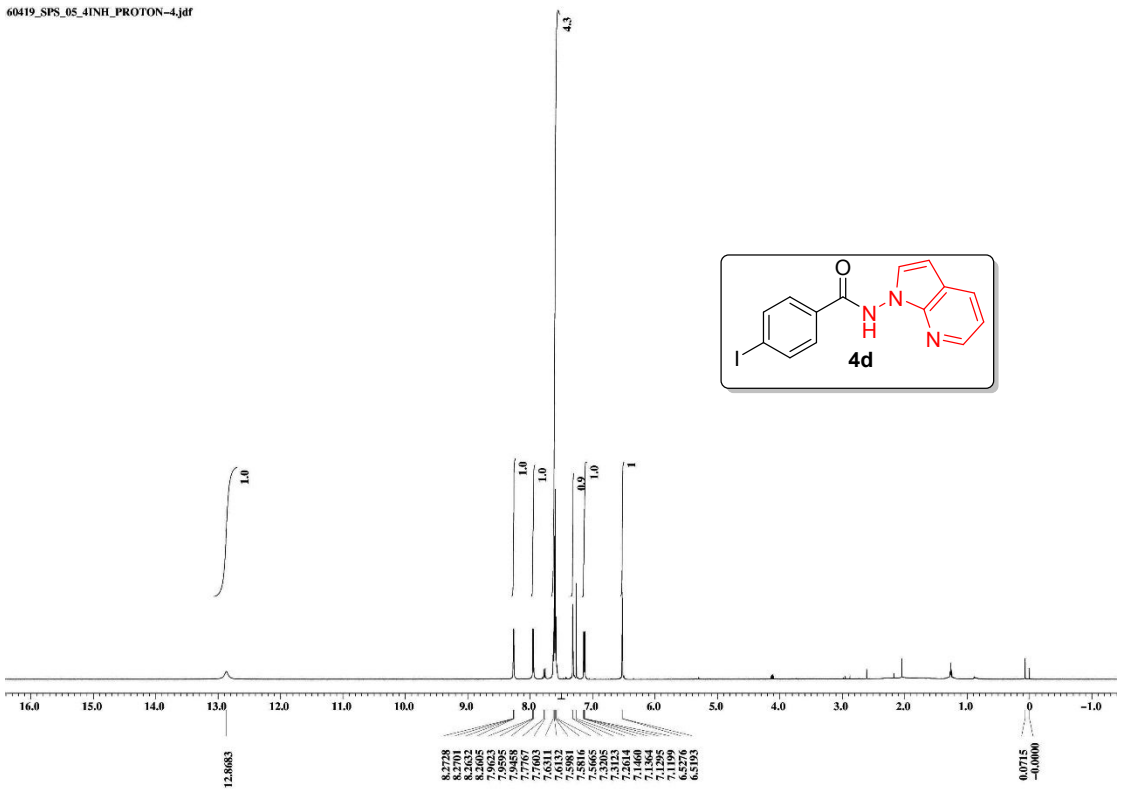

Fig. S9. ^{1}H NMR spectrum of **4d** (500 MHz, $CDCl_3$)

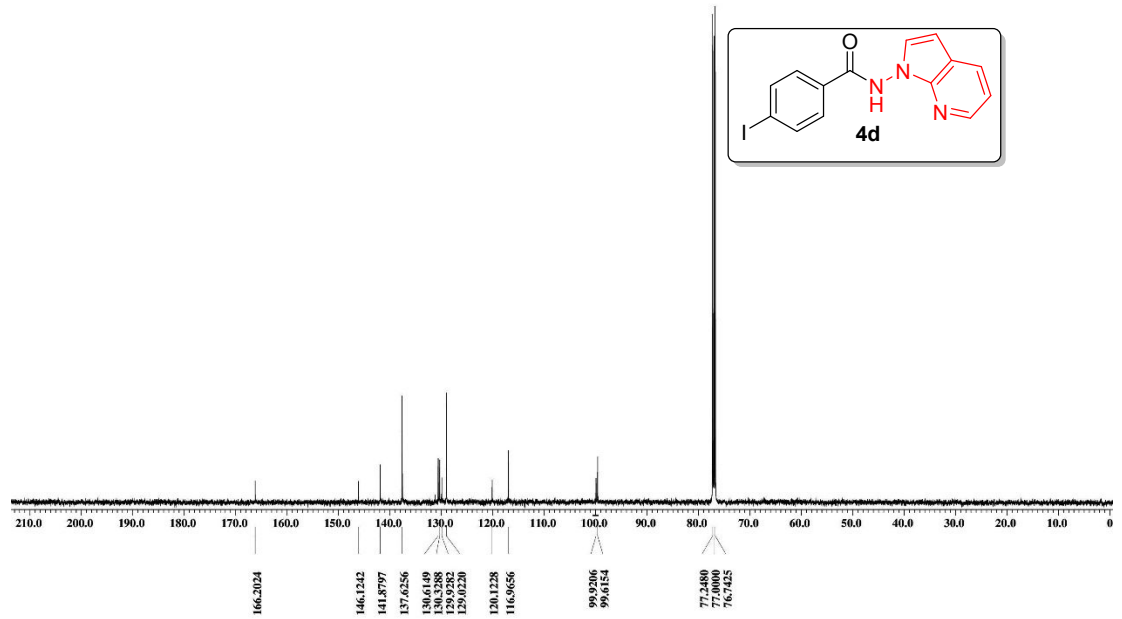

Fig. S10. ^{1}H NMR spectrum of **4d** (125 MHz, $CDCl_3$)

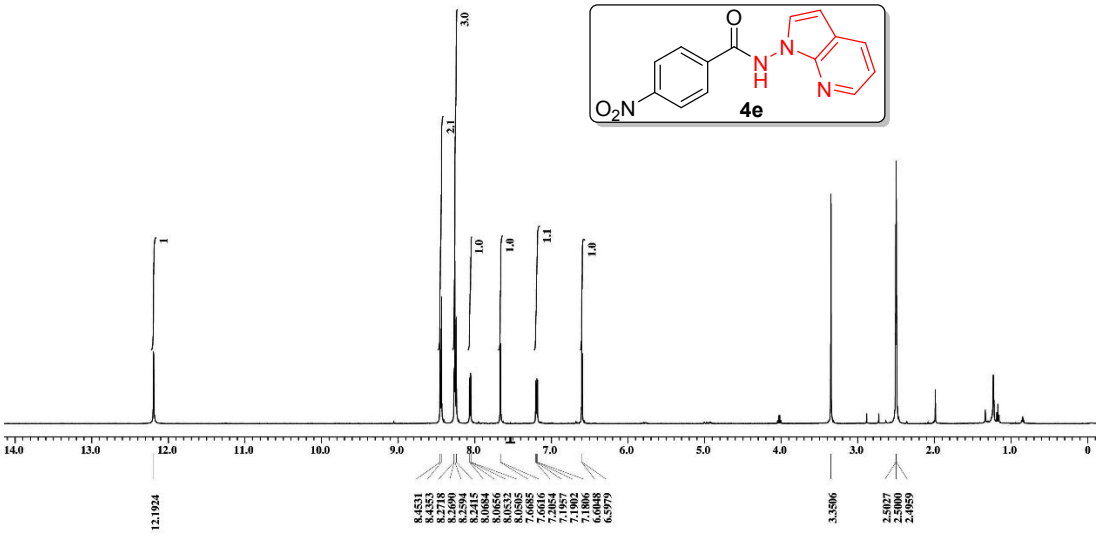

Fig. S11. ^{1}H NMR spectrum of **4e** (500 MHz, DMSO-d_6)

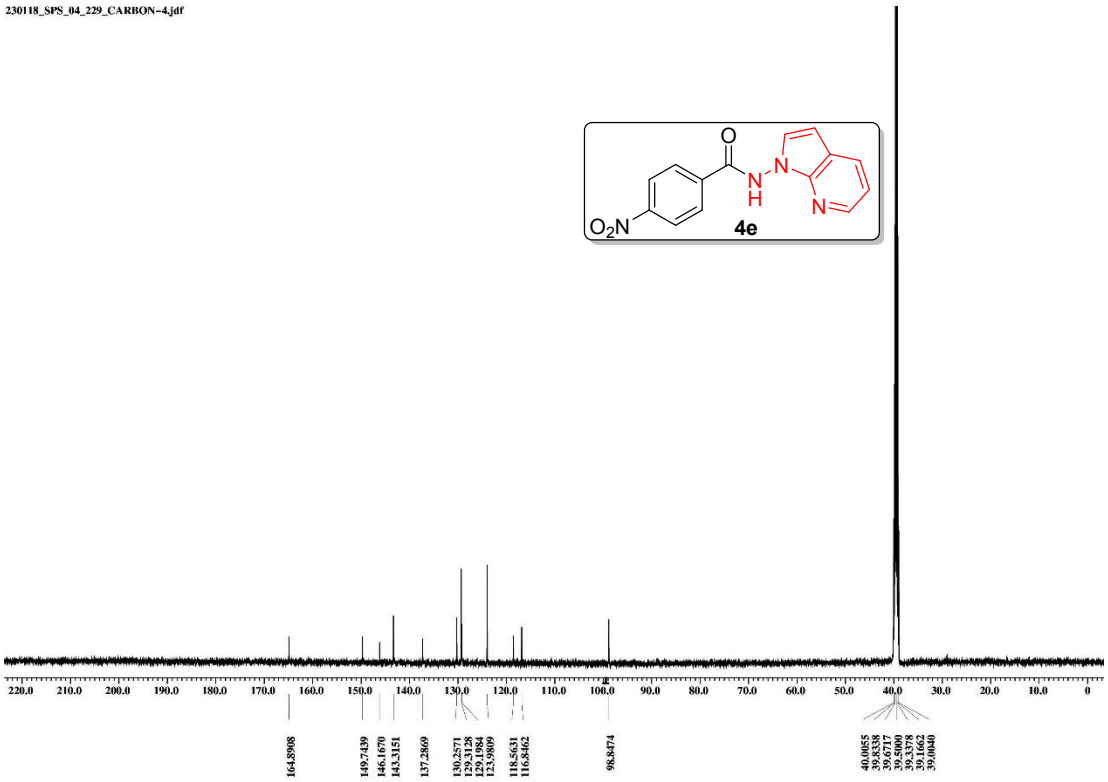

Fig. S12. ^{13}C NMR spectrum of **4e** (125 MHz, DMSO-d_6)

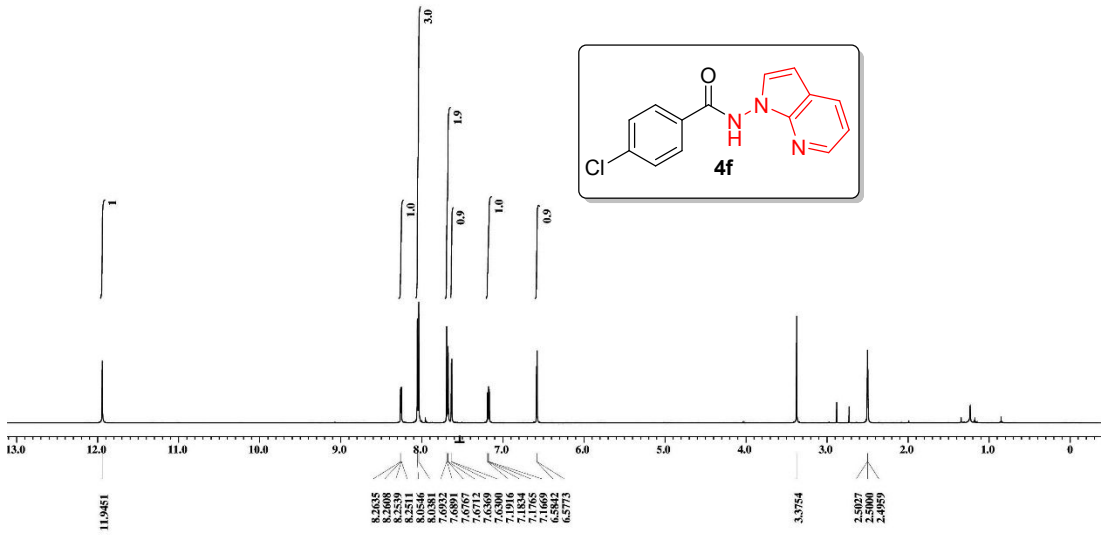

Fig. S13. ^{1}H NMR spectrum of **4f** (500 MHz, DMSO-d_6)

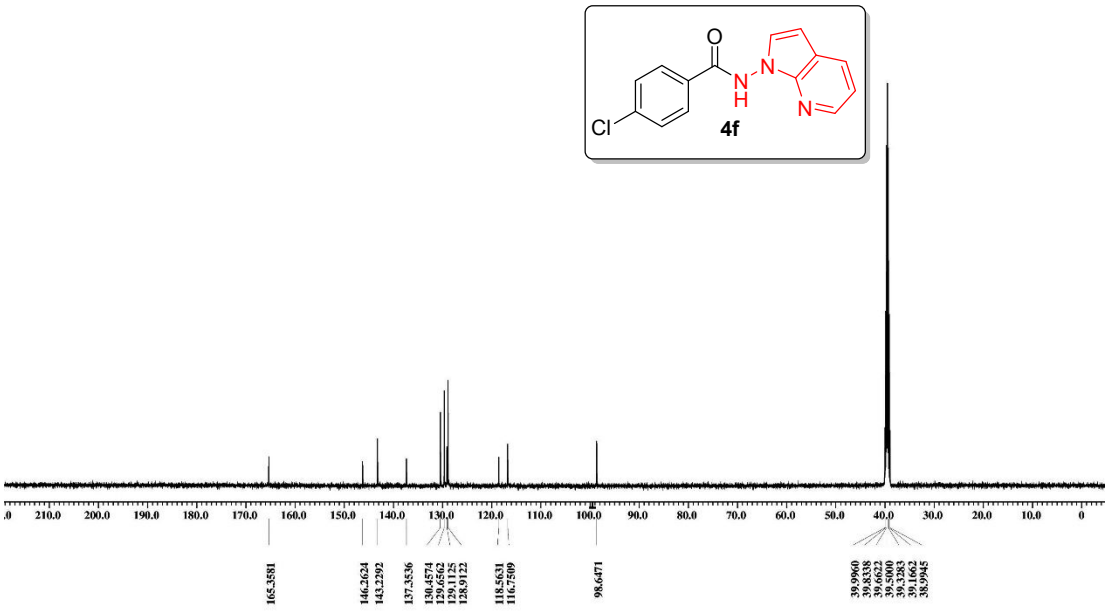

Fig. S14. ^{13}C NMR spectrum of **4f** (125 MHz, DMSO-d_6)

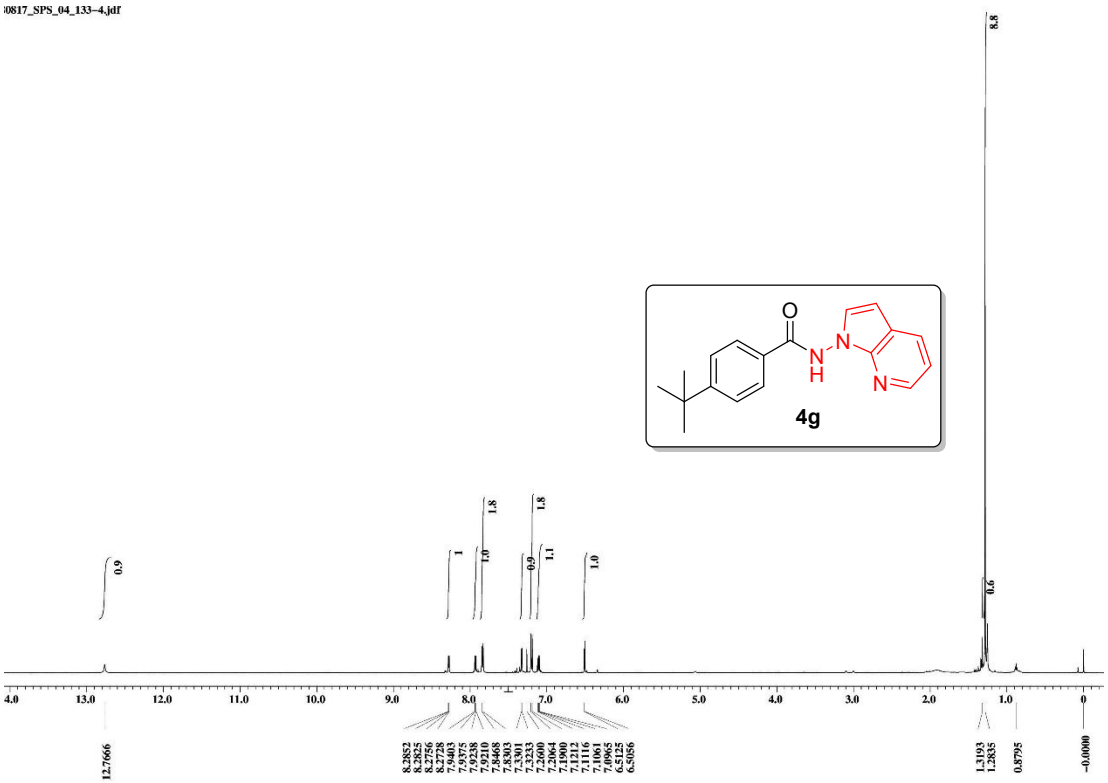

Fig. S15. ^{1}H NMR spectrum of **4g** (500 MHz, $CDCl_3$)

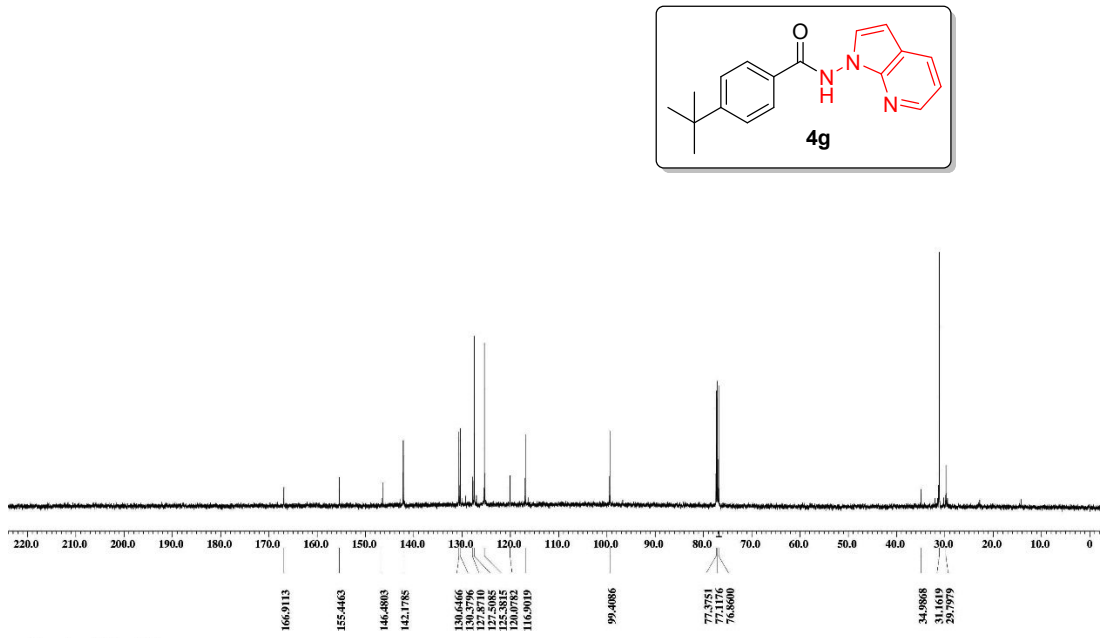

Fig. S16. ^{13}C NMR spectrum of **4g** (125 MHz, $CDCl_3$)

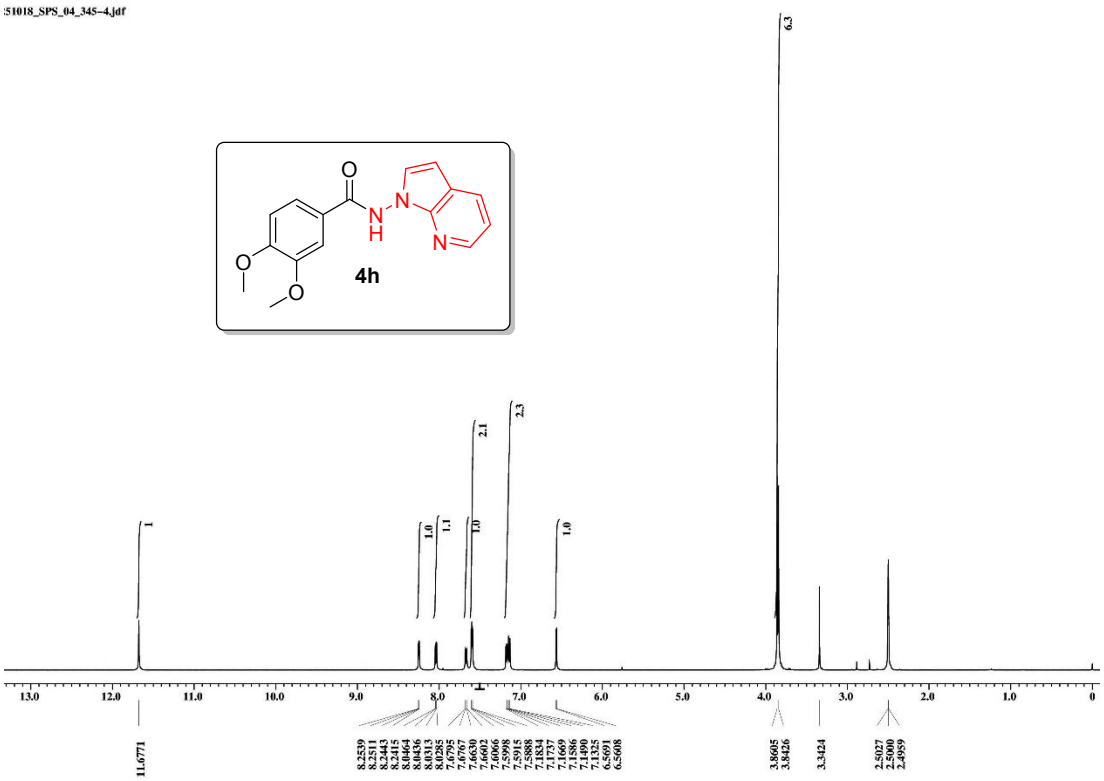

Fig. S17. ^{1}H NMR spectrum of **4h** (500 MHz, DMSO-d_6)

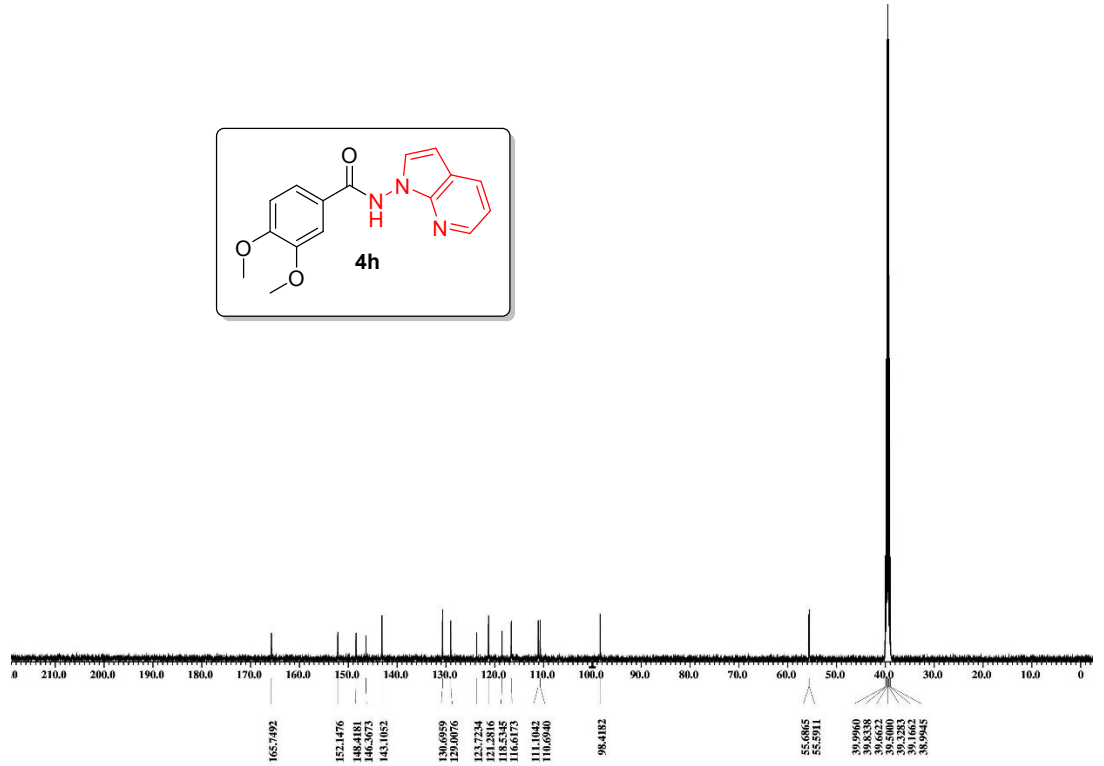

Fig. S18. ^{13}C NMR spectrum of **4h** (125 MHz, DMSO-d_6)

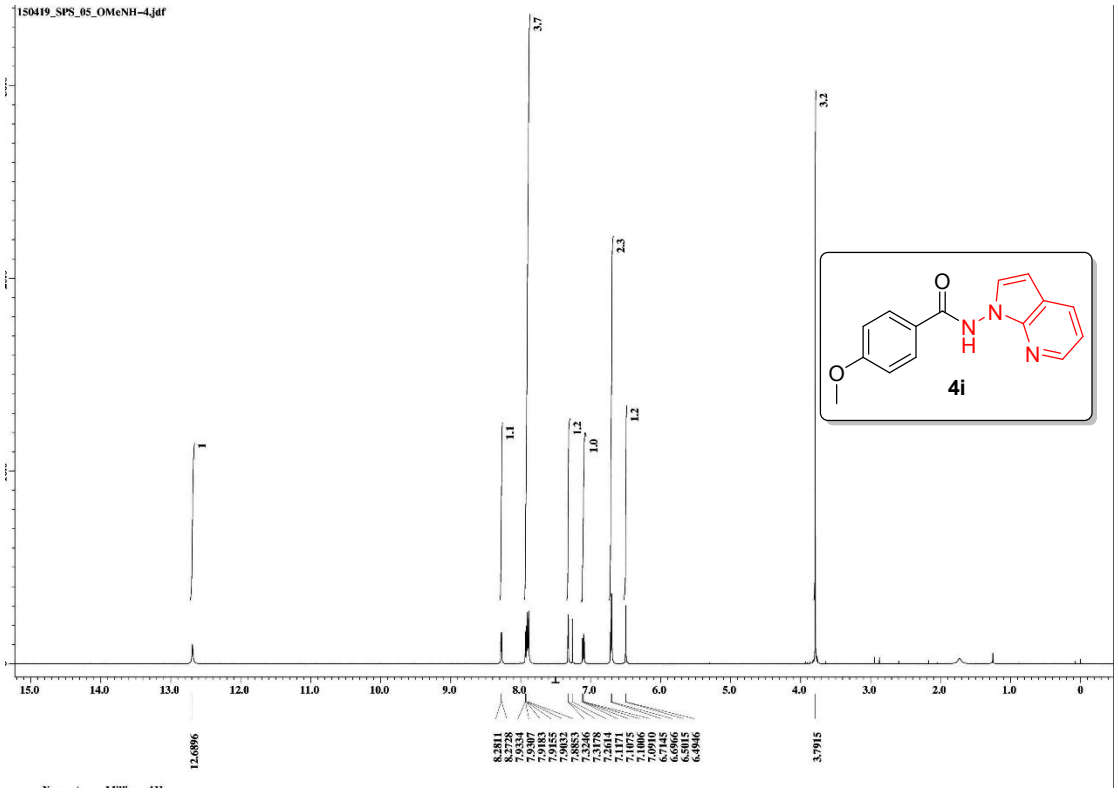

Fig. S19. ^{1}H NMR spectrum of **4i** (500 MHz, $CDCl_3$)

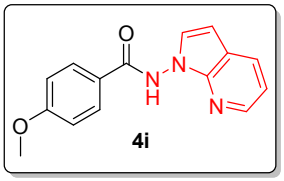

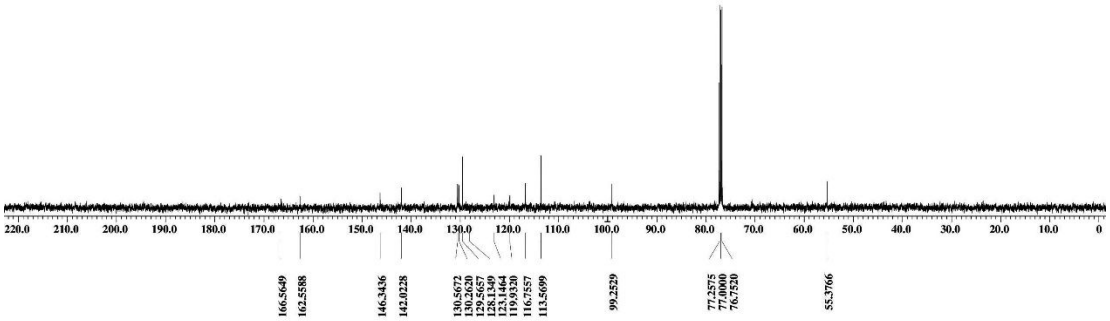

Fig. S20. ^{1}H NMR spectrum of **4i** (125 MHz, $CDCl_3$)

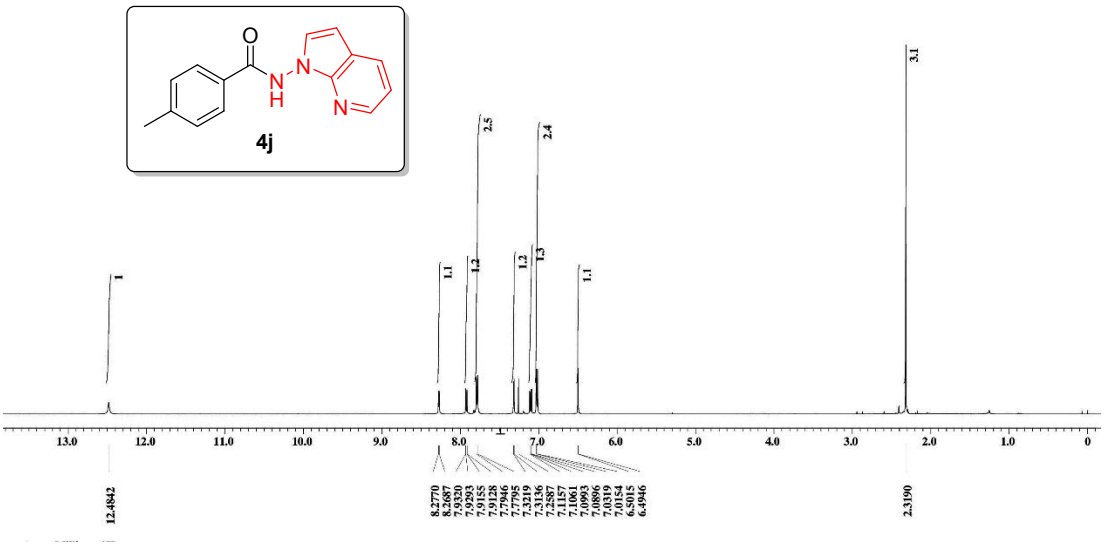

Fig. S21. ^{1}H NMR spectrum of **4j** (500 MHz, $CDCl_3$)

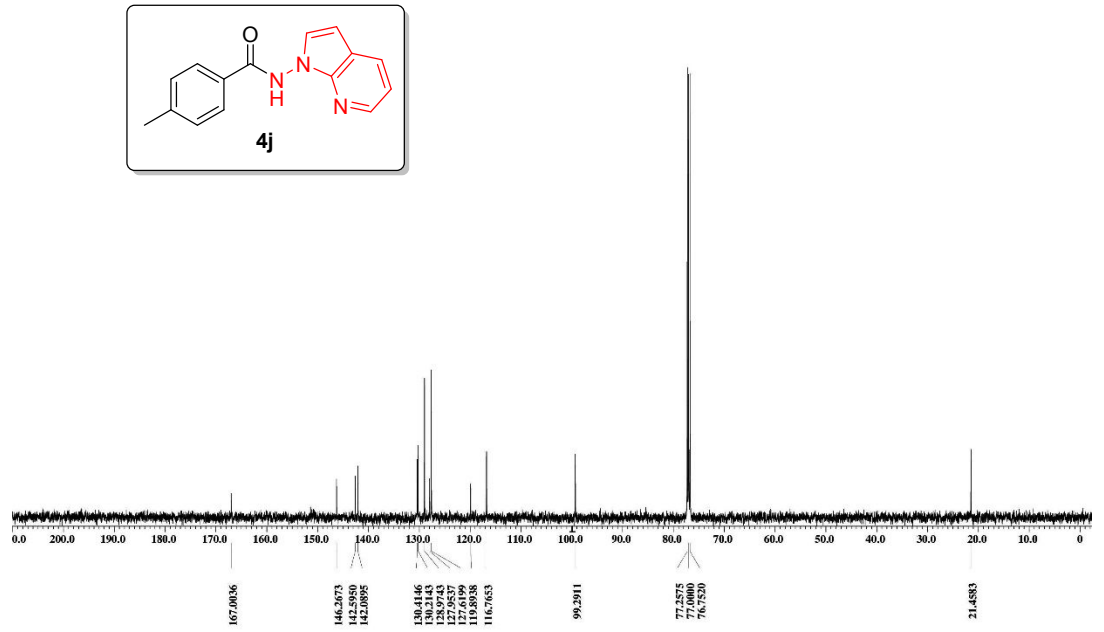

Fig. S22. ^{13}C NMR spectrum of **4j** (125 MHz, $CDCl_3$)

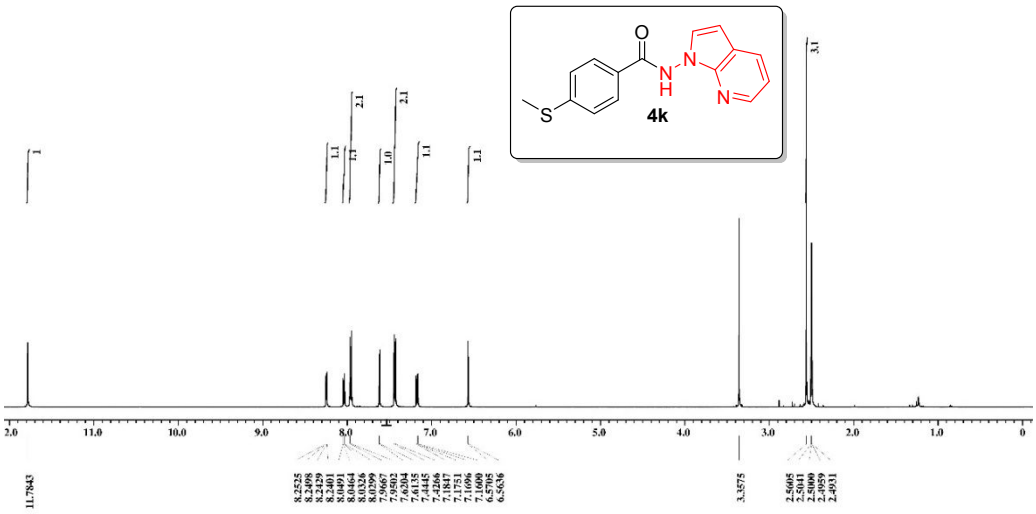

Fig. S23. ^{1}H NMR spectrum of **4k** (500 MHz, DMSO-d_6)

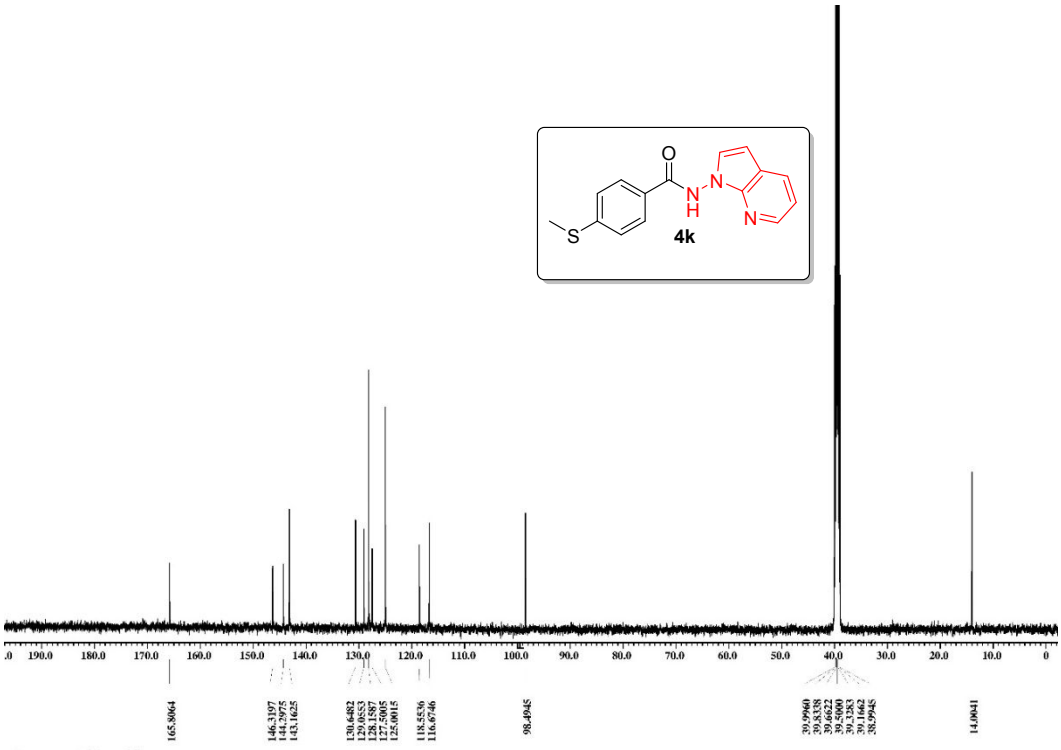

Fig. S24. ^{13}C NMR spectrum of **4k** (125 MHz, DMSO-d_6)

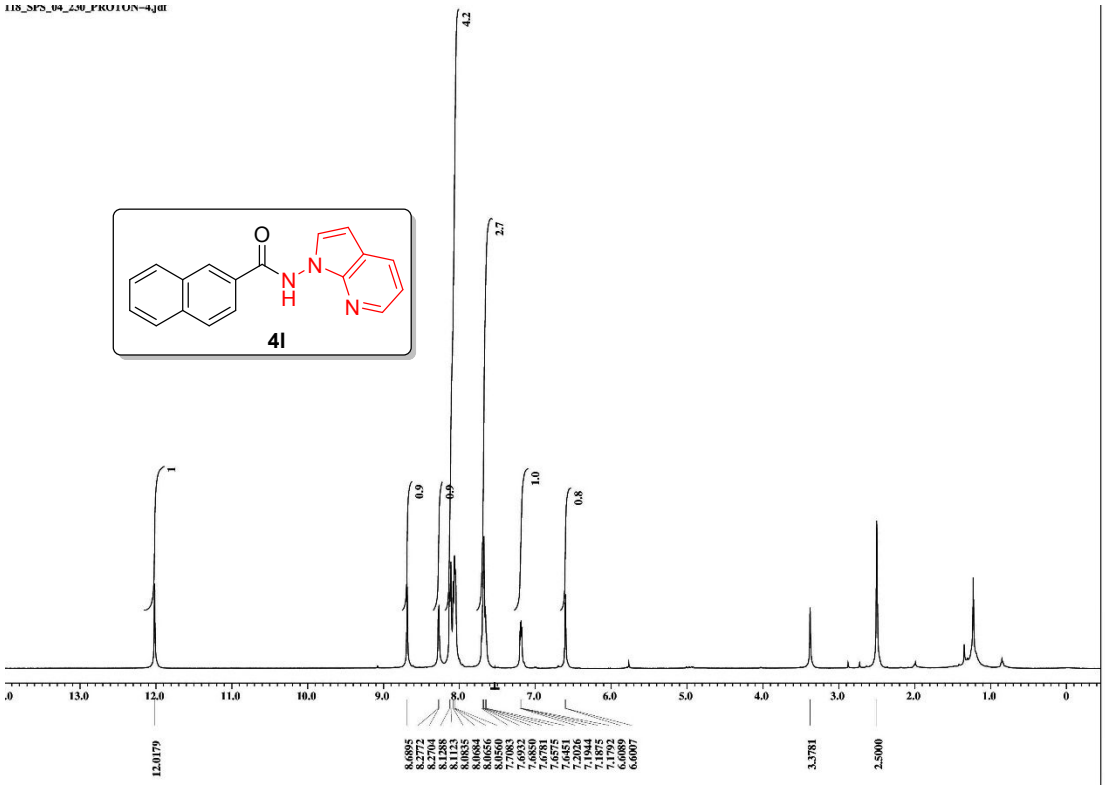

Fig. S25. ^{1}H NMR spectrum of **4l** (500 MHz, DMSO-d_6)

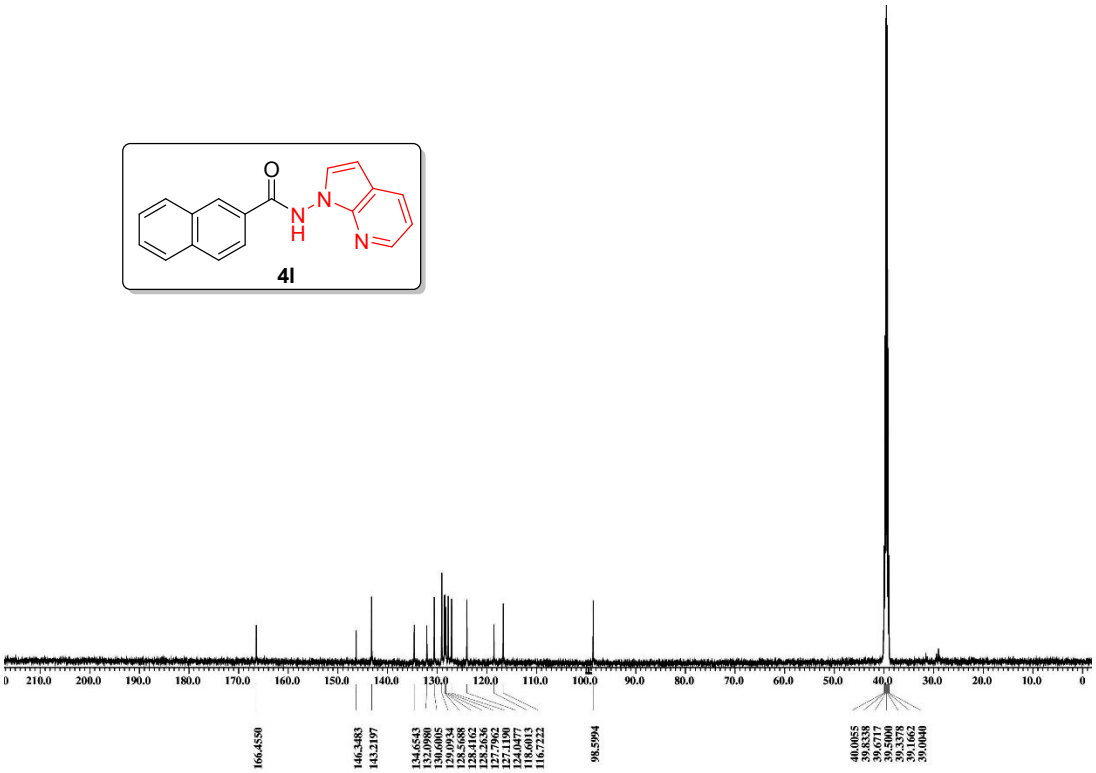

Fig. S26. ^{13}C NMR spectrum of **4l** (125 MHz, DMSO-d_6)

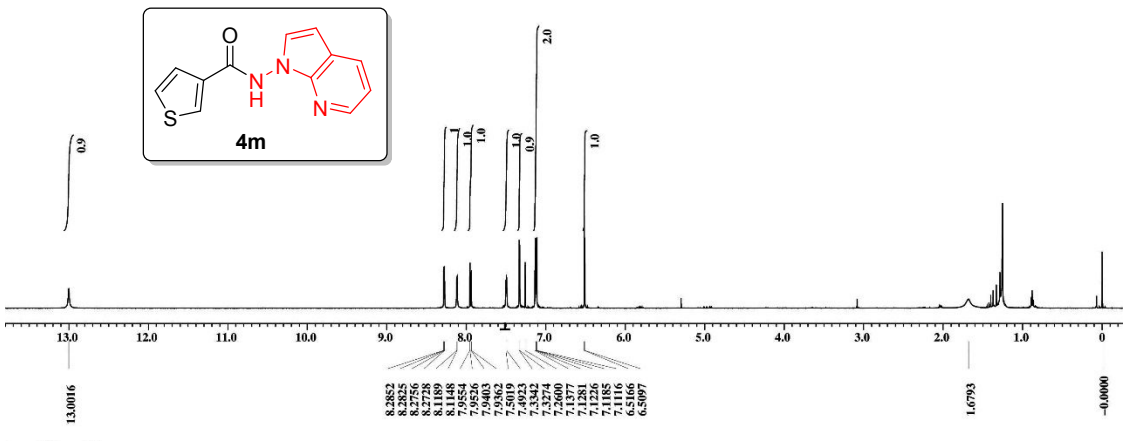

Fig. S27. ^{1}H NMR spectrum of **4m** (500 MHz, $CDCl_3$)

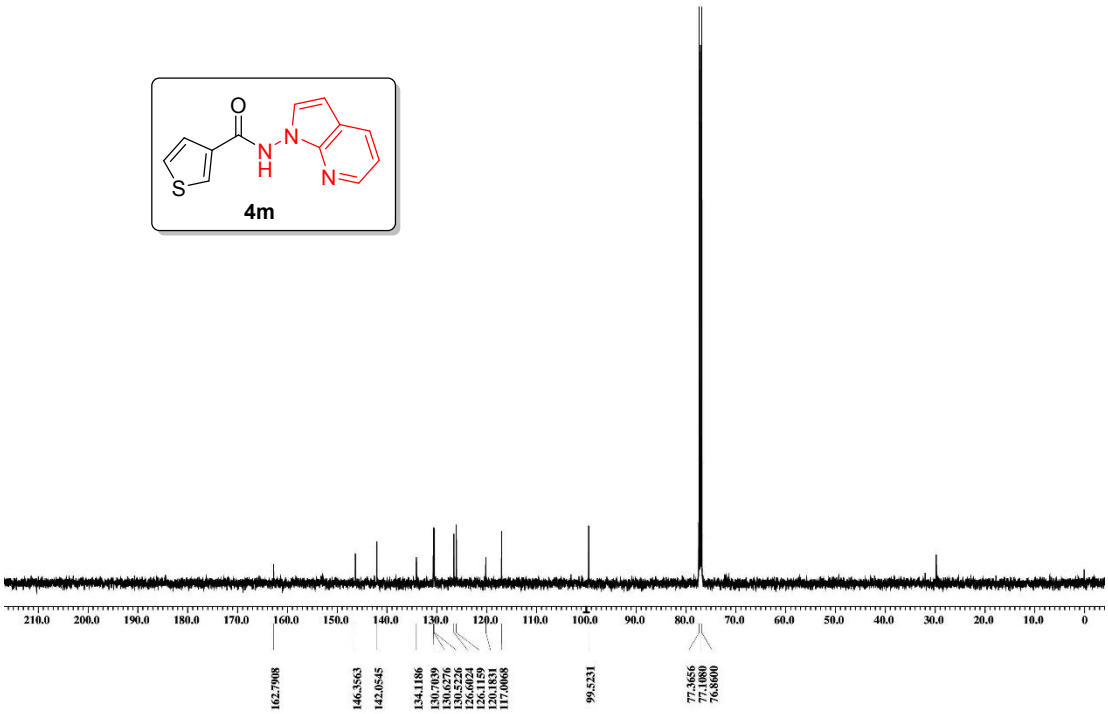

Fig. S28. ^{13}C NMR spectrum of **4m** (125 MHz, $CDCl_3$)

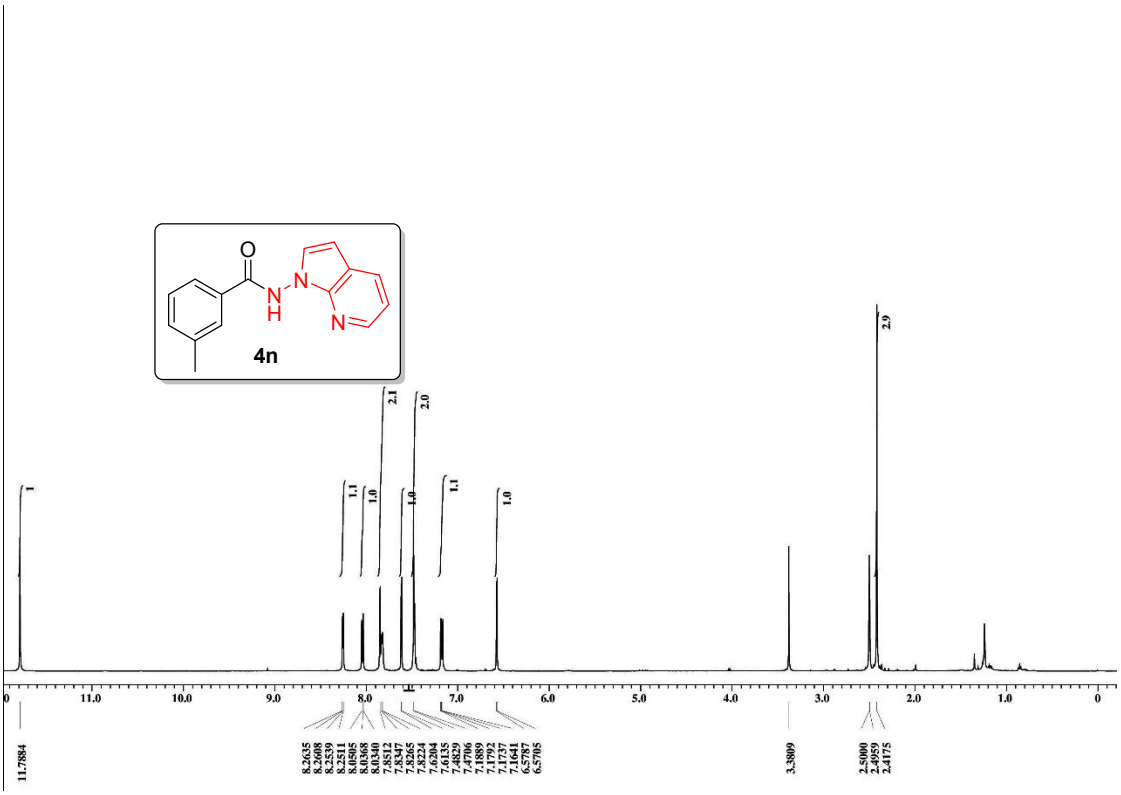

Fig. S29. ^{1}H NMR spectrum of **4n** (500 MHz, DMSO-d_6)

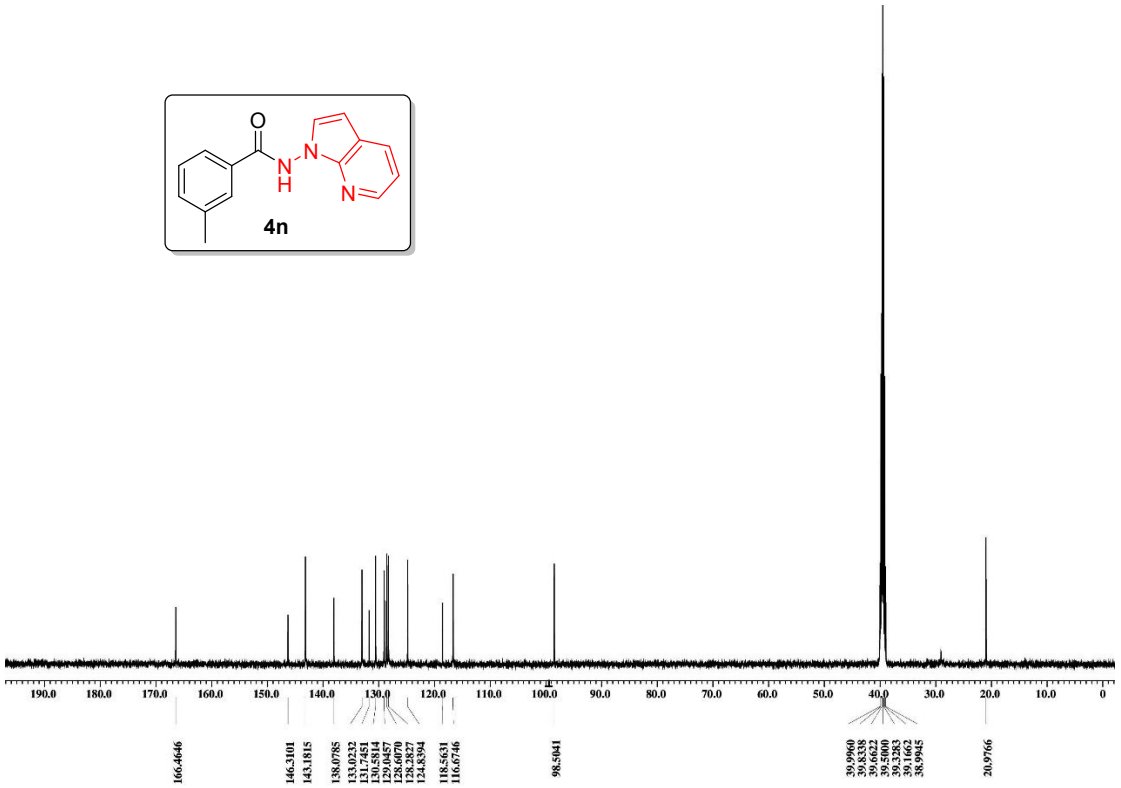

Fig. S30. ^{13}C NMR spectrum of **4n** (125 MHz, DMSO-d_6)

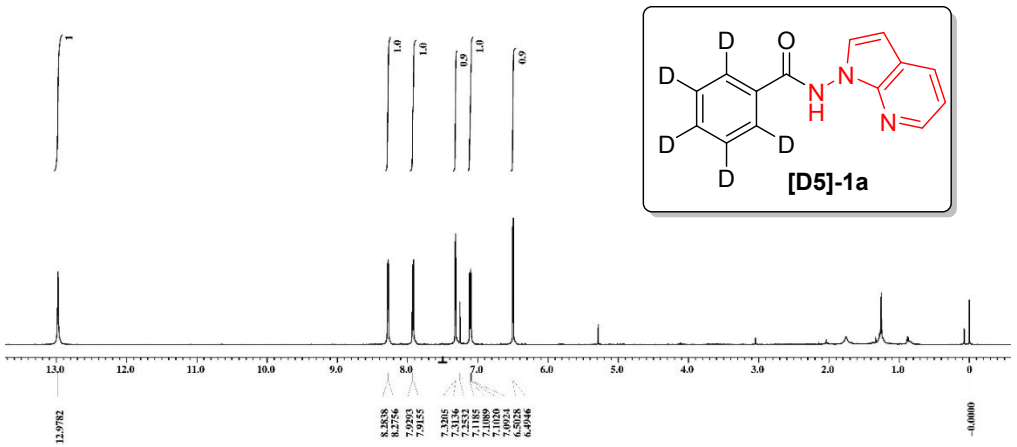

Fig. S31. ^{1}H NMR spectrum of **[D_5]-1a** (500 MHz, $CDCl_3$)

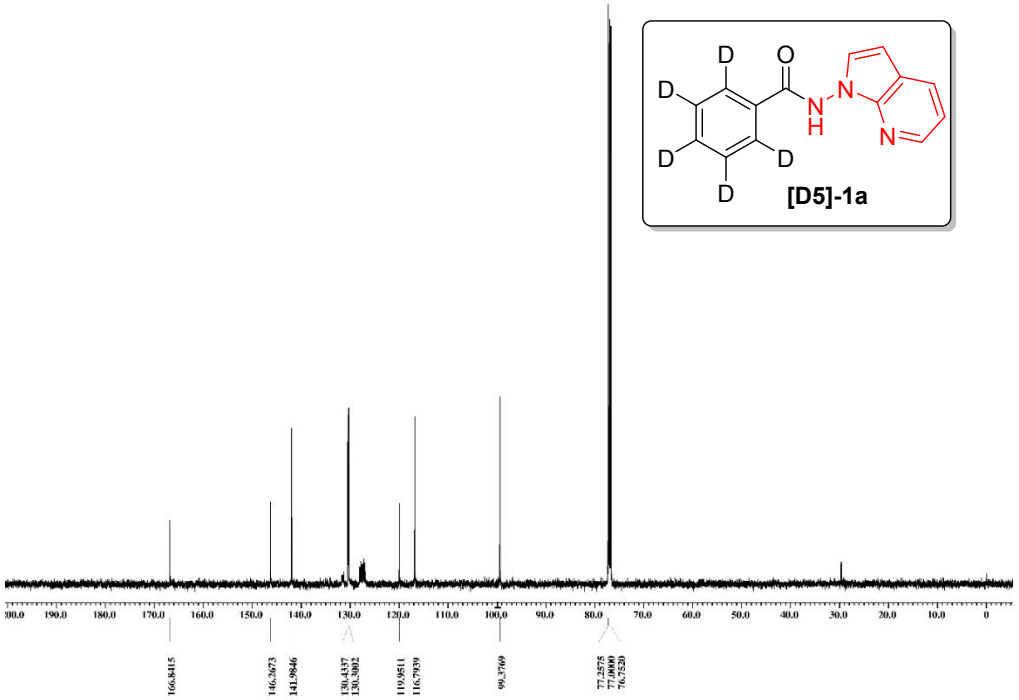

Fig. S32. ^{13}C NMR spectrum of **[D_5]-1a** (125 MHz, $CDCl_3$)

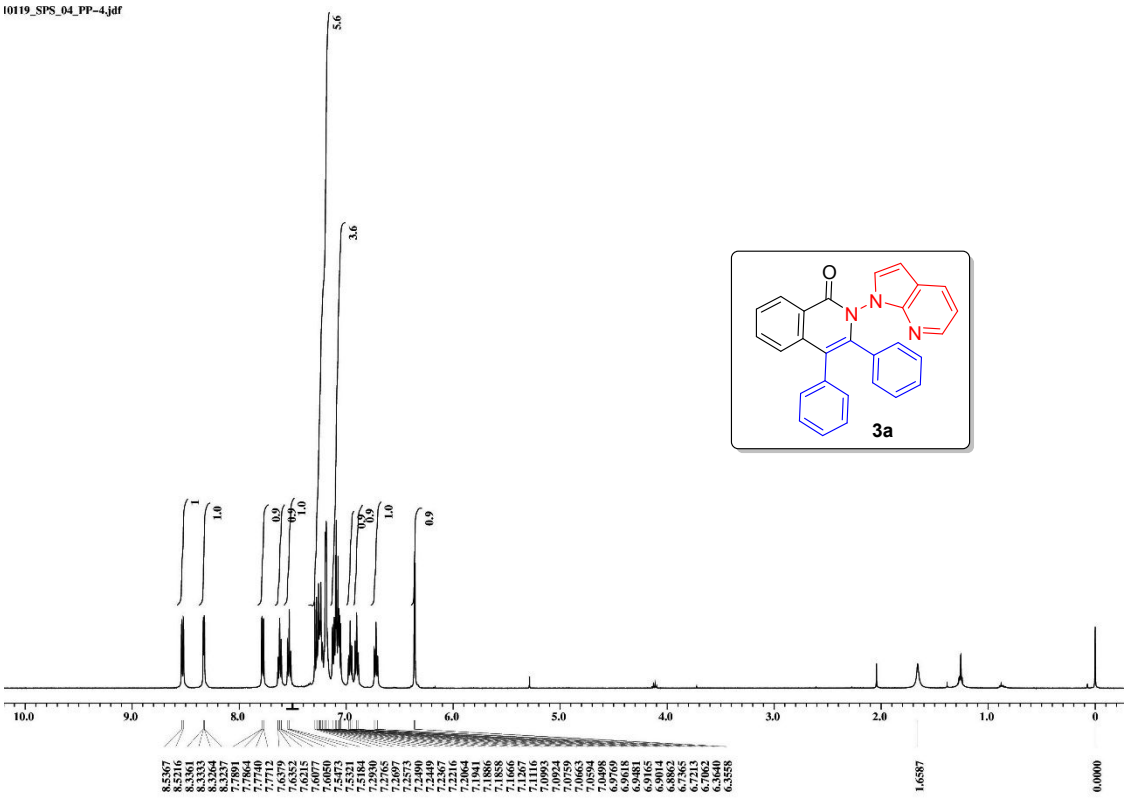

Fig. S33. ^{1}H NMR spectrum of **3a** (500 MHz, $CDCl_3$)

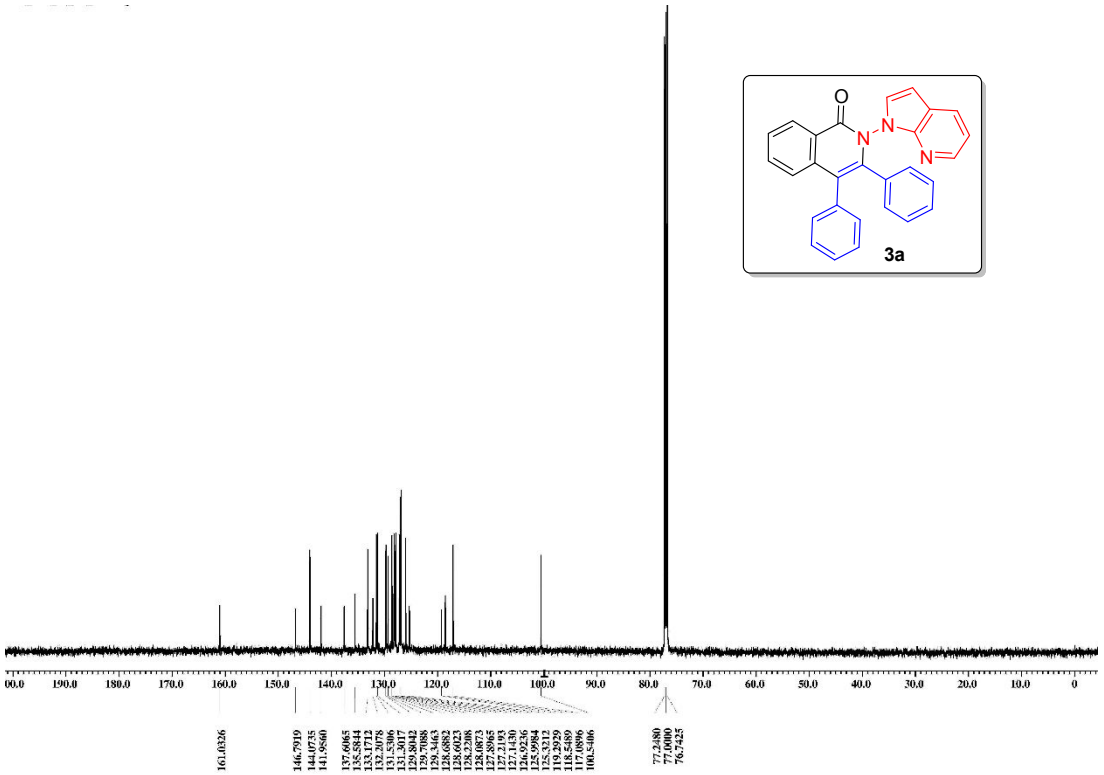

Fig. S34. ^{13}C NMR spectrum of **3a** (125 MHz, $CDCl_3$)

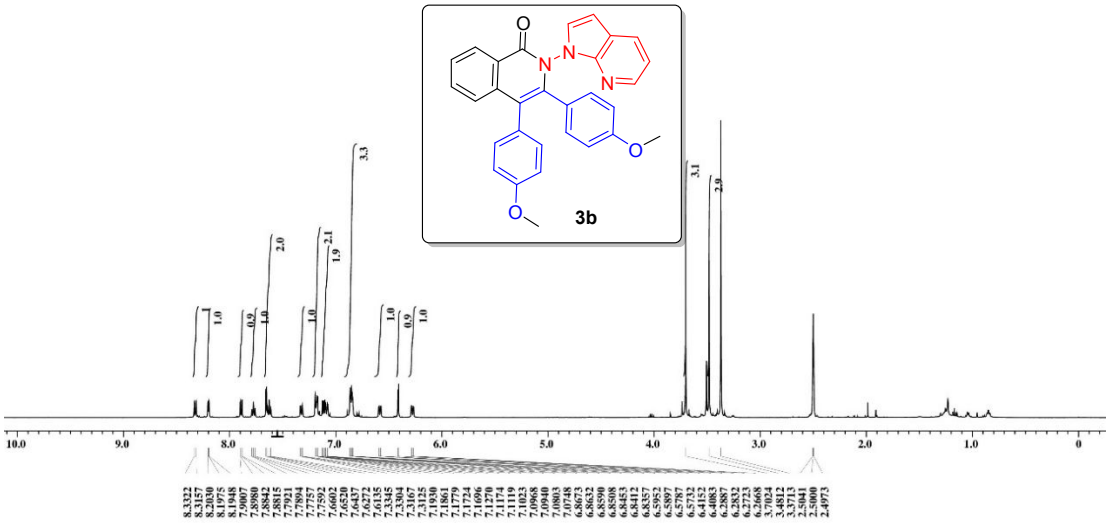

Fig. S35. ^{1}H NMR spectrum of **3b** (500 MHz, DMSO)

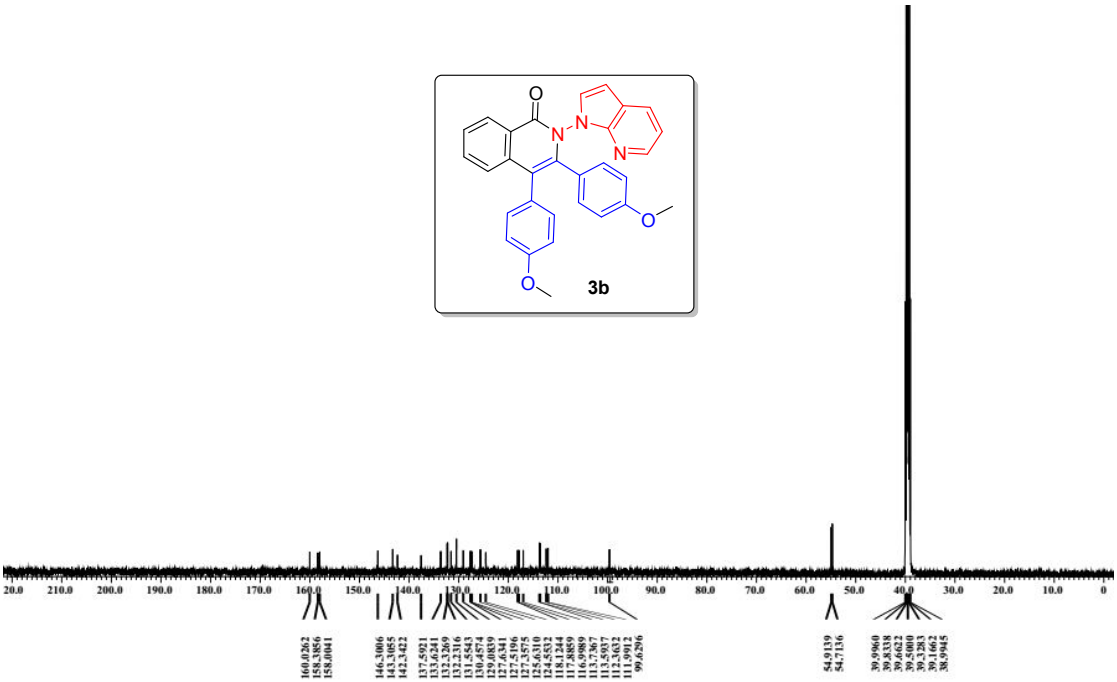

Fig. S36. ^{13}C NMR spectrum of **3b** (125 MHz, DMSO)

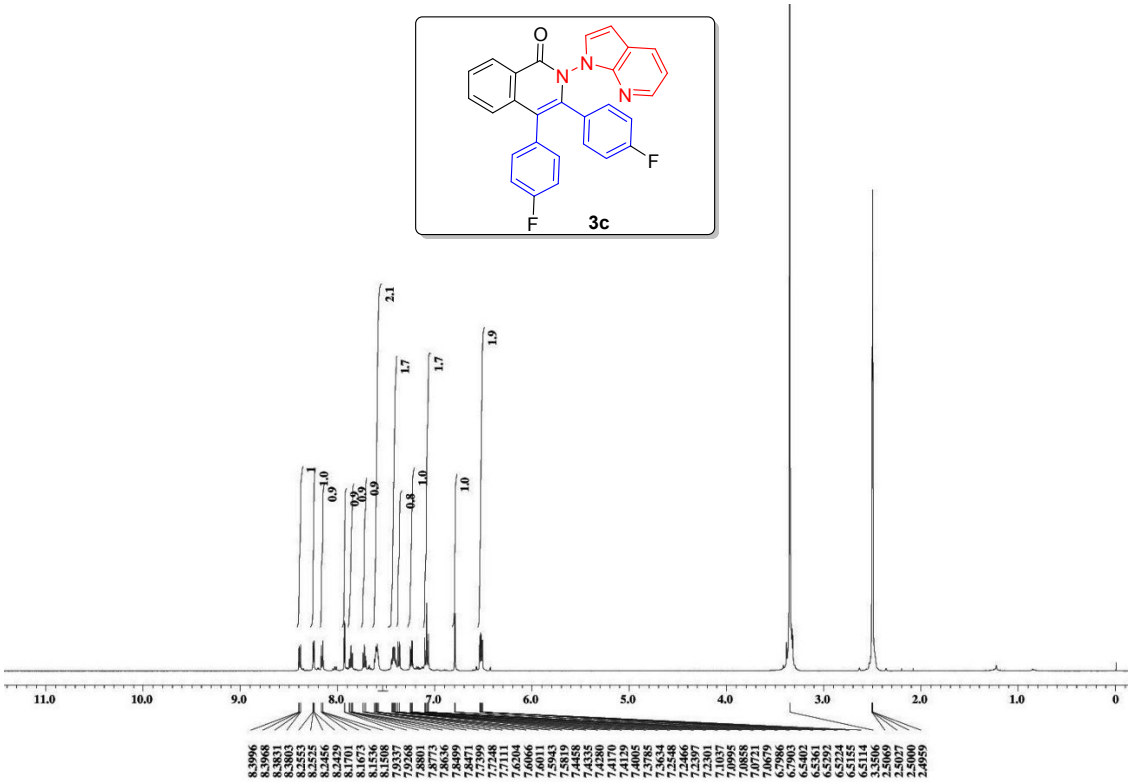

Fig. S37. ^{1}H NMR spectrum of **3c** (500 MHz, $CDCl_3$)

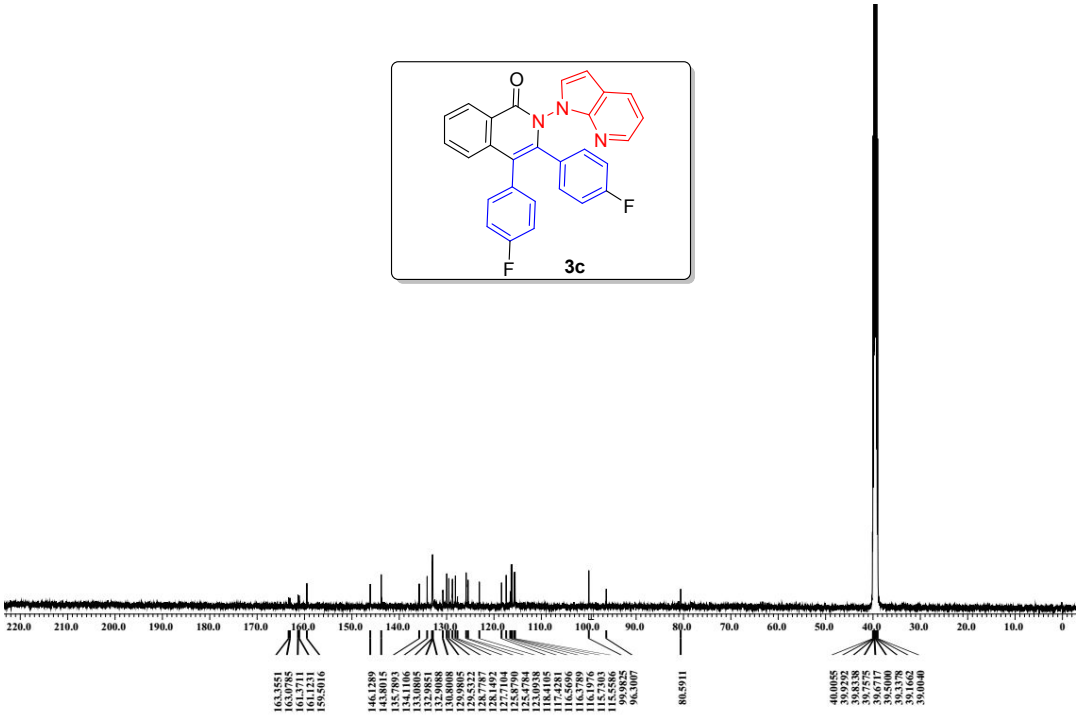

Fig. S38. ^{13}C NMR spectrum of **3c** (125 MHz, $CDCl_3$)

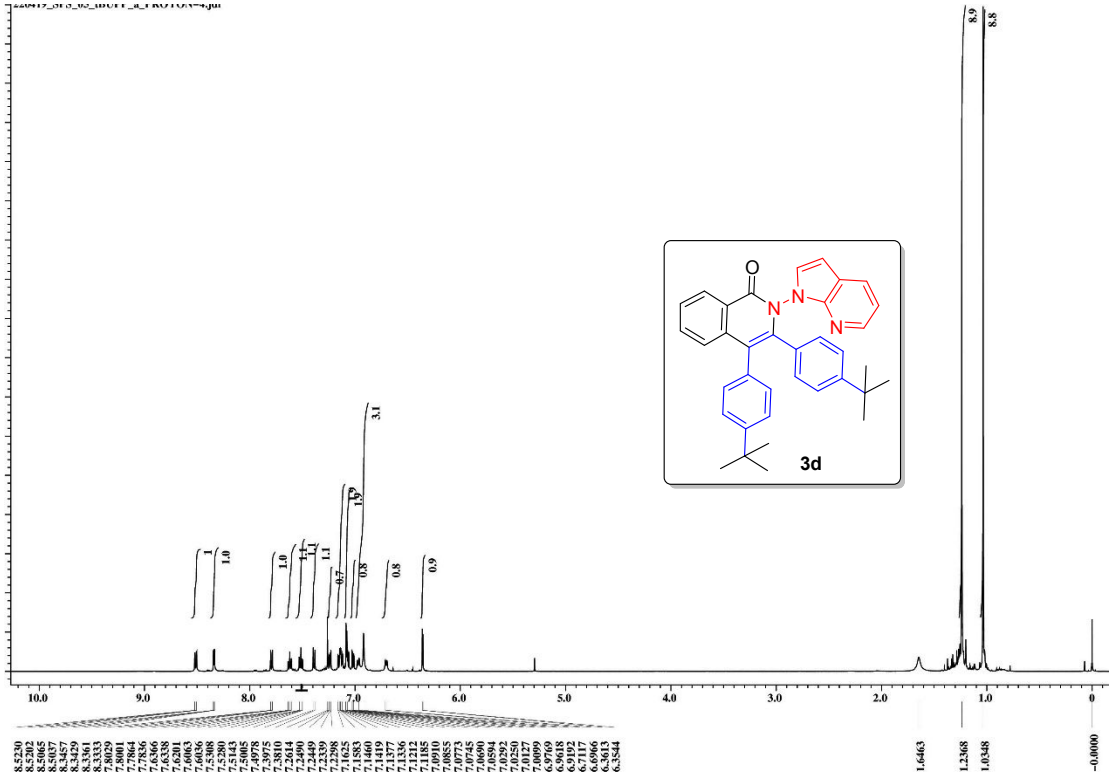

Fig. S39. ^{1}H NMR spectrum of **3d** (500 MHz, $CDCl_3$)

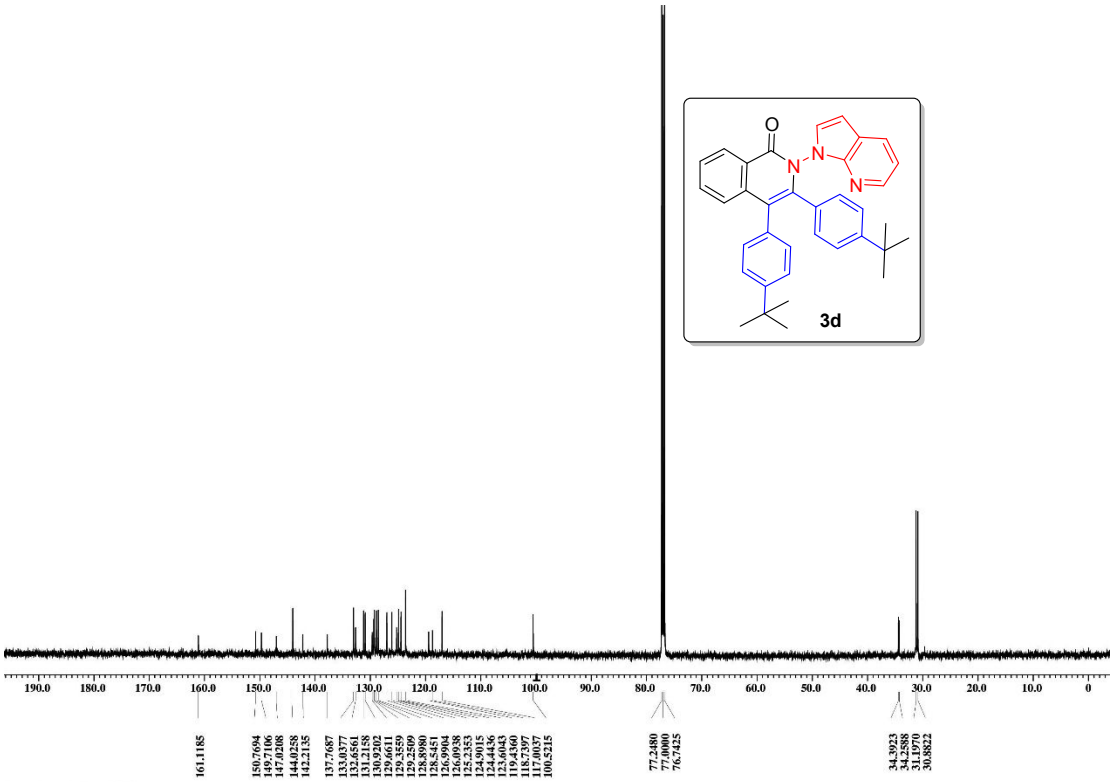

Fig. S40. ^{13}C NMR spectrum of **3d** (125 MHz, $CDCl_3$)

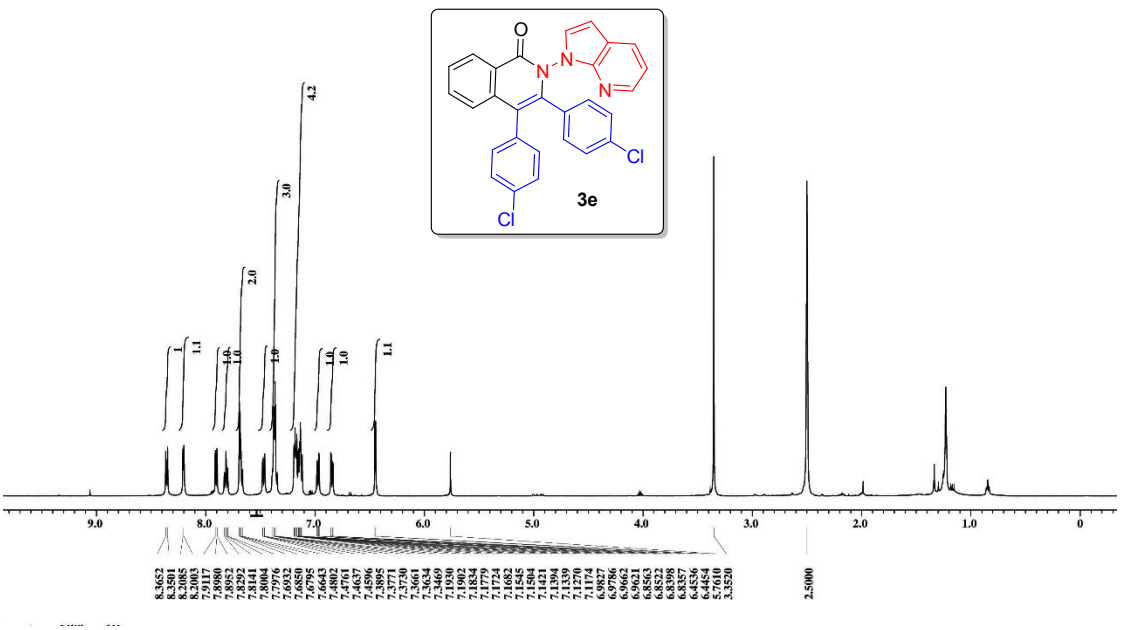

Fig. S41. ^{1}H NMR spectrum of **3e** (500 MHz, DMSO)

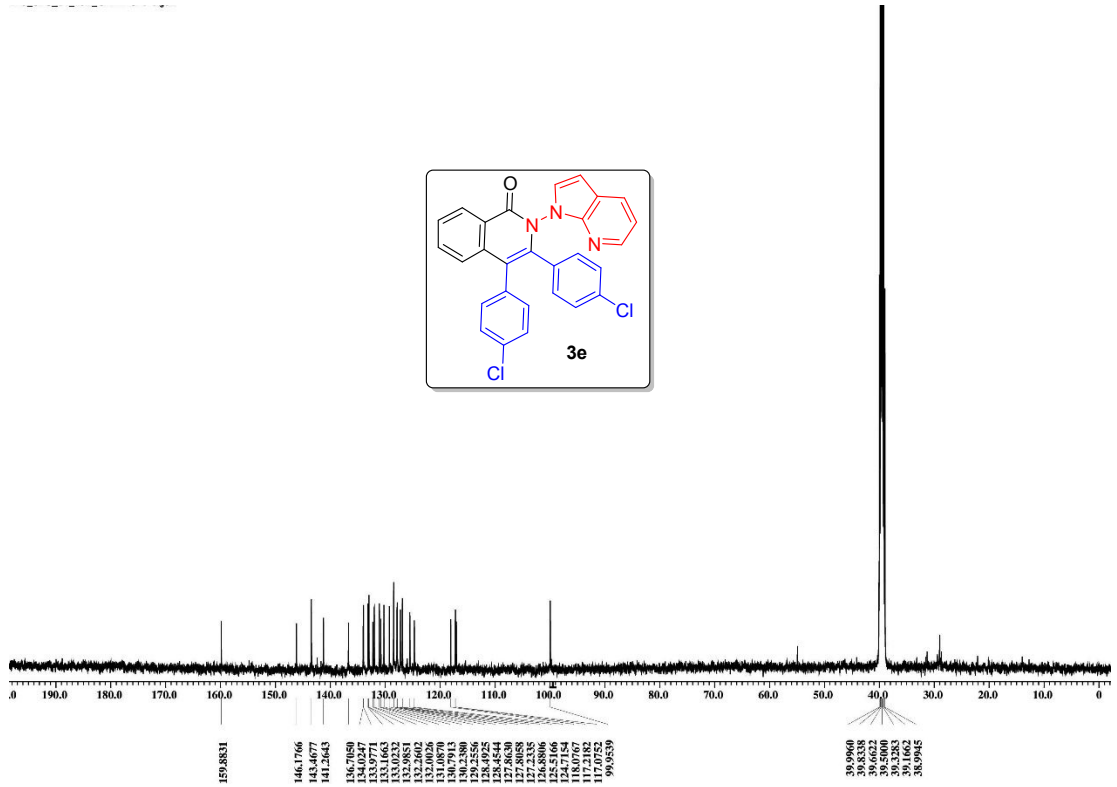

Fig. S42. ^{13}C NMR spectrum of **3e** (125 MHz, DMSO)

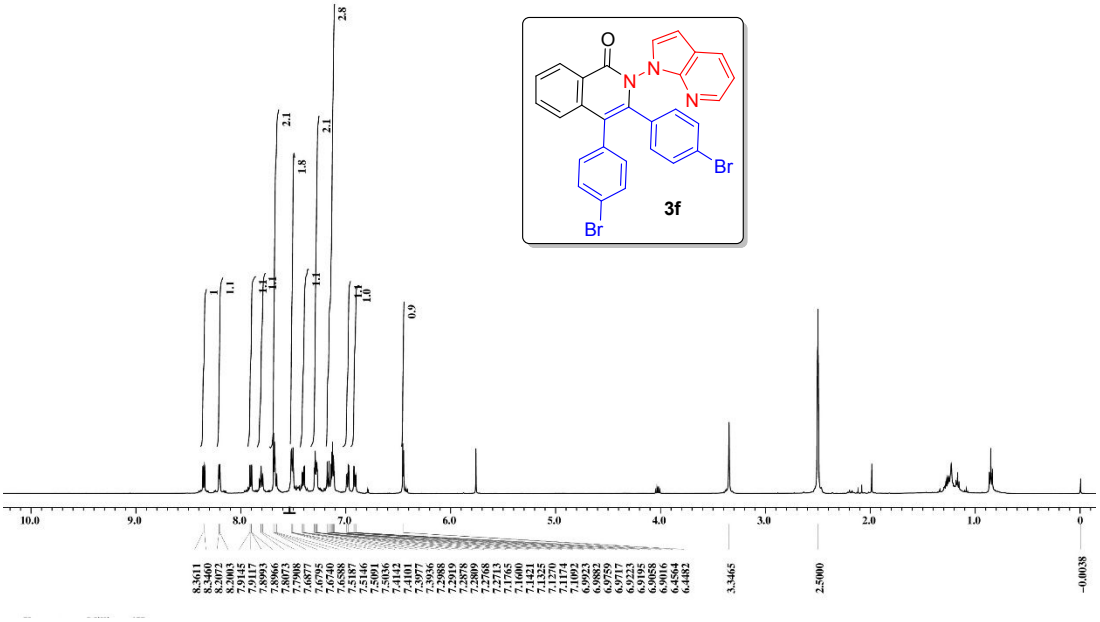

Fig. S43. ^{1}H NMR spectrum of **3f** (500 MHz, DMSO)

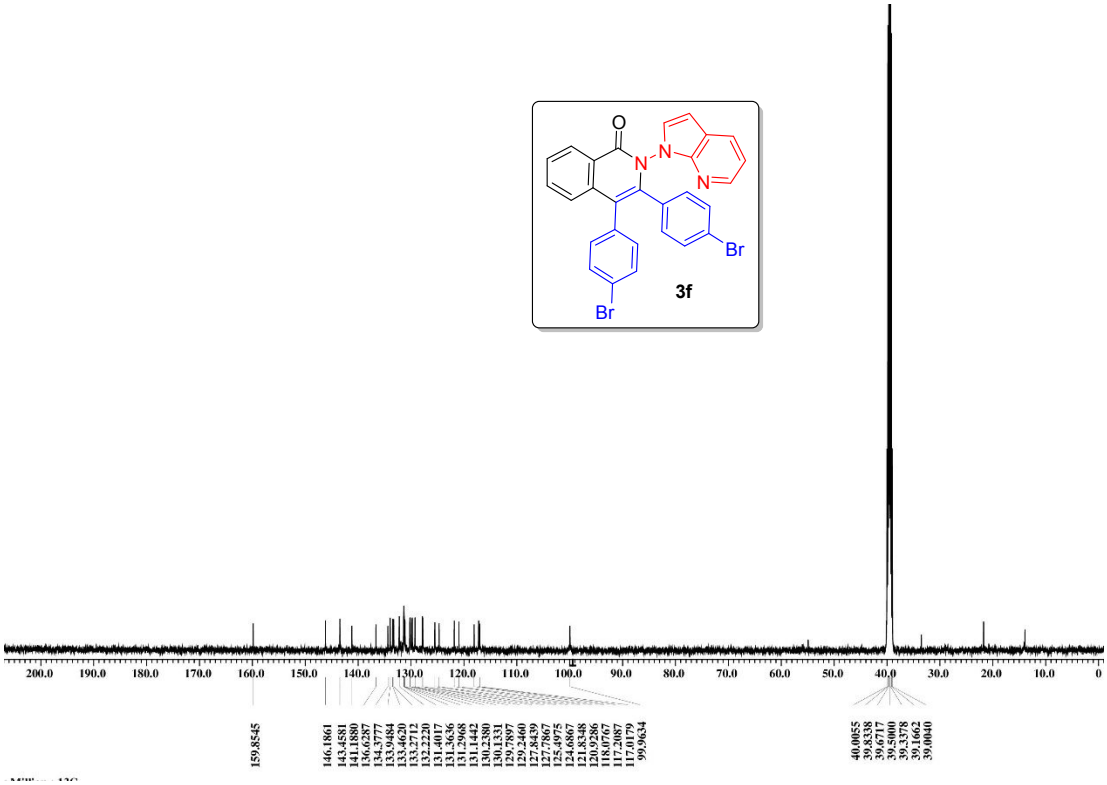

Fig. S44. ^{13}C NMR spectrum of **3f** (125 MHz, DMSO)

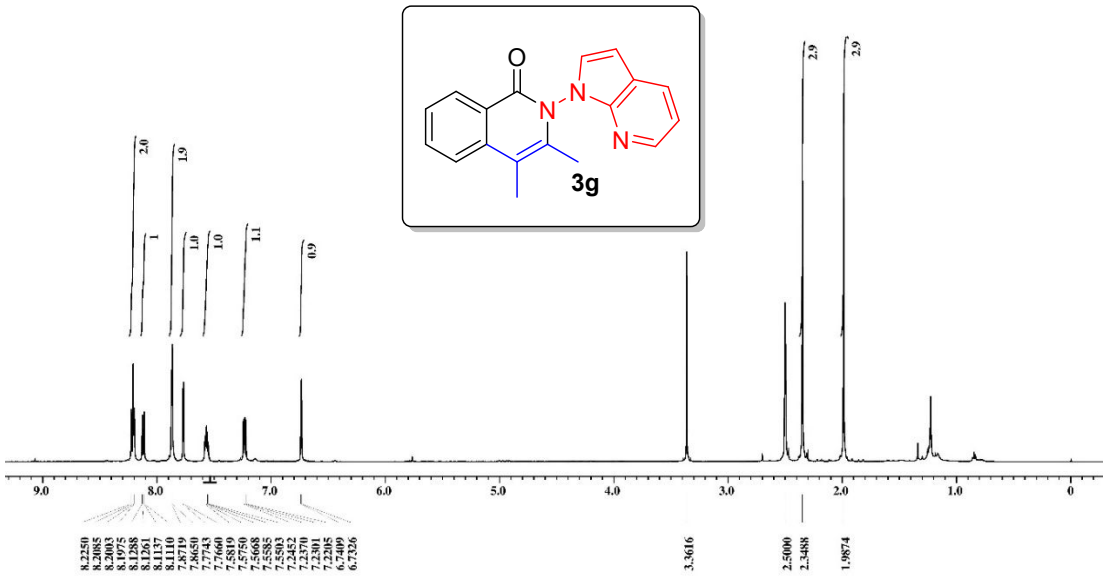

Fig. S45. ^{1}H NMR spectrum of **3g** (500 MHz, DMSO)

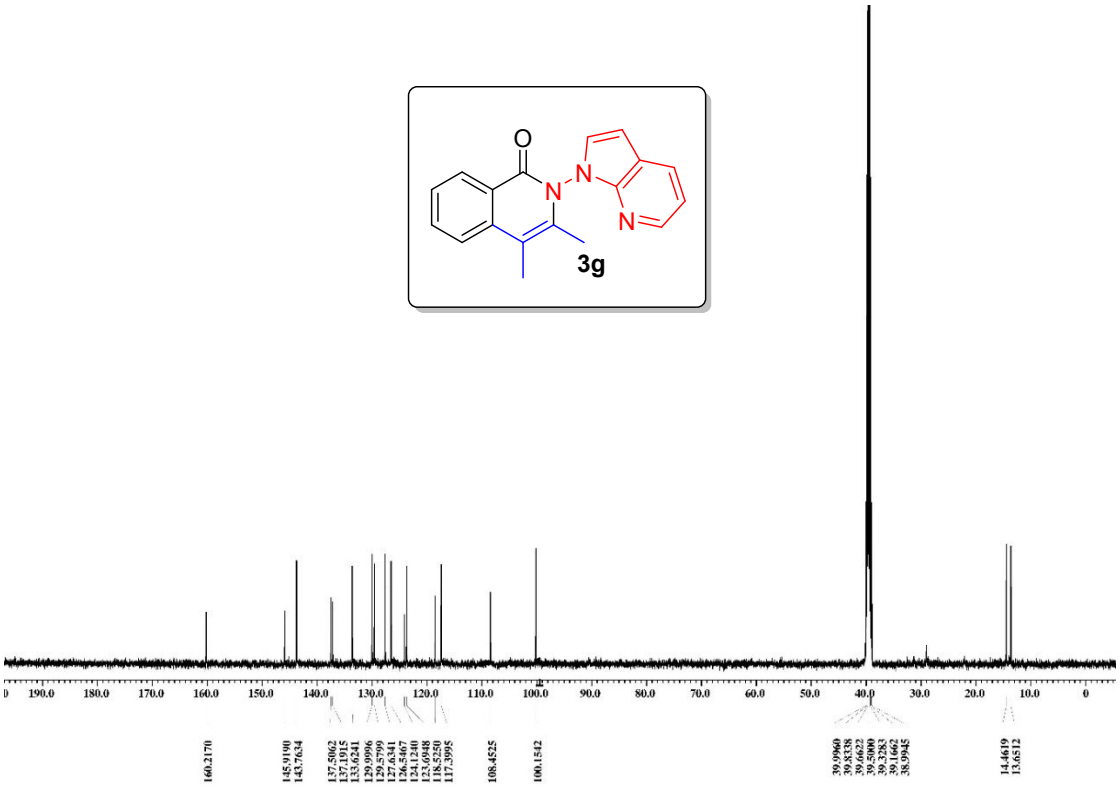

Fig. S46. ^{13}C NMR spectrum of **3g** (125 MHz, DMSO)

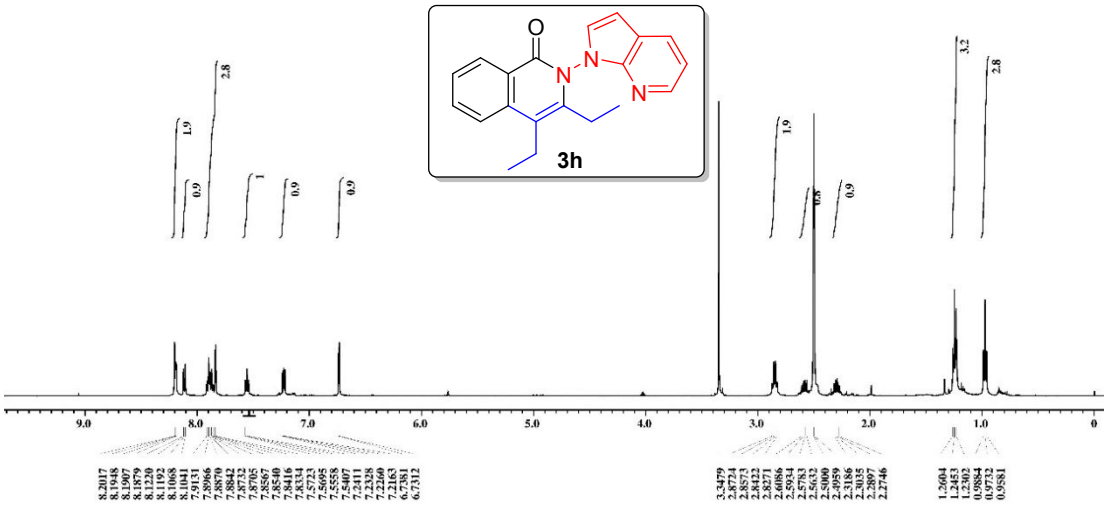

Fig. S47. ^{1}H NMR spectrum of **3h** (500 MHz, DMSO)

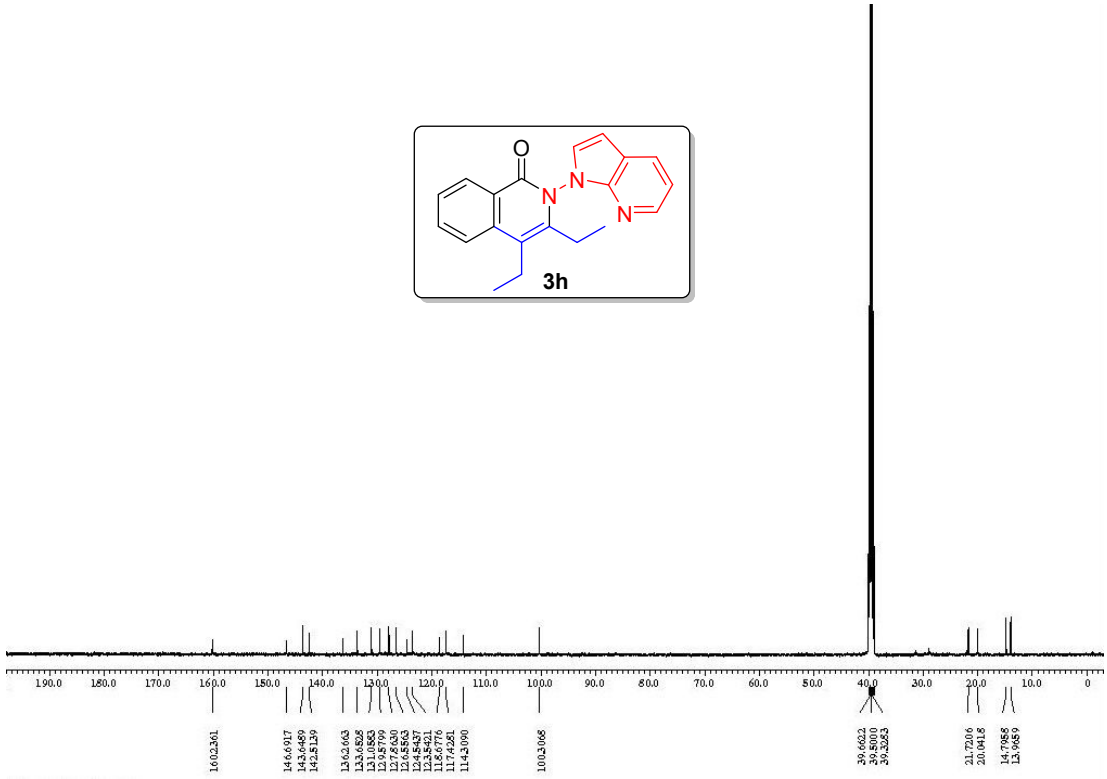

Fig. S48. ^{13}C NMR spectrum of **3h** (125 MHz, DMSO)

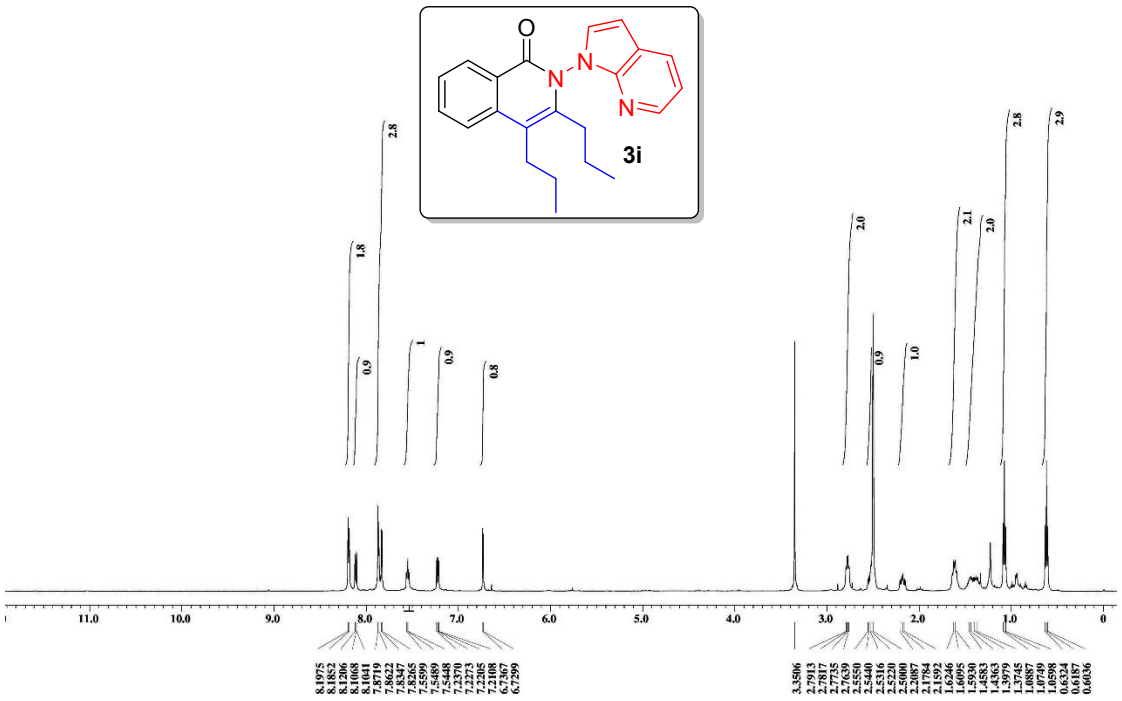

Fig. S49. ^{1}H NMR spectrum of **3i** (500 MHz, DMSO)

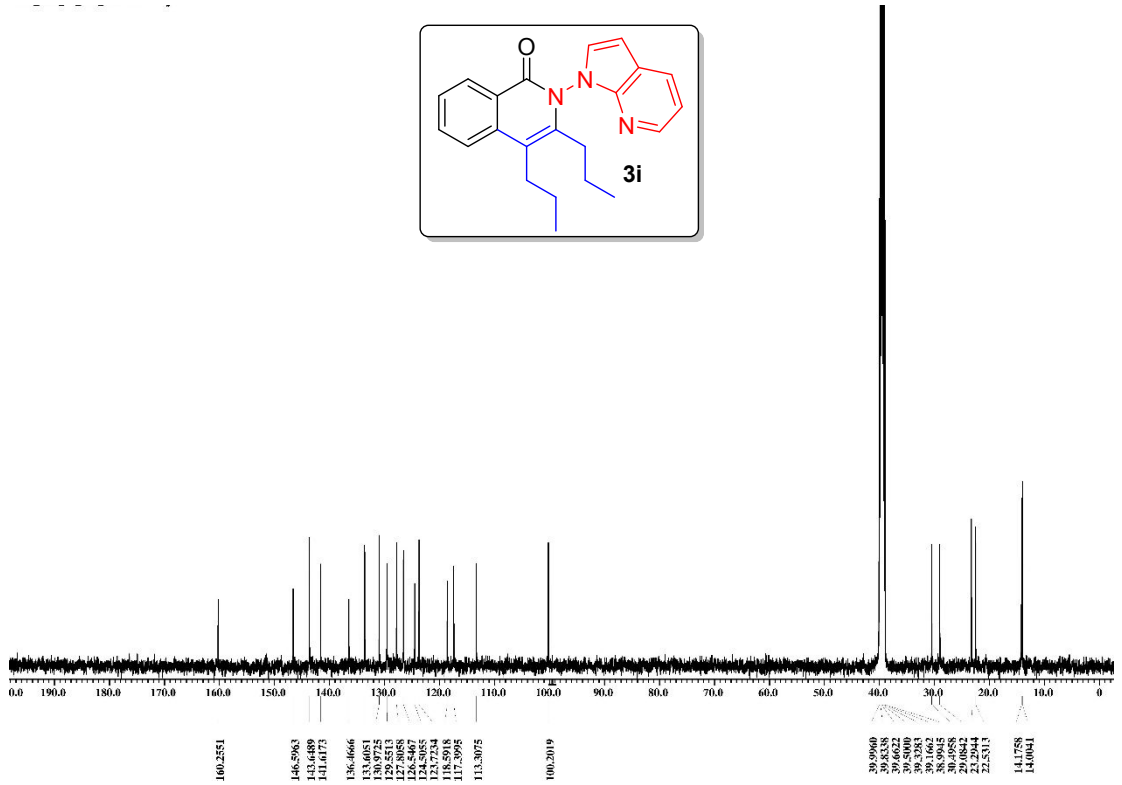

Fig. S50. ^{13}C NMR spectrum of **3i** (125 MHz, DMSO)

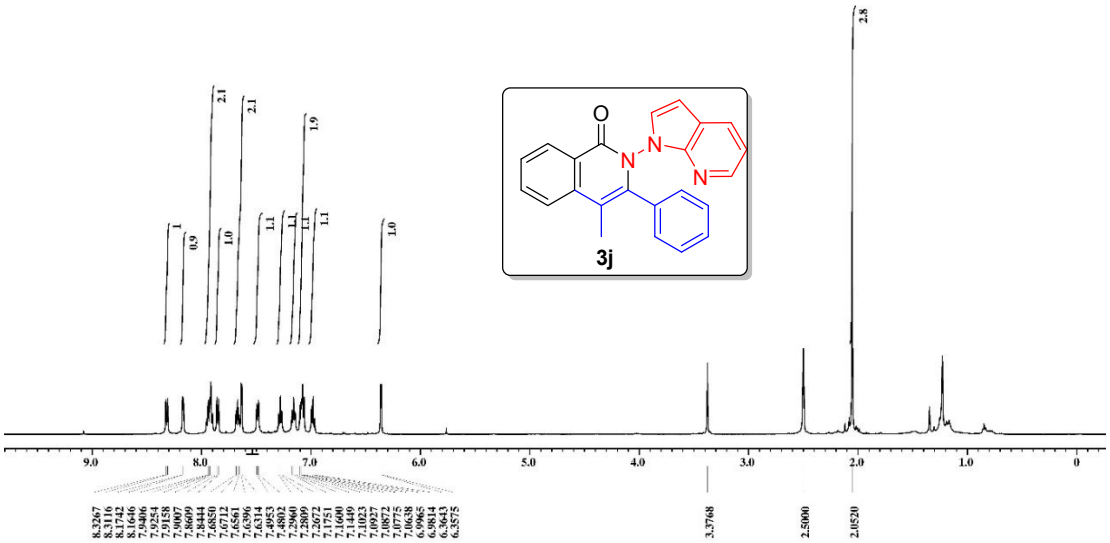

Fig. S51. ^{1}H NMR spectrum of **3j** (500 MHz, DMSO)

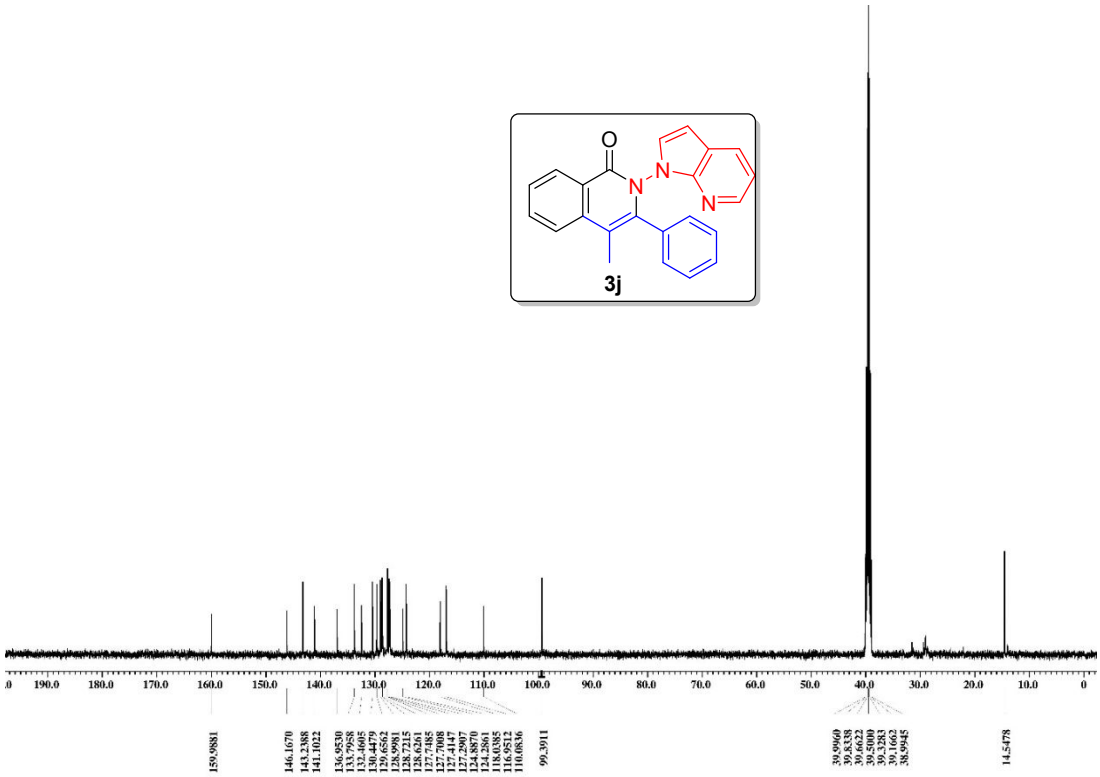

Fig. S52. ^{13}C NMR spectrum of **3j** (125 MHz, DMSO)

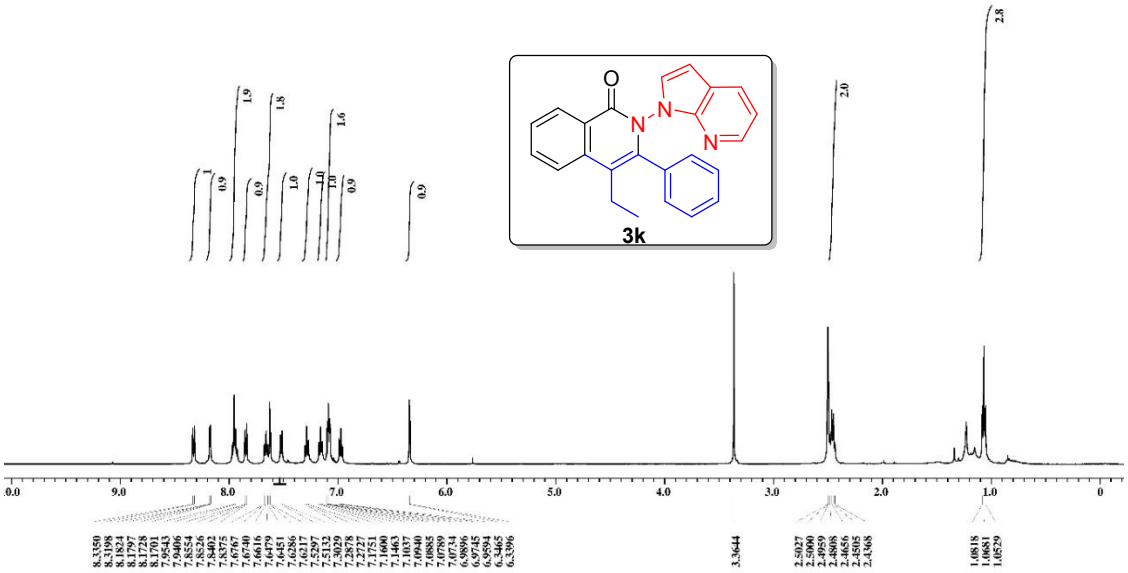

Fig. S53. ^{1}H NMR spectrum of **3k** (500 MHz, DMSO)

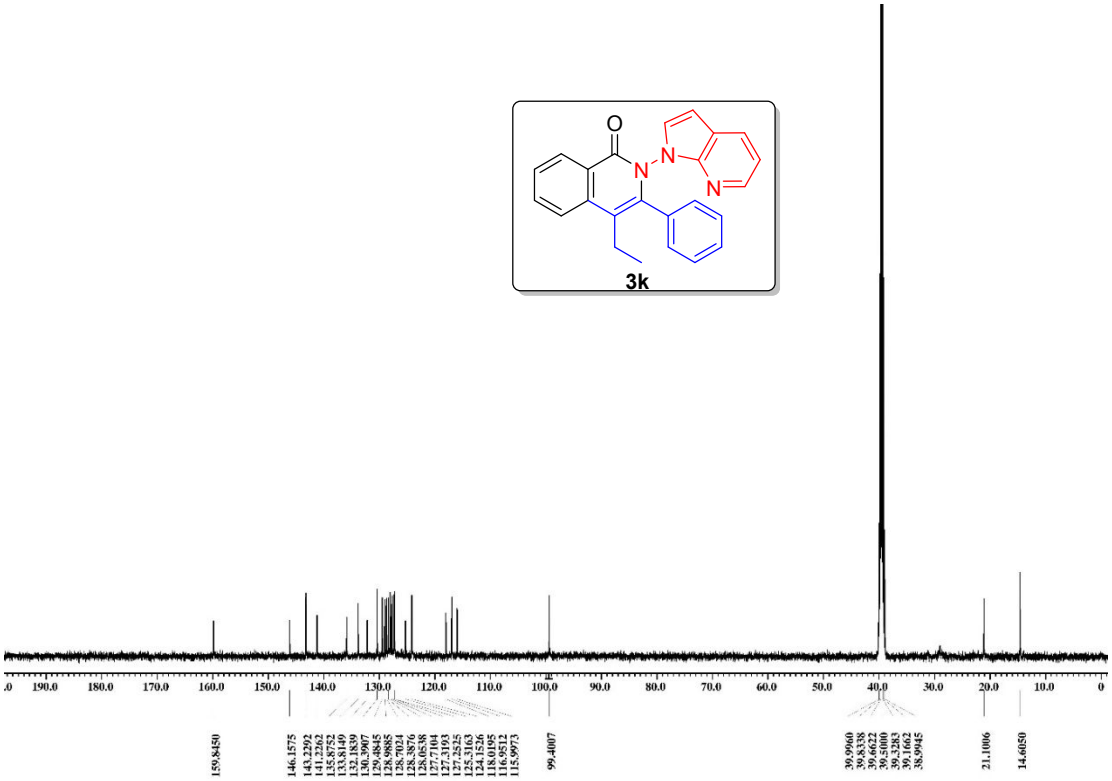

Fig. S54. ^{13}C NMR spectrum of **3k** (125 MHz, DMSO)

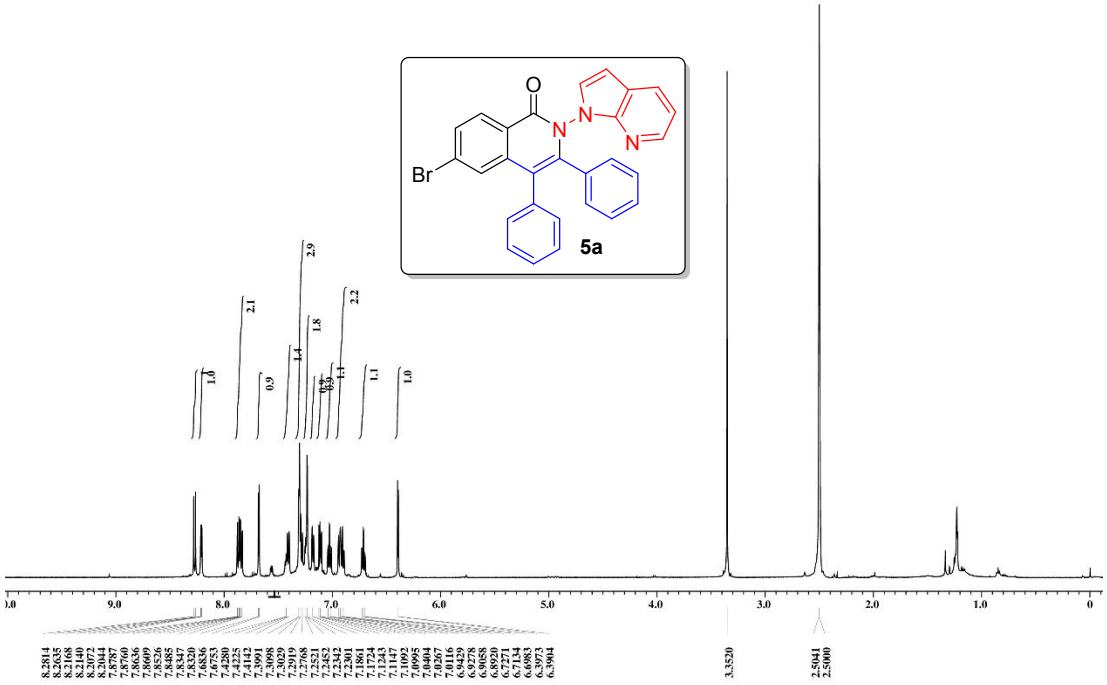

Fig. S55. ^{1}H NMR spectrum of **5a** (500 MHz, DMSO)

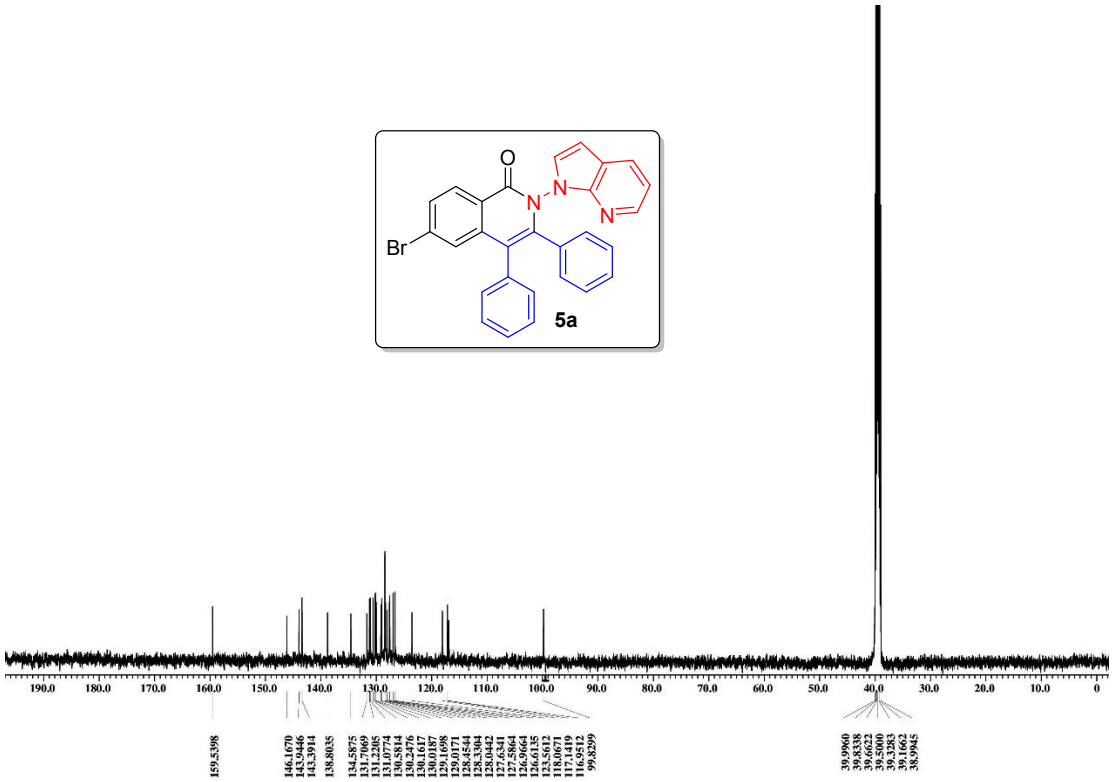

Fig. S56. ^{13}C NMR spectrum of **5a** (125 MHz, DMSO)

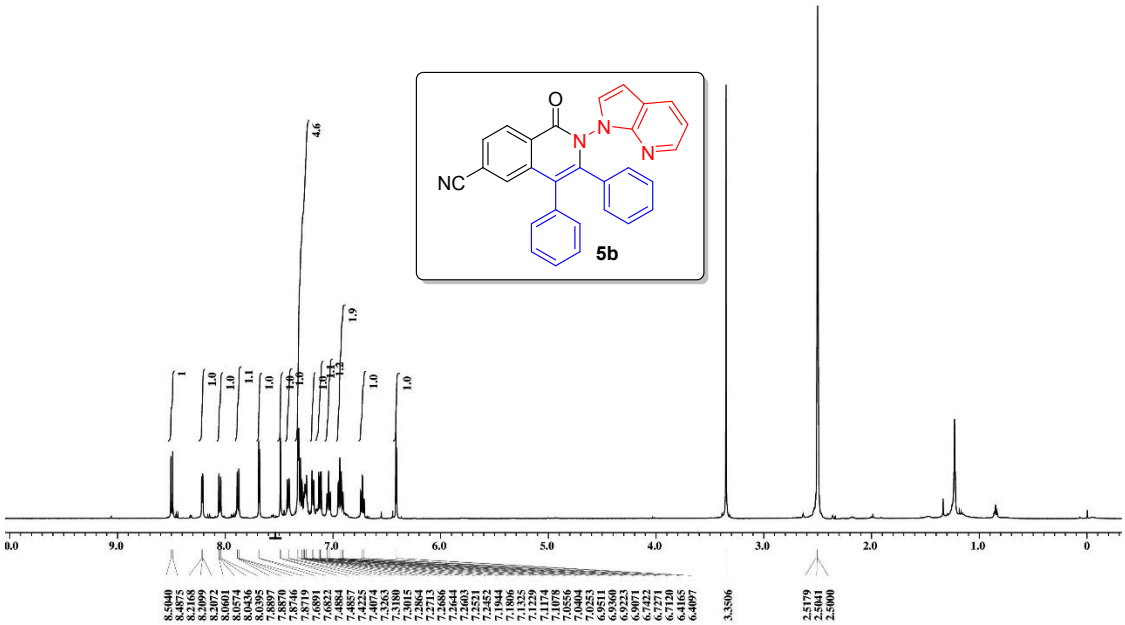

Fig. S57. ^{1}H NMR spectrum of **5b** (500 MHz, DMSO)

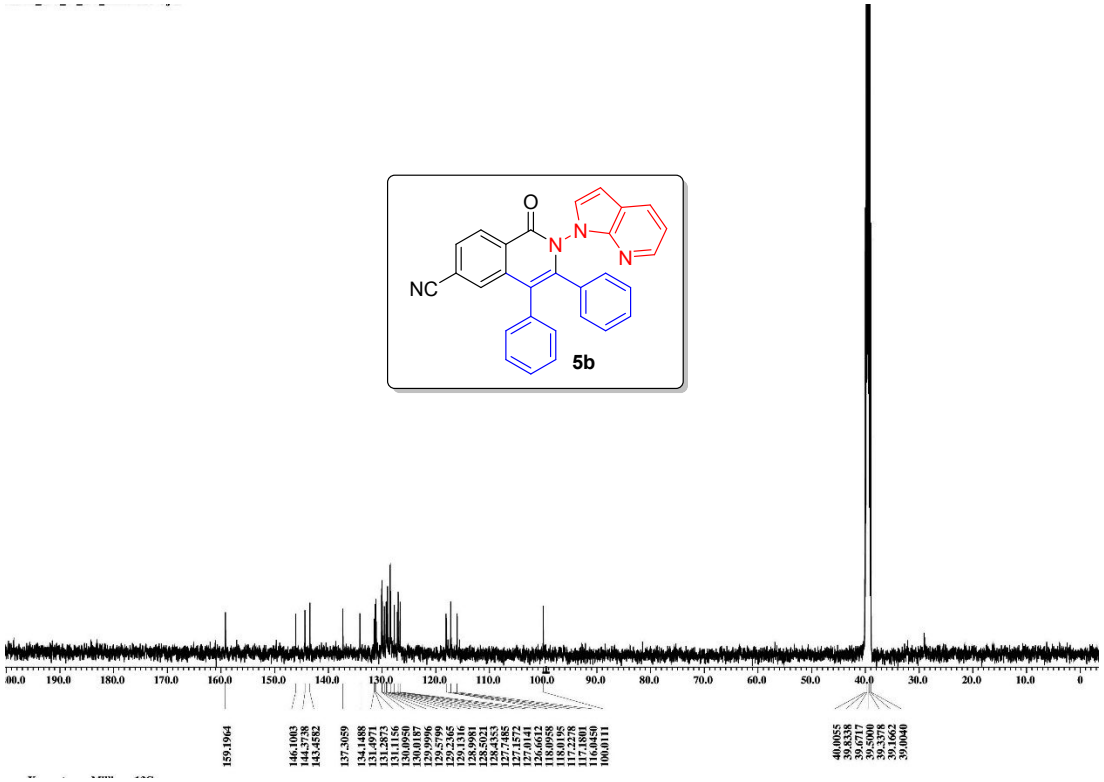

Fig. S58. ^{13}C NMR spectrum of **5b** (125 MHz, DMSO)

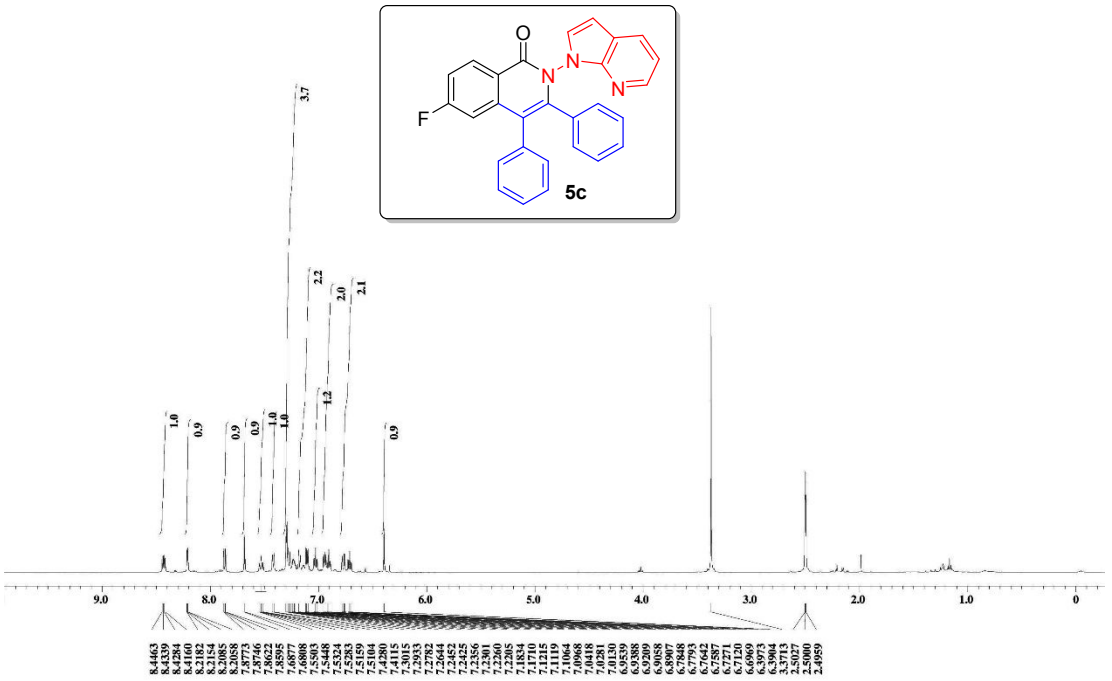

Fig. S59. ^{1}H NMR spectrum of **5c** (500 MHz, DMSO)

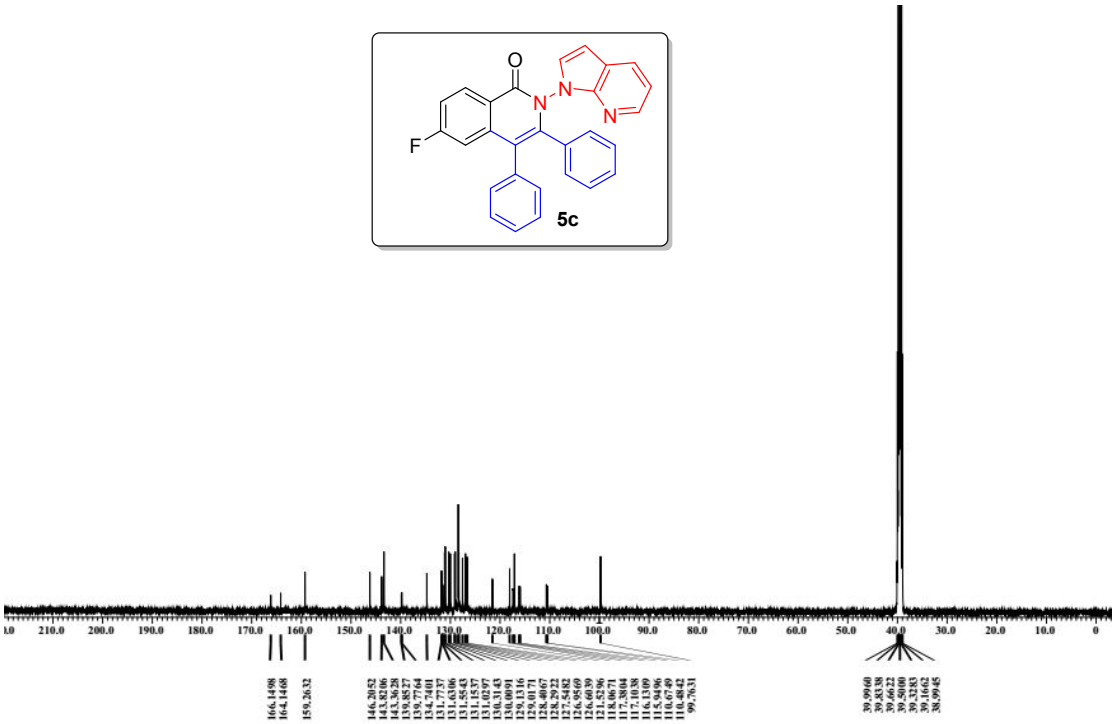

Fig. S60. ^{13}C NMR spectrum of **5c** (125 MHz, DMSO)

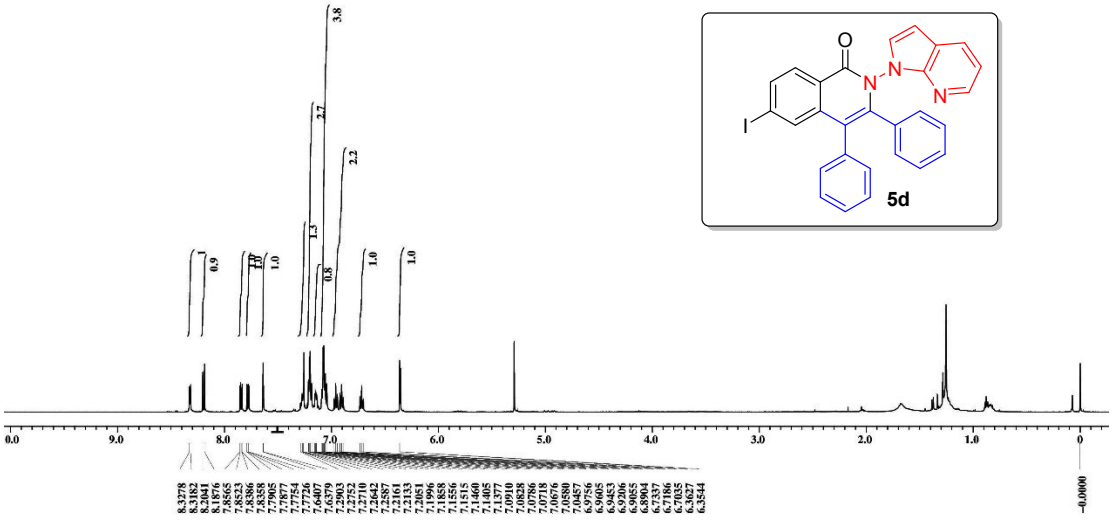

Fig. S61. ^{1}H NMR spectrum of **5d** (500 MHz, $CDCl_3$)

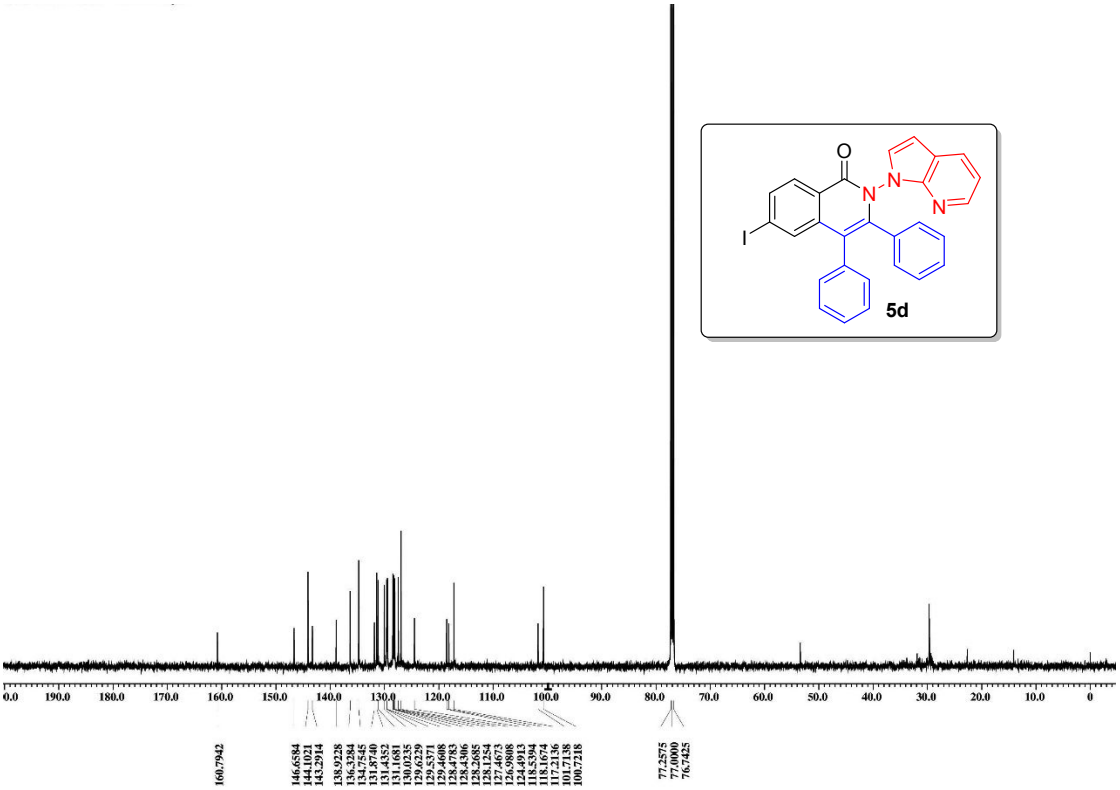

Fig. S62. ^{13}C NMR spectrum of **5d** (125 MHz, $CDCl_3$)

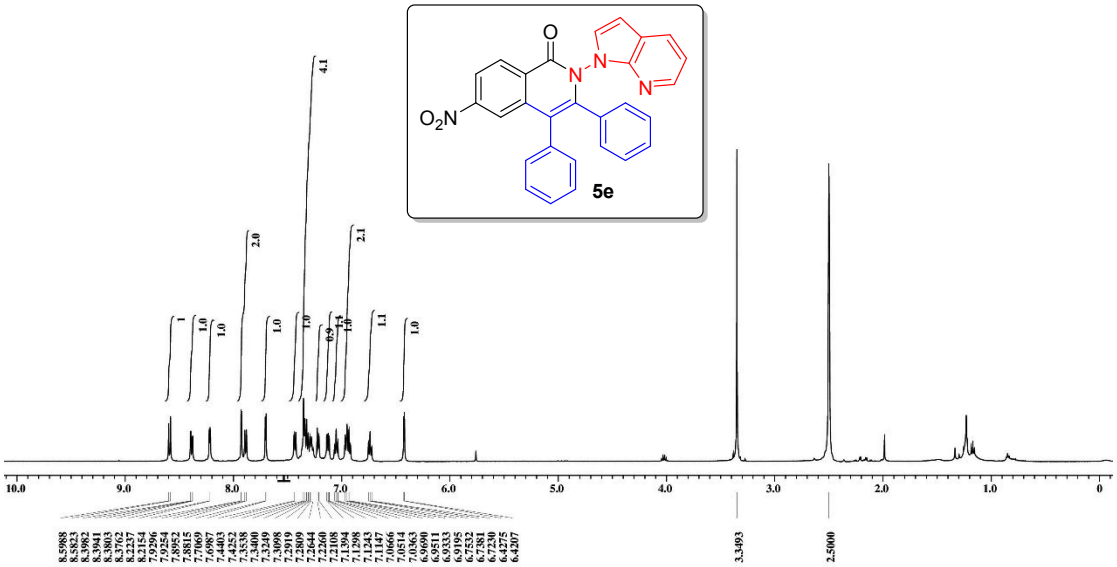

Fig. S63. ^{1}H NMR spectrum of **5e** (500 MHz, DMSO)

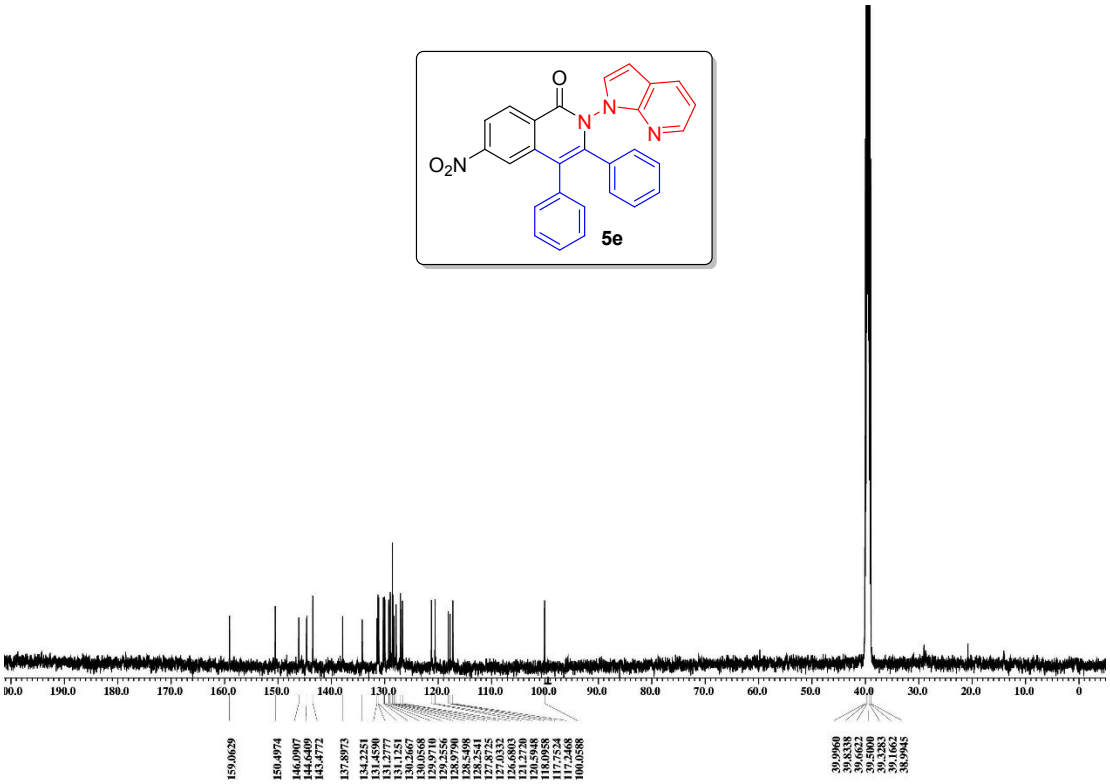

Fig. S64. ^{13}C NMR spectrum of **5e** (125 MHz, DMSO)

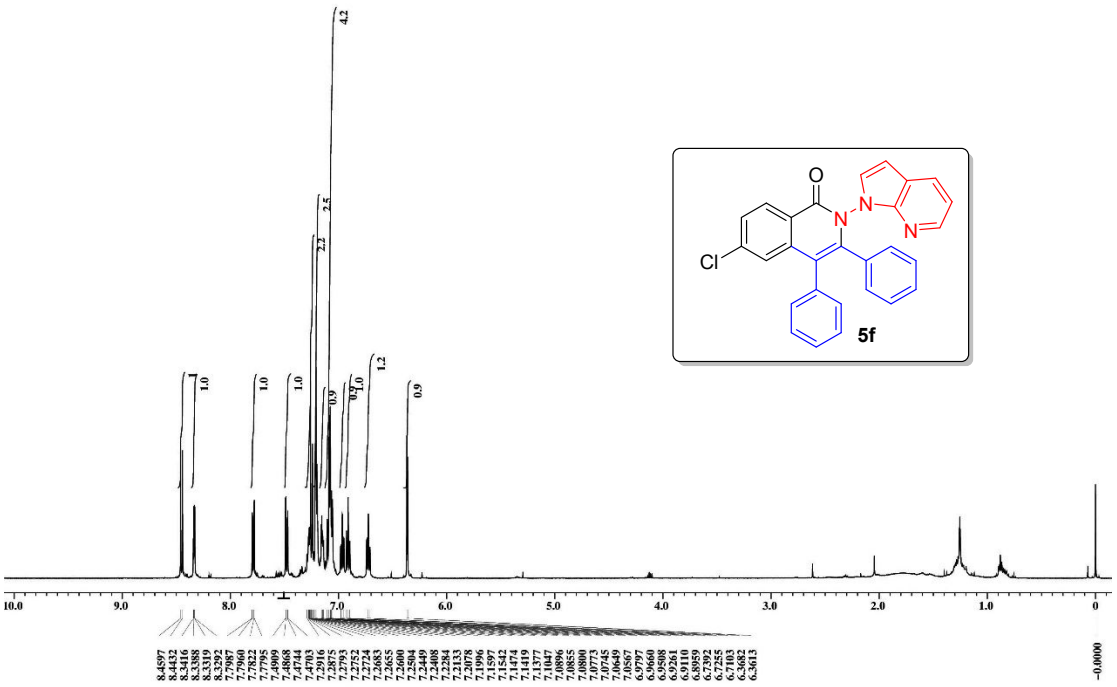

Fig. S65. ^{1}H NMR spectrum of **5f** (500 MHz, $CDCl_3$)

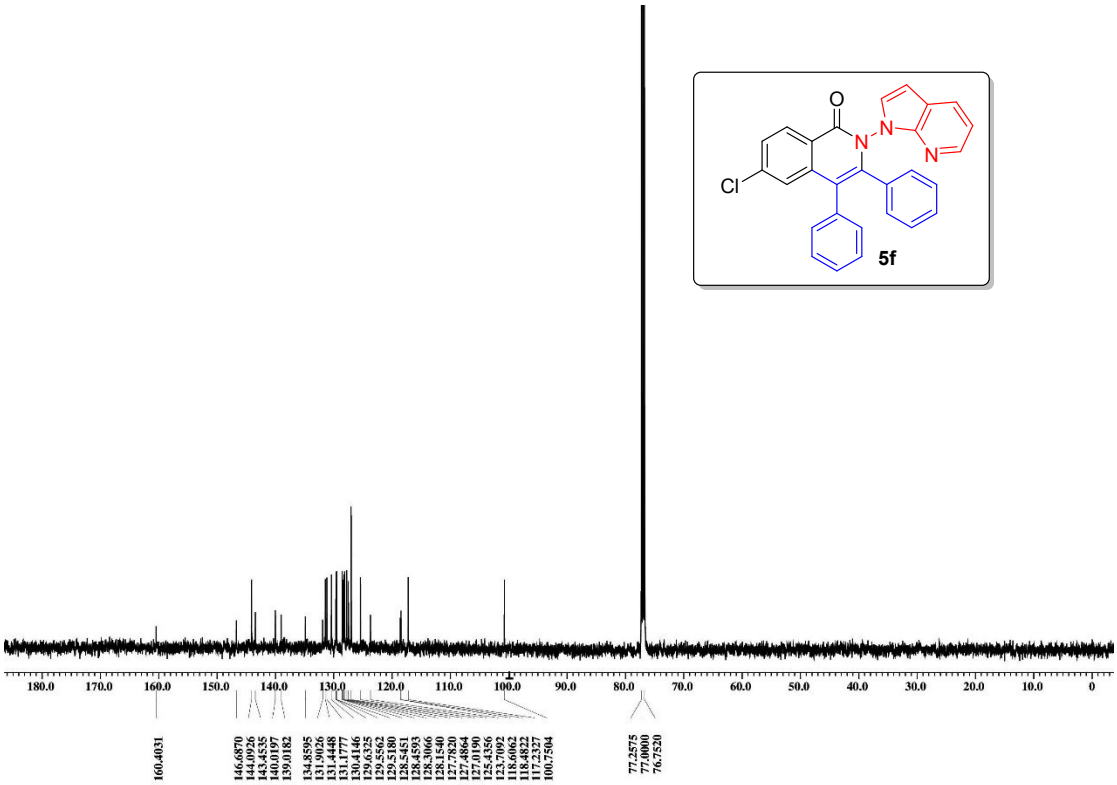

Fig. S66. ^{13}C NMR spectrum of **5f** (125 MHz, $CDCl_3$)

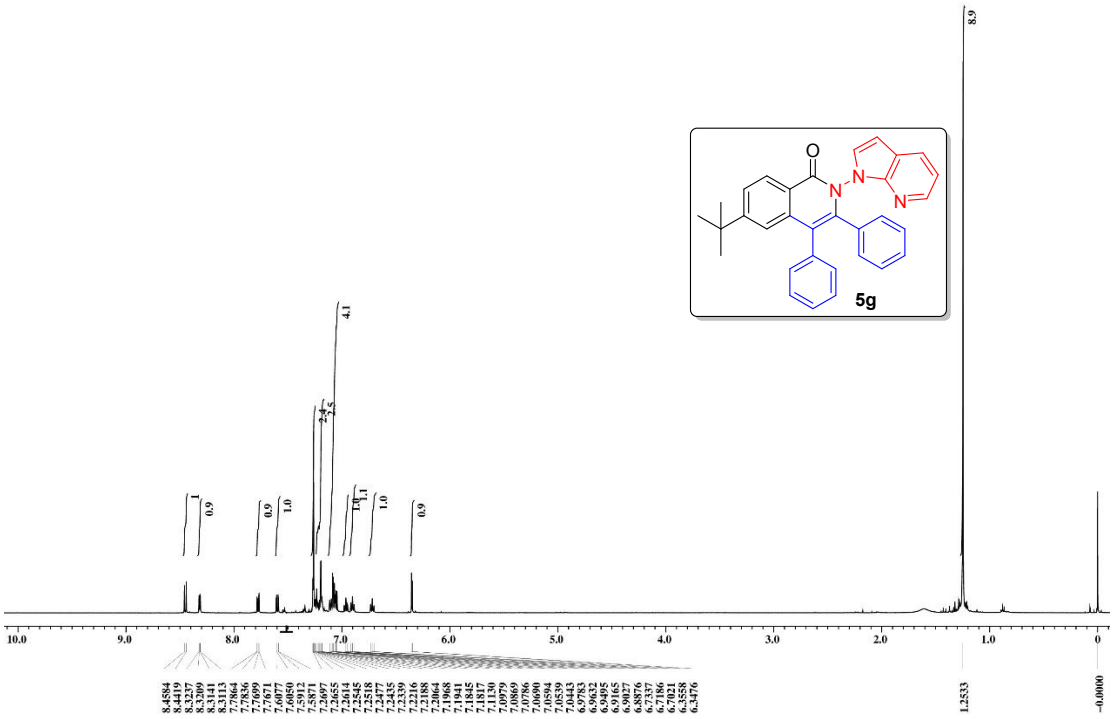

Fig. S67. ^{1}H NMR spectrum of **5g** (500 MHz, $CDCl_3$)

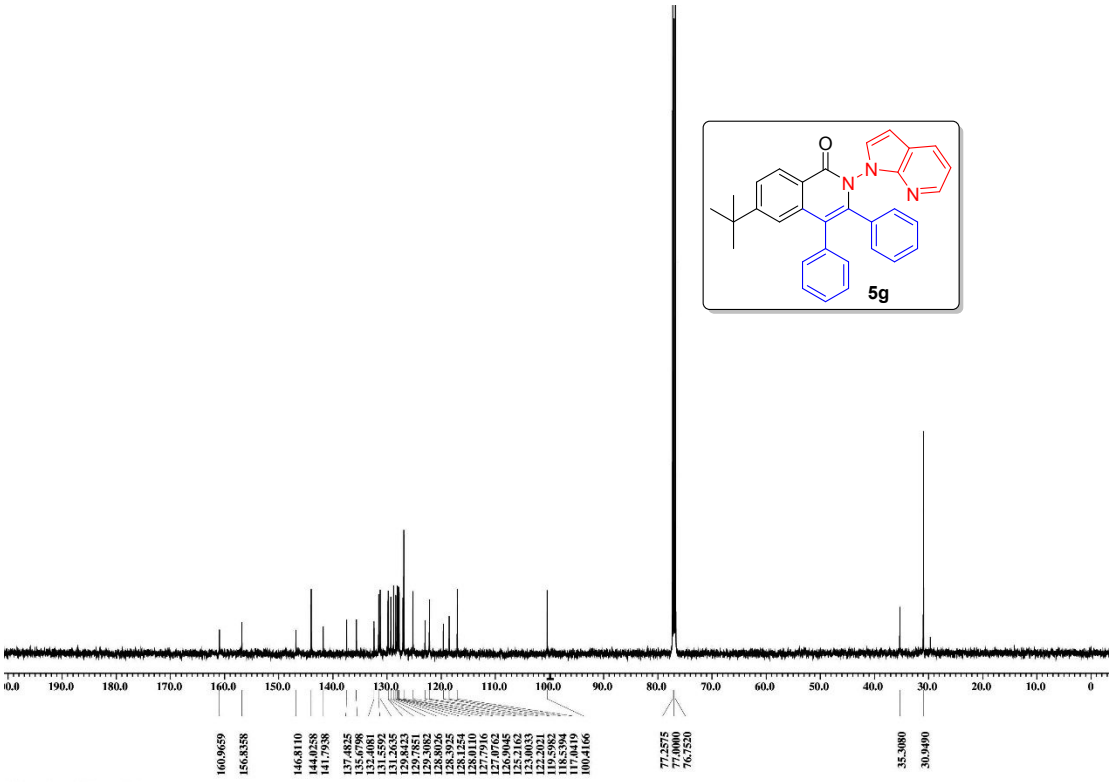

Fig. S68. ^{13}C NMR spectrum of **5g** (125 MHz, $CDCl_3$)

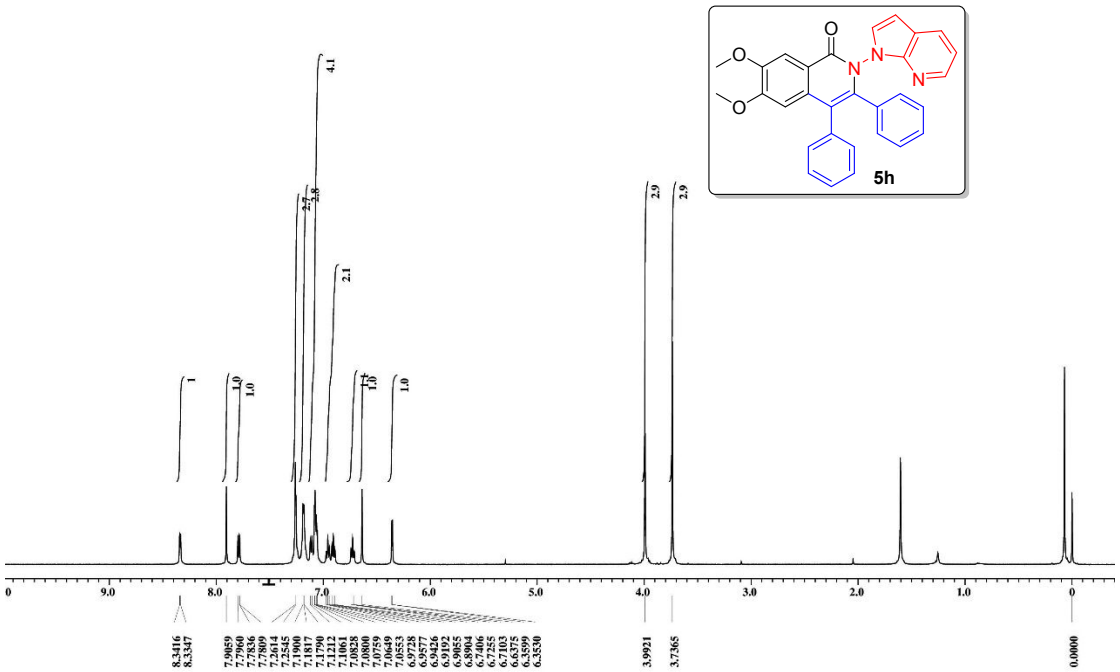

Fig. S69. ^{1}H NMR spectrum of **5h** (500 MHz, $CDCl_3$)

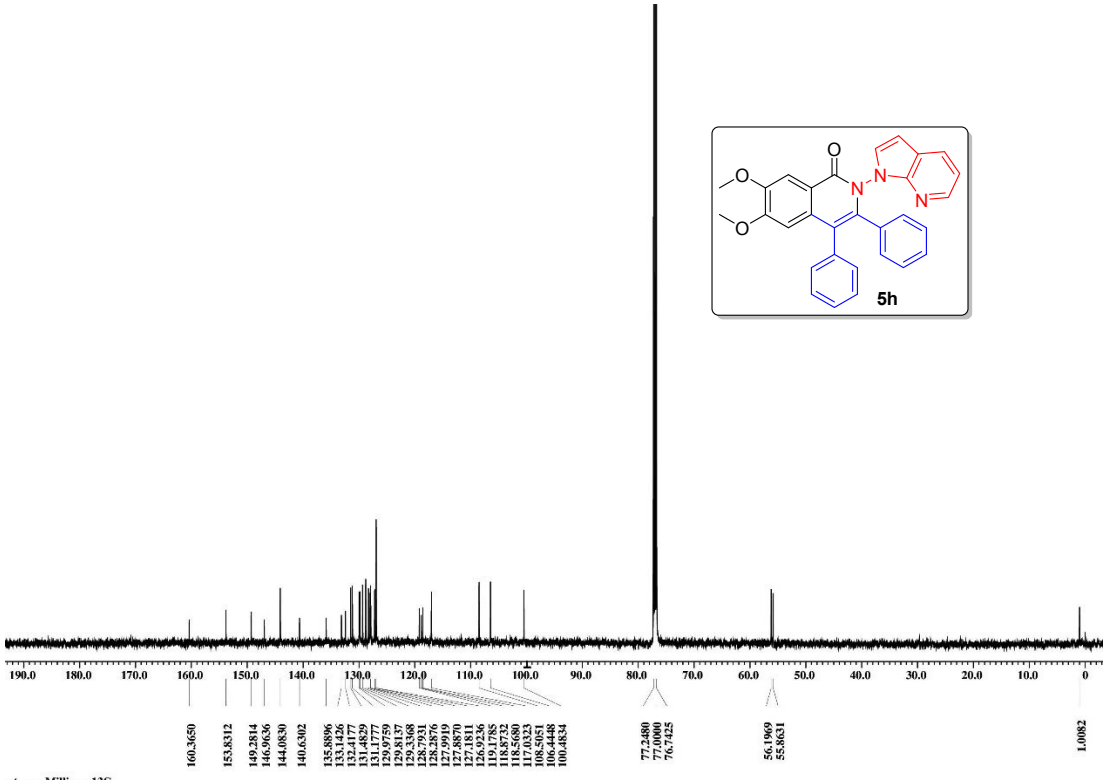

Fig. S70. ^{13}C NMR spectrum of **5h** (125 MHz, $CDCl_3$)

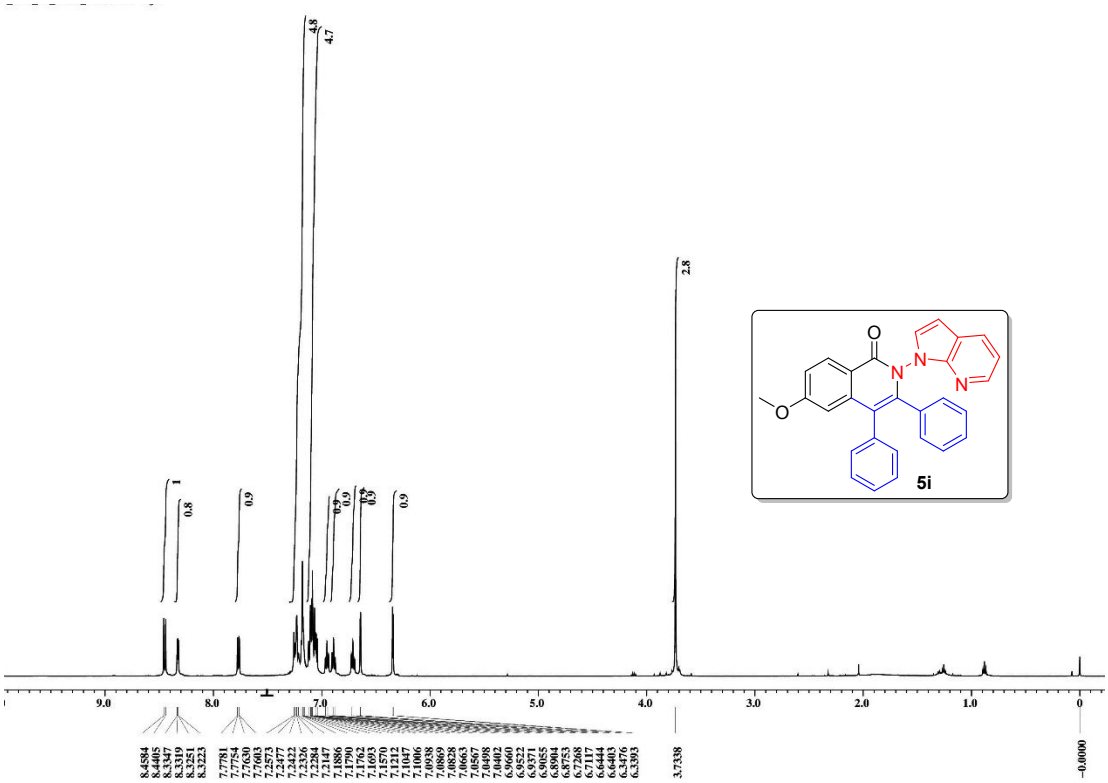

Fig. S71. ^{1}H NMR spectrum of **5i** (500 MHz, $CDCl_3$)

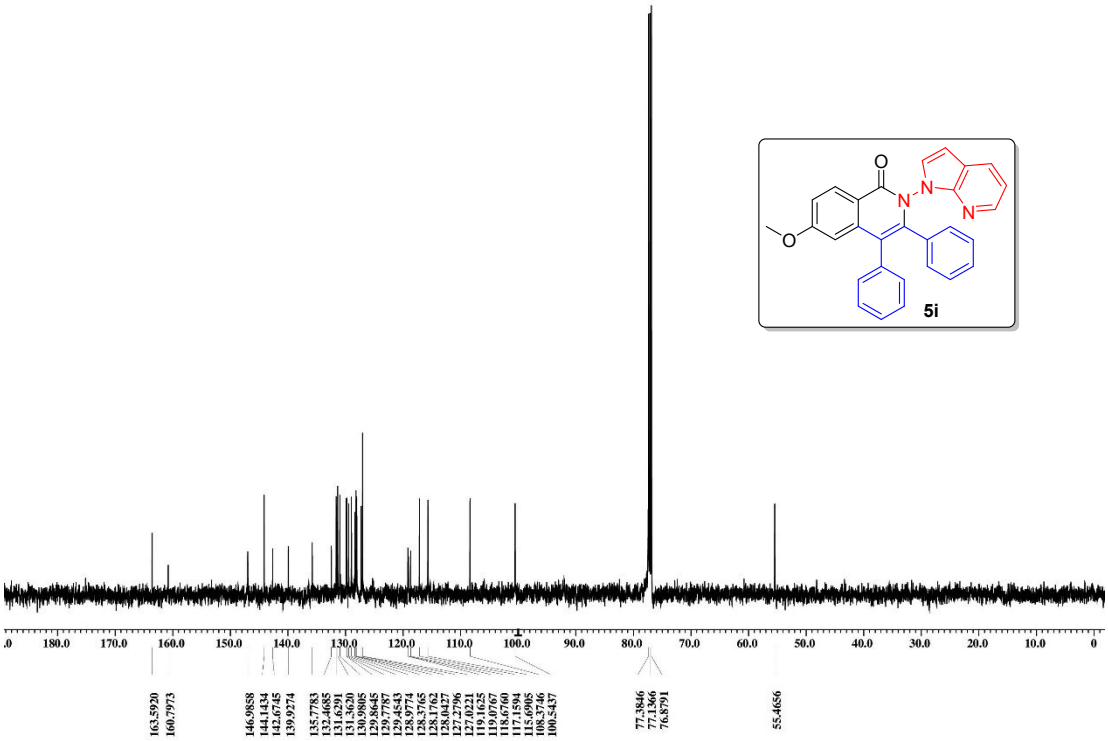

Fig. S72. ^{13}C NMR spectrum of **5i** (125 MHz, $CDCl_3$)

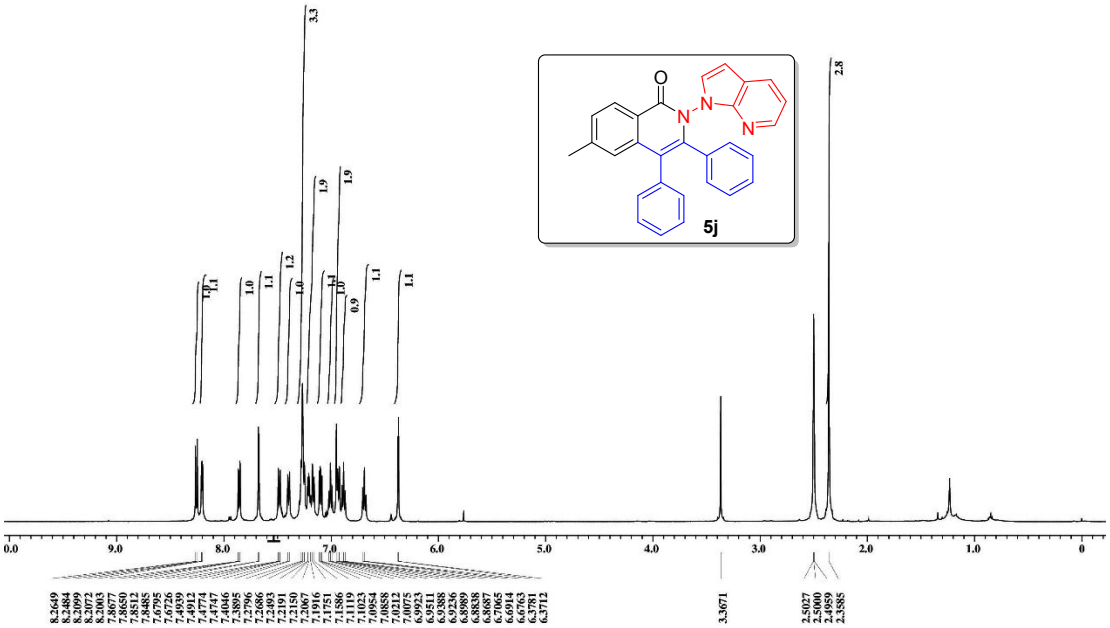

Fig. S73. ^{1}H NMR spectrum of **5j** (500 MHz, DMSO)

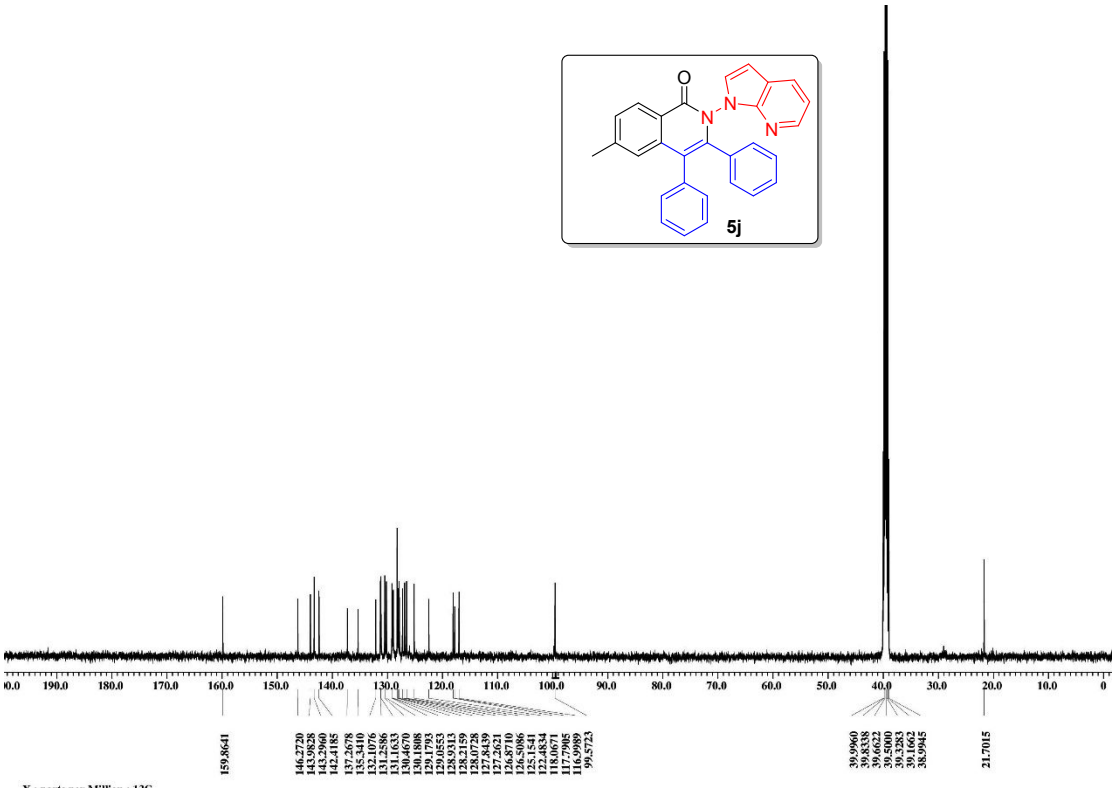

Fig. S74. ^{13}C NMR spectrum of **5j** (125 MHz, DMSO)

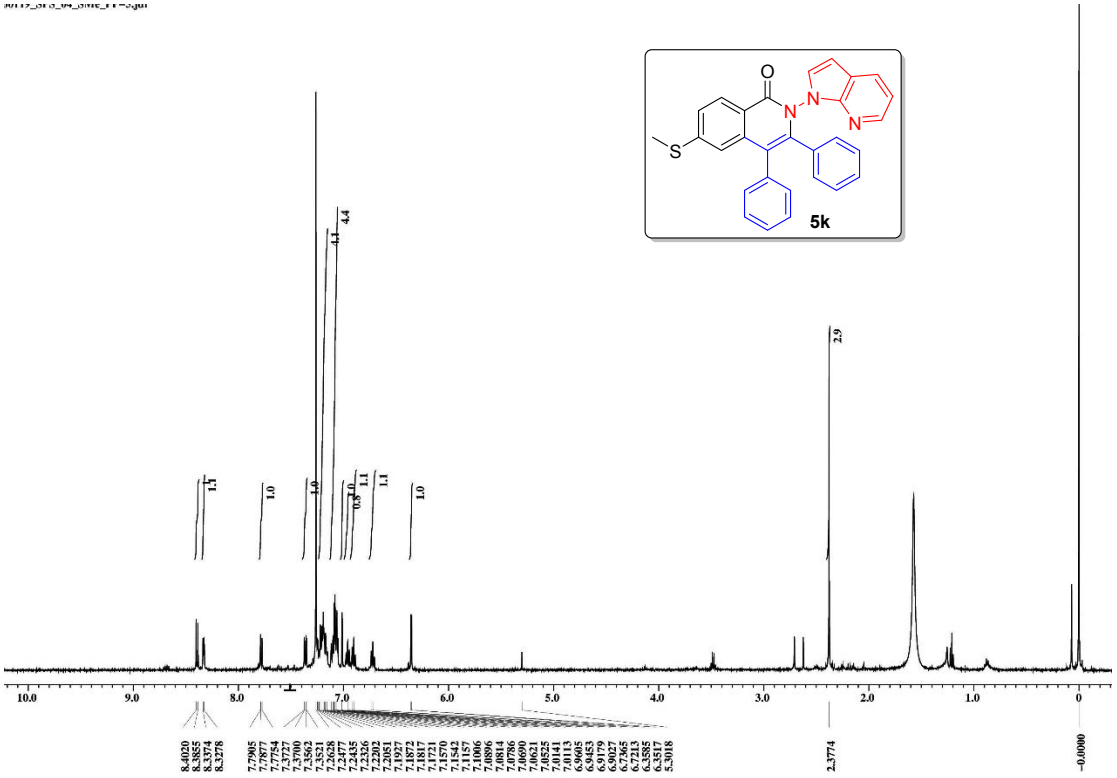

Fig. S75. ^{1}H NMR spectrum of **5k** (500 MHz, $CDCl_3$)

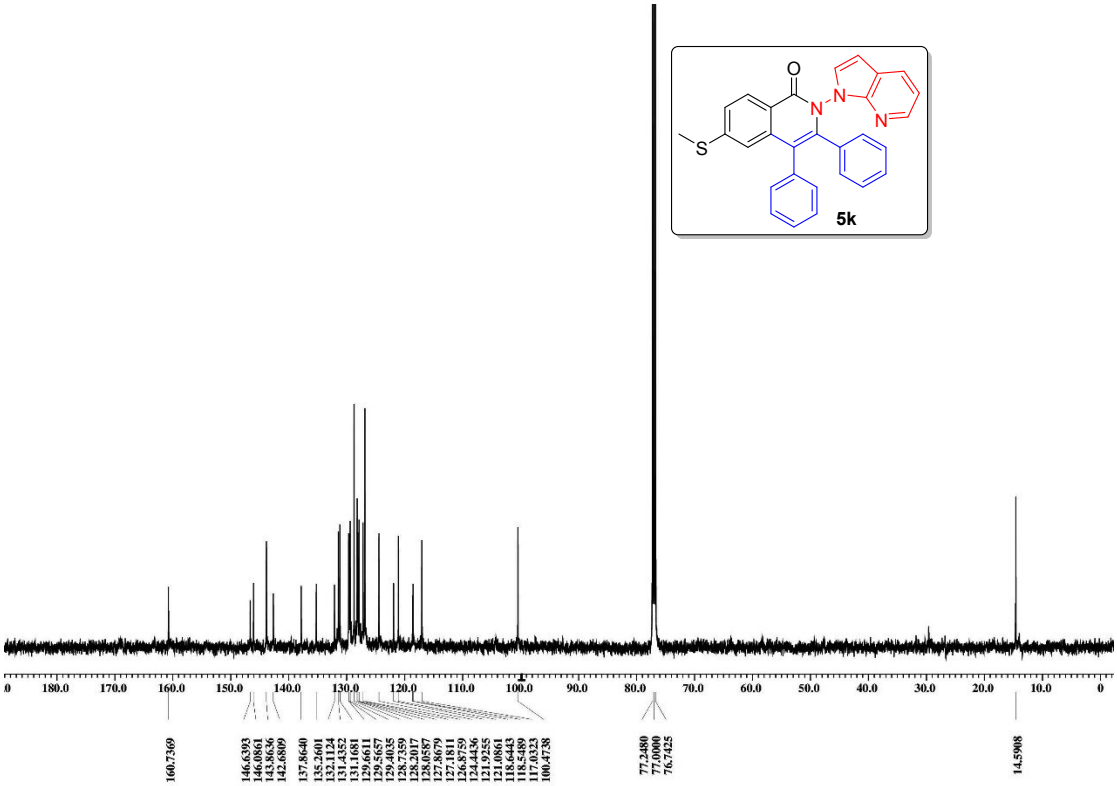

Fig. S76. ^{13}C NMR spectrum of **5k** (125 MHz, $CDCl_3$)

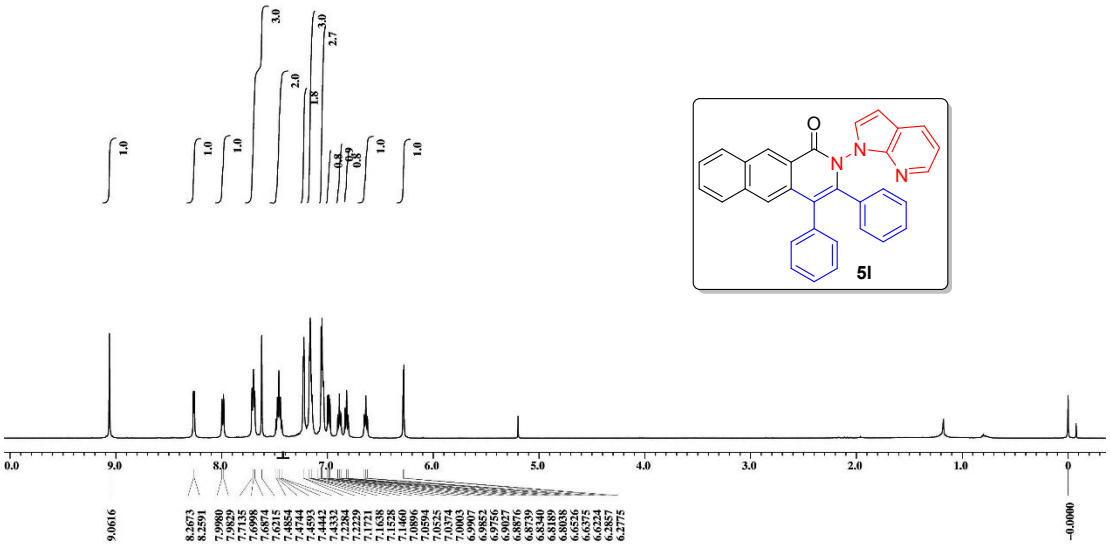

Fig. S77. ^{1}H NMR spectrum of **5l** (500 MHz, $CDCl_3$)

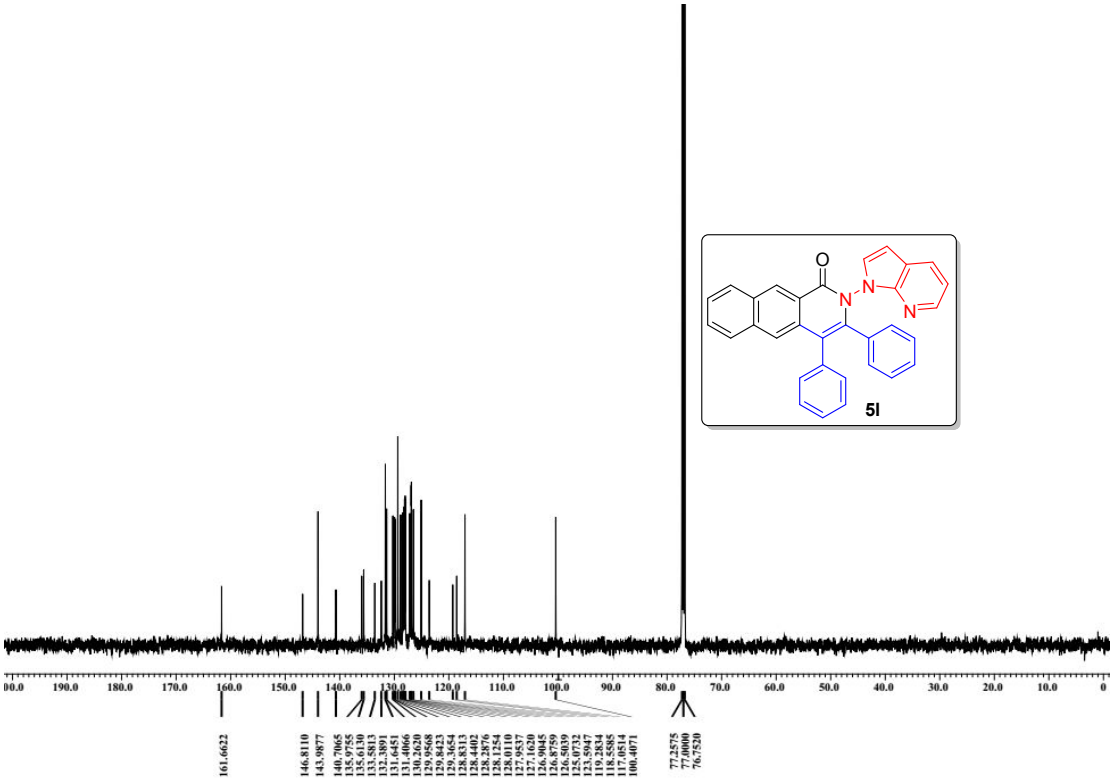

Fig. S78. ^{13}C NMR spectrum of **5l** (125 MHz, $CDCl_3$)

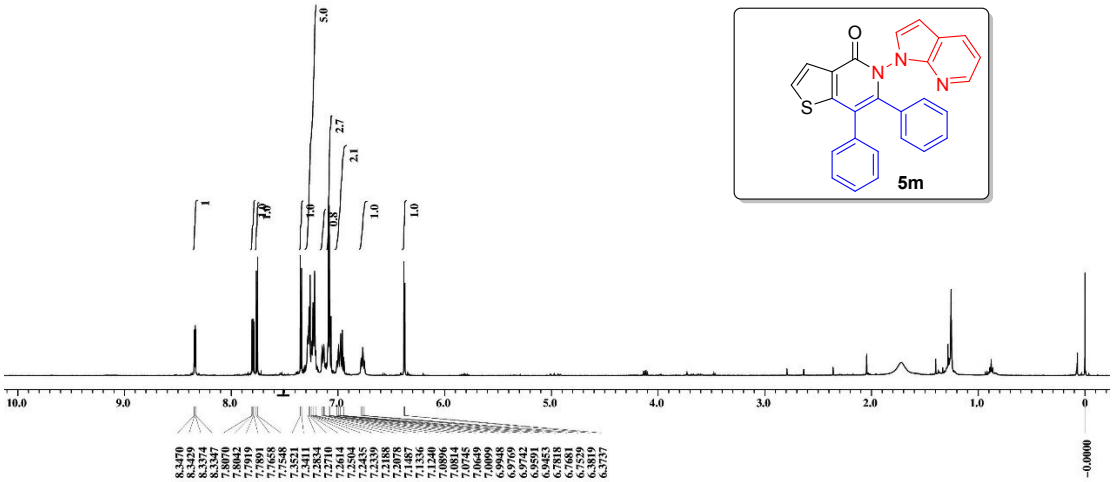

Fig. S79. ^{1}H NMR spectrum of **5m** (500 MHz, $CDCl_3$)

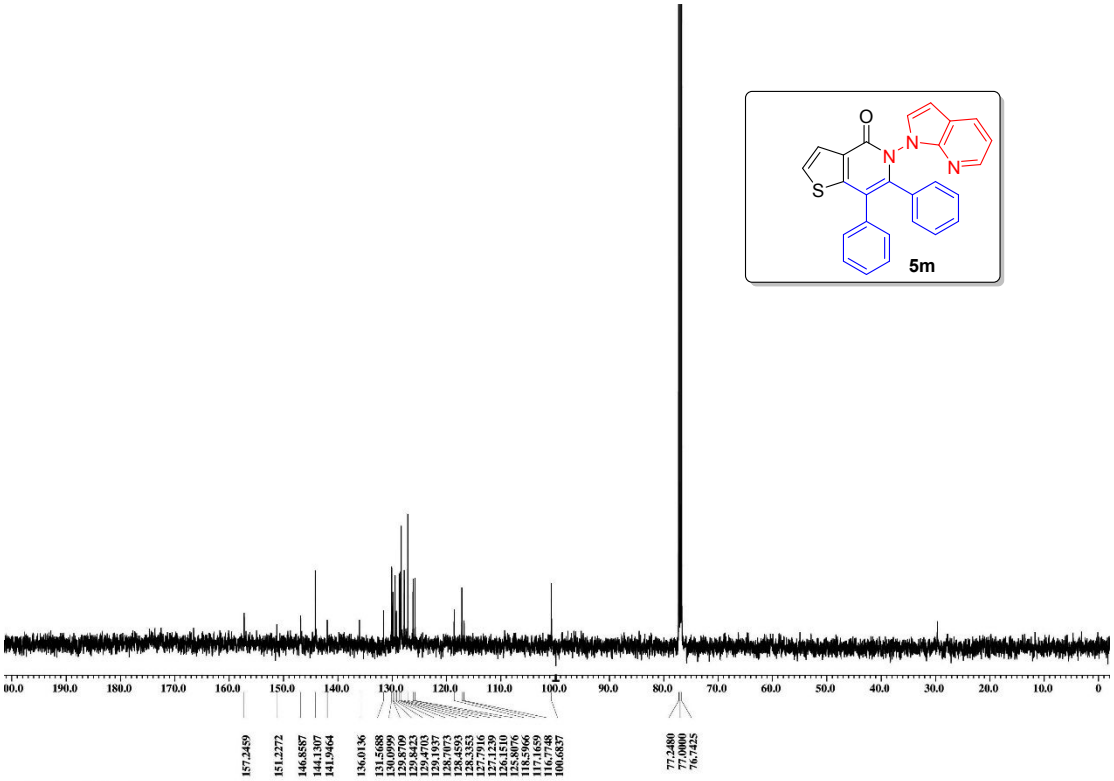

Fig. S80. ^{13}C NMR spectrum of **5m** (125 MHz, $CDCl_3$)

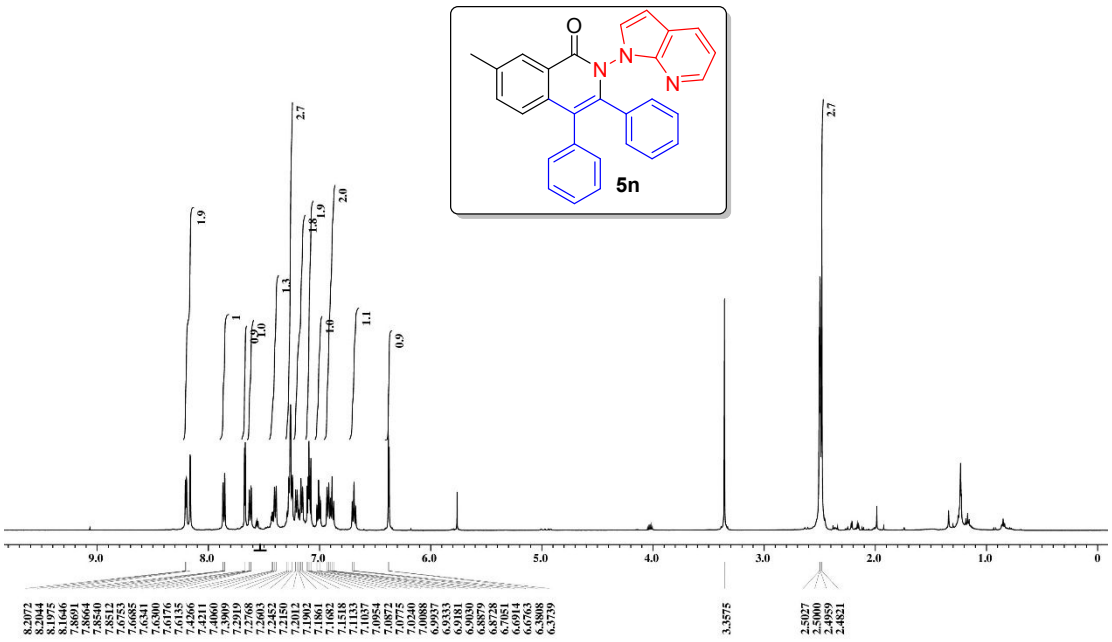

Fig. S81. ^{1}H NMR spectrum of **5n** (500 MHz, DMSO)

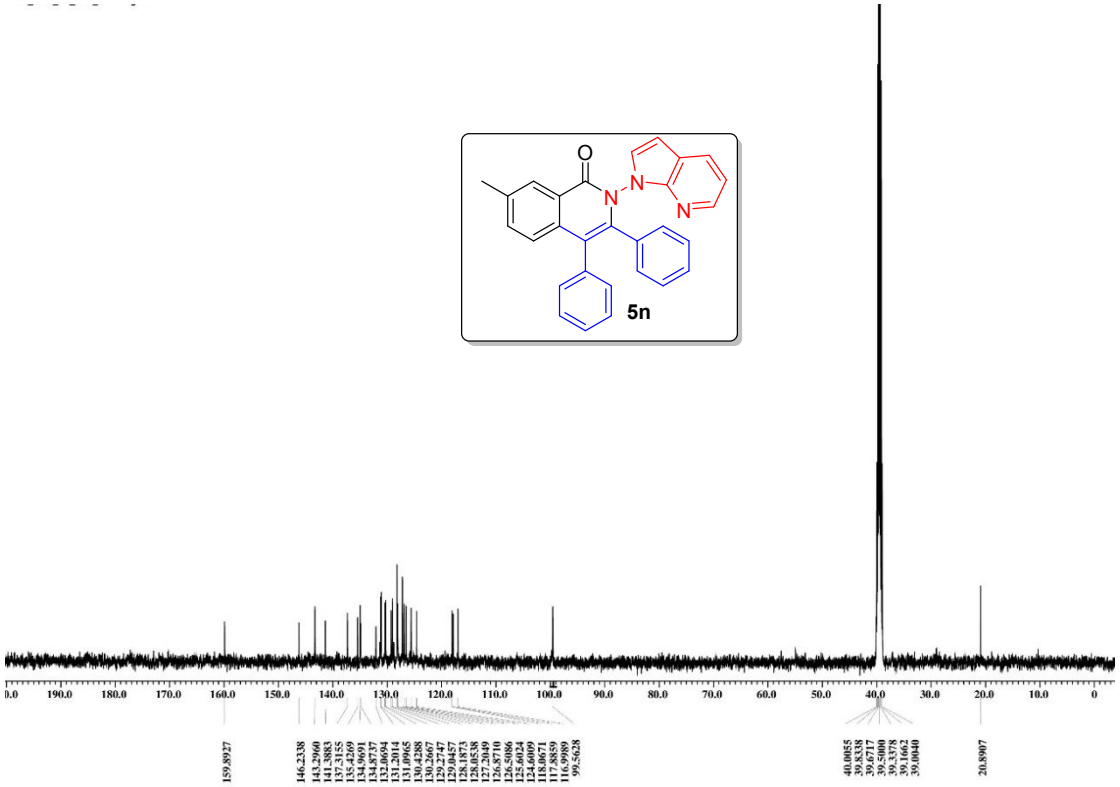

Fig. S82. ^{13}C NMR spectrum of **5n** (125 MHz, DMSO)

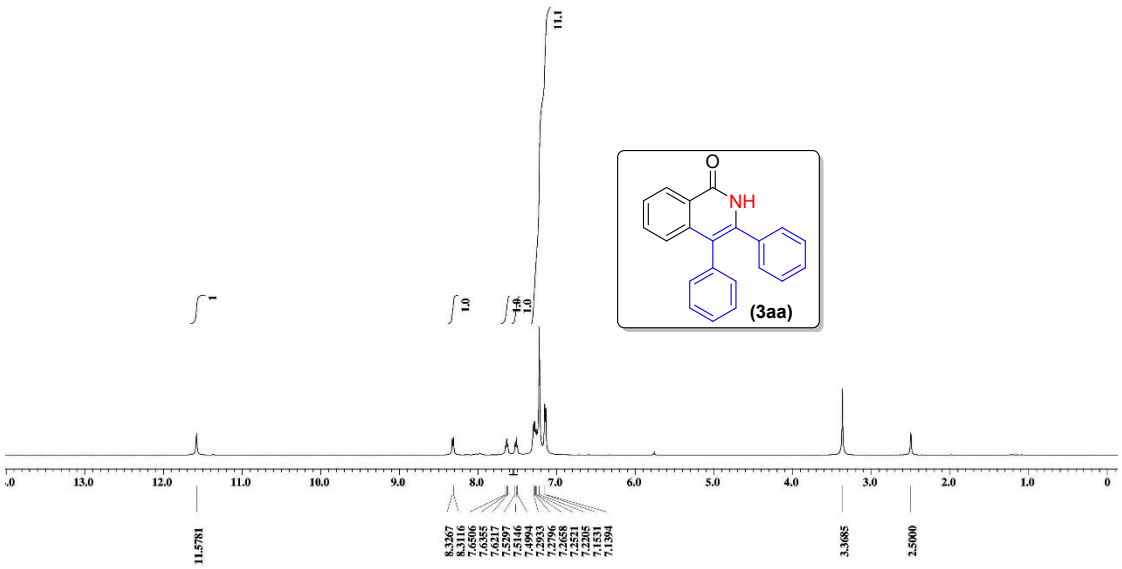

Fig. S83. ^{1}H NMR spectrum of **3aa** (500 MHz, DMSO)

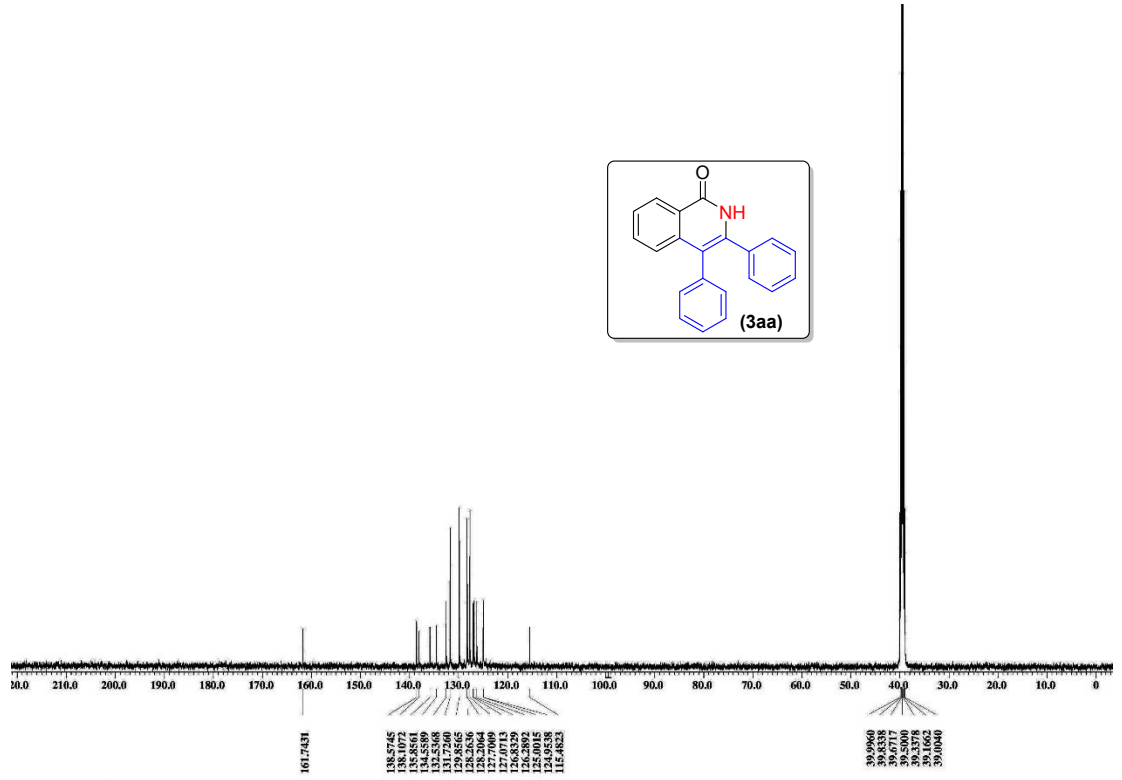

Fig. S84. ^{13}C NMR spectrum of **3aa** (125 MHz, DMSO)

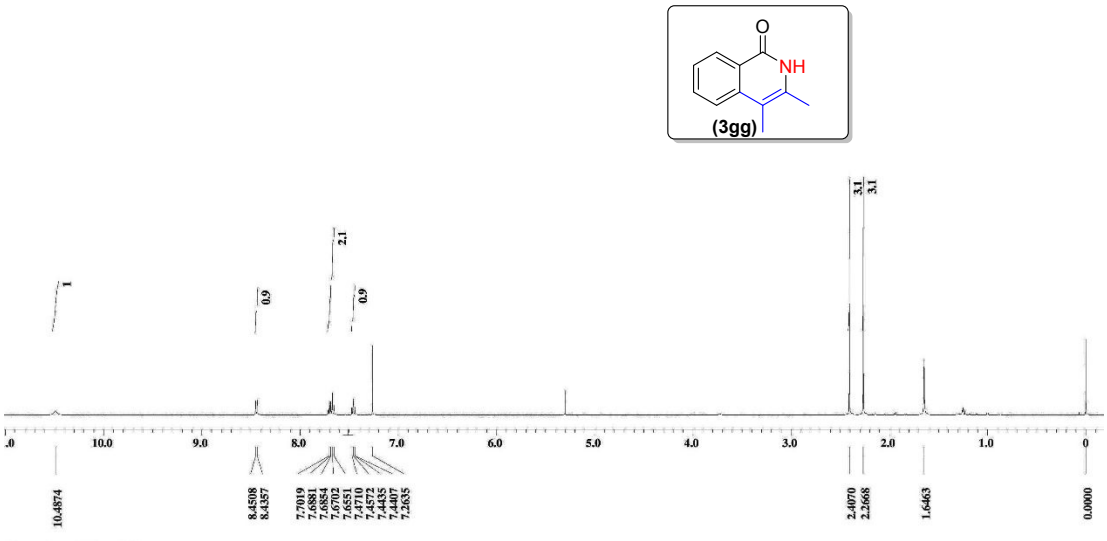

Fig. S85. ^{1}H NMR spectrum of **3gg** (500 MHz, $CDCl_3$)

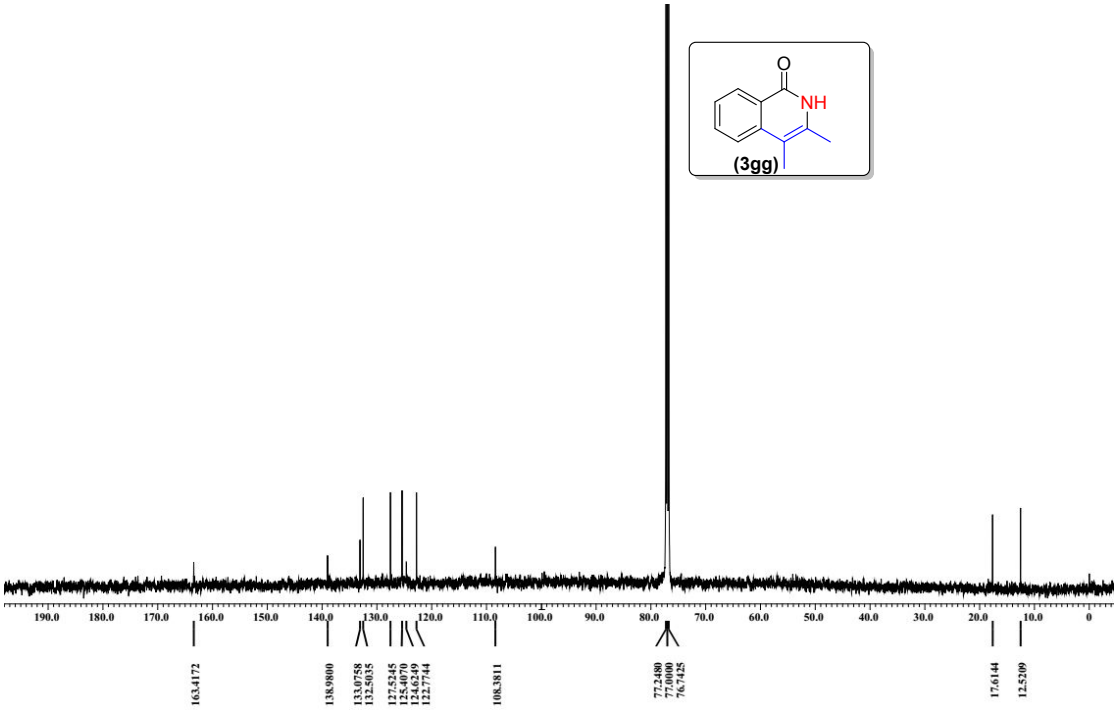

Fig. S86. ^{13}C NMR spectrum of **3gg** (125 MHz, $CDCl_3$)

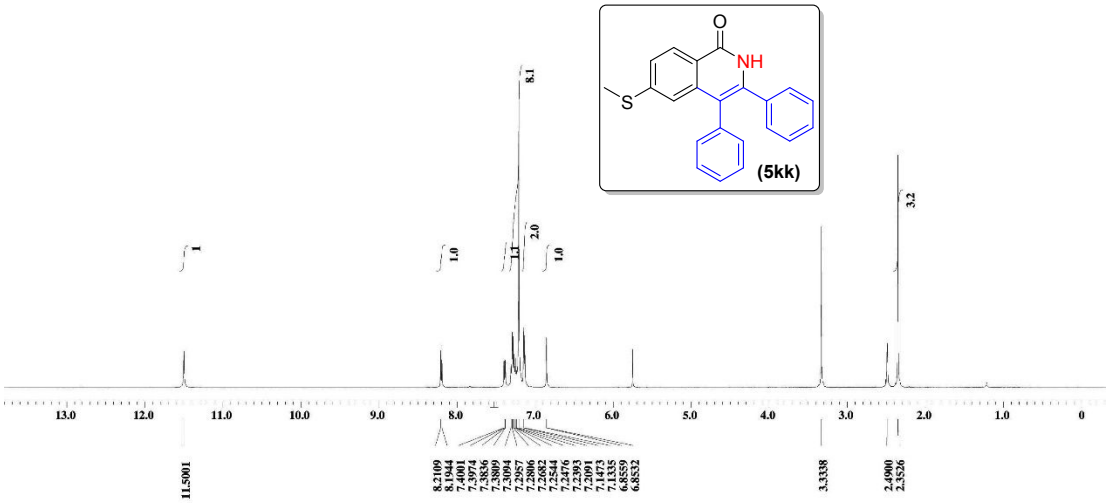

Fig. S87. ^{1}H NMR spectrum of **5kk** (500 MHz, DMSO)

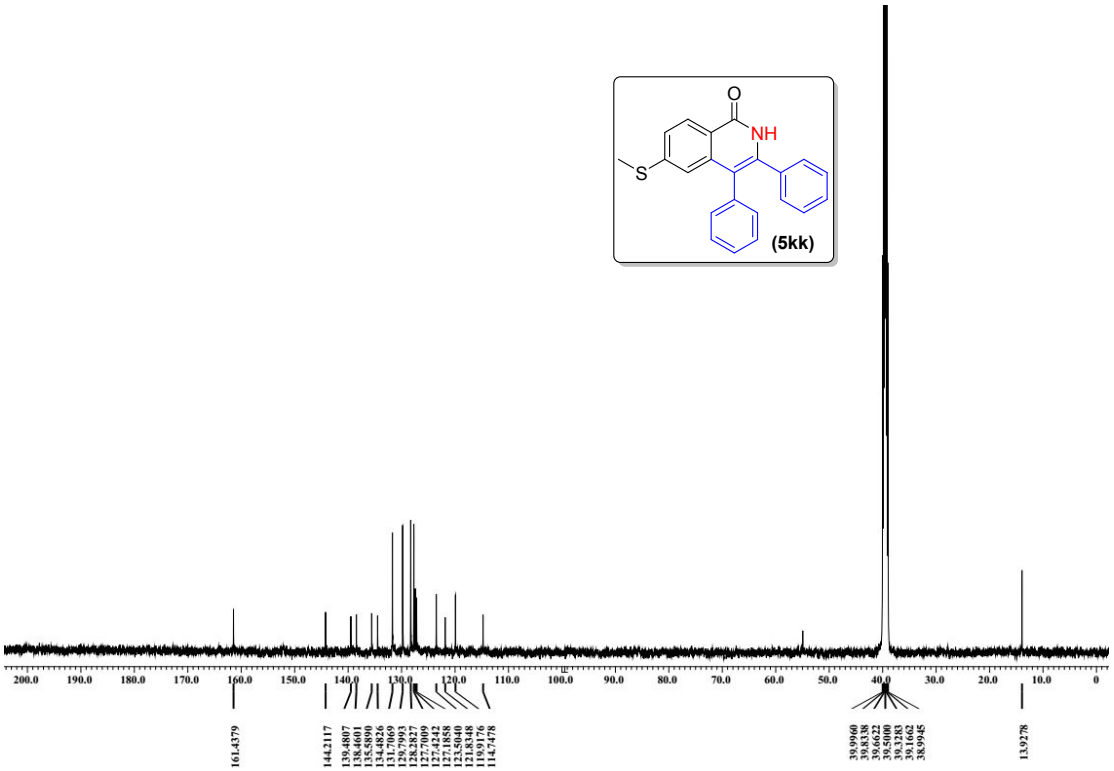

Fig. S88. ^{13}C NMR spectrum of **5kk** (125 MHz, DMSO)

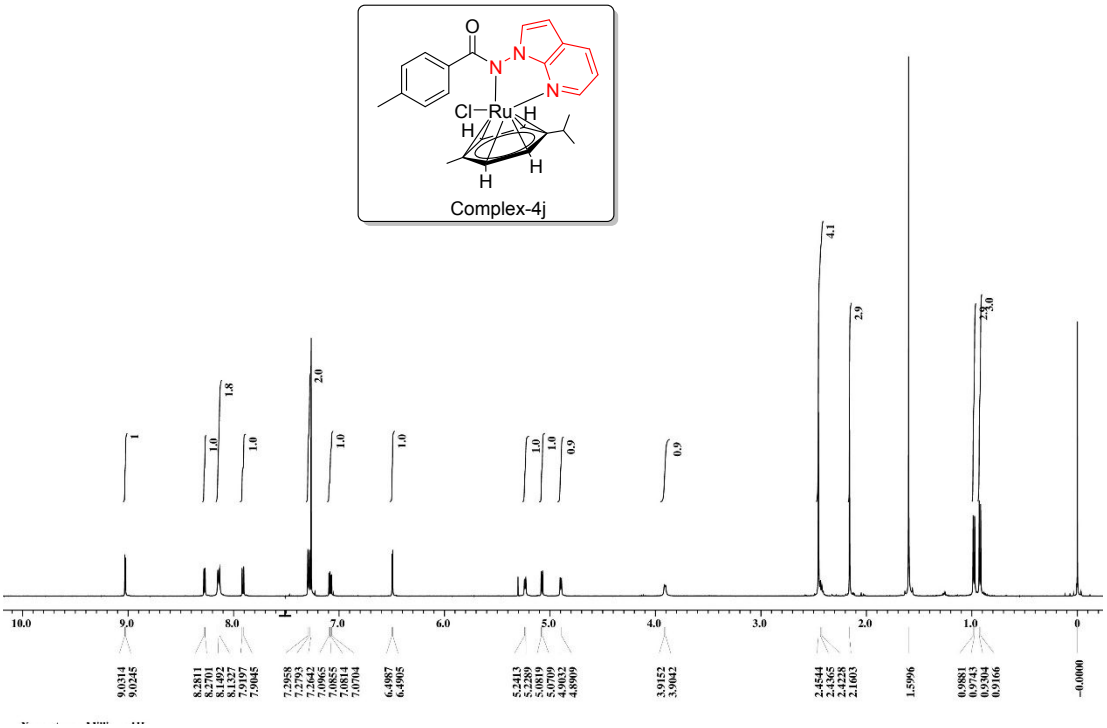

Fig. S89. ^{1}H NMR spectrum of **complex-4j** (500 MHz, $CDCl_3$)

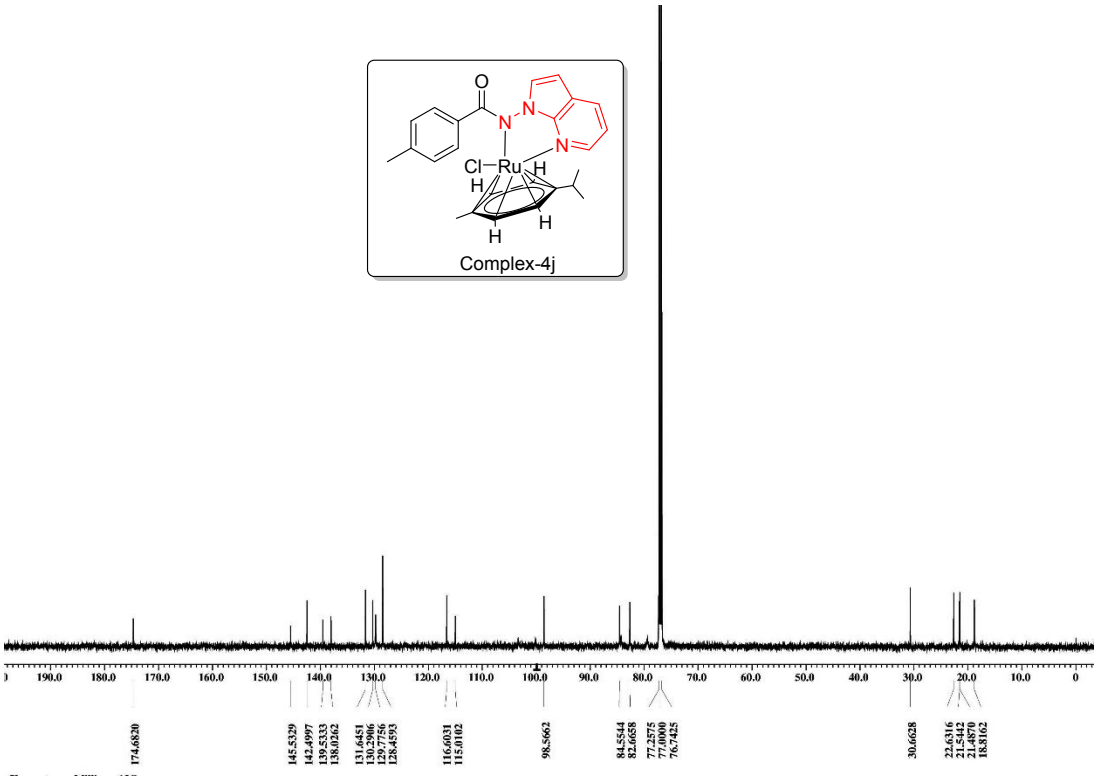

Fig. S90. ^{13}C NMR spectrum of **complex-4k** (125 MHz, $CDCl_3$)

4. X-ray Crystallographic Analysis of 1a, 3k & complex-4j':

4a. crystal structure of 1a

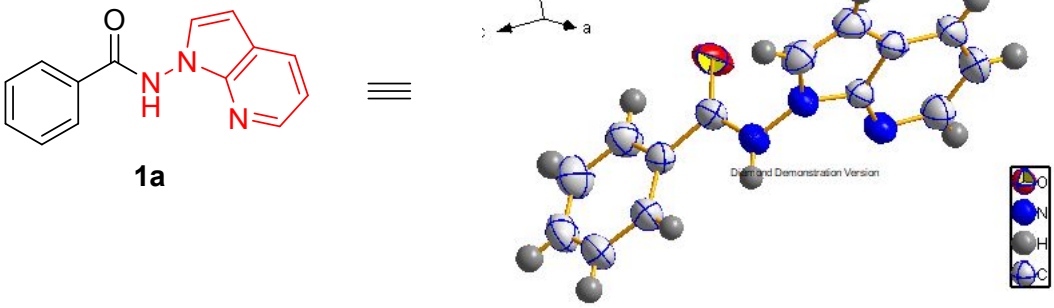

CCDC: 1868212

Table S2. Crystal data and structure refinement for

Identification code	
Empirical formula	$C_{14}H_{11}N_3O$
Formula weight	237.26
Temperature/K	293(2)
Crystal system	monoclinic
Space group	$P2_1/c$
a/Å	11.8814(4)
b/Å	19.4570(4)
c/Å	11.4871(4)
α/°	90.00
β/°	115.705(4)
γ/°	90.00
Volume/Å^3	2392.74(11)
Z	8
ρ_{calc}mg/mm^3	1.317
m/mm^{-1}	0.698
F(000)	1136.0
Crystal size/mm^3	0.258 × 0.137 × 0.099
2Θ range for data collection	8.26 to 133.66°
Index ranges	$-13 \leq h \leq 14$, $-16 \leq k \leq 23$, $-13 \leq l \leq 10$

Reflections collected	7757
Independent reflections	4196[R(int) = 0.0290]
Data/restraints/parameters	4196/0/325
Goodness-of-fit on F^2	1.035
Final R indexes [I>=2σ (I)]	R_1 = 0.0459, wR_2 = 0.1248
Final R indexes [all data]	R_1 = 0.0530, wR_2 = 0.1335
Largest diff. peak/hole / e $Å^{-3}$	0.28/-0.28

4b. Crystal Structure of 3k

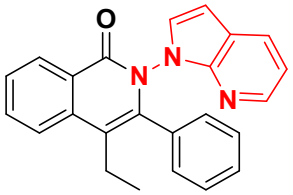

3k

≡

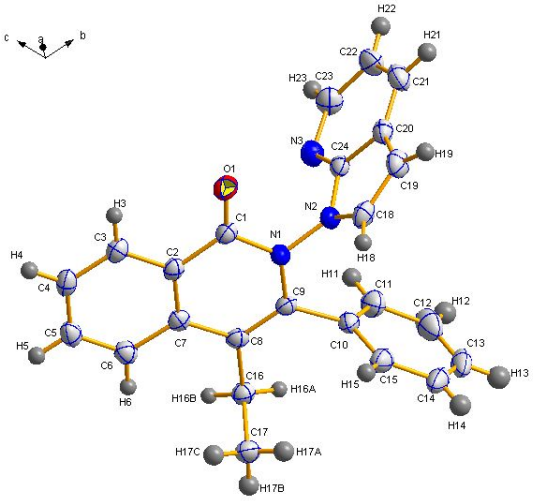

CCDC :1868597

Table S3. Crystal data and structure refinement for

Identification code	
Empirical formula	$C_{24}H_{19}N_3O$
Formula weight	365.42
Temperature/K	150.00(10)
Crystal system	triclinic
Space group	P-1
a/Å	9.2805(5)
b/Å	12.3962(7)
c/Å	16.8806(8)
α/°	107.261(5)
β/°	92.112(4)
γ/°	95.307(5)
Volume/$Å^3$	1842.38(17)

Z	4
ρ_{calc}mg/mm^3	1.314
m/mm^{-1}	0.082
F(000)	878.0
Crystal size/mm^3	0.33 × 0.25 × 0.133
2Θ range for data collection	3.46 to 56.68°
Index ranges	$-10 \leq h \leq 11$, $-16 \leq k \leq 15$, $-20 \leq l \leq 22$
Reflections collected	11201
Independent reflections	7946[R(int) = 0.0186]
Data/restraints/parameters	7946/0/507
Goodness-of-fit on F^2	1.040
Final R indexes [I>=2σ (I)]	R_1 = 0.0483, wR_2 = 0.1073
Final R indexes [all data]	R_1 = 0.0638, wR_2 = 0.1187
Largest diff. peak/hole / e Å^{-3}	0.23/-0.21

4c. Crystal Structure of complex-4j'

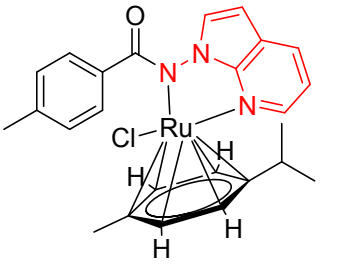

Complex-4j'

≡

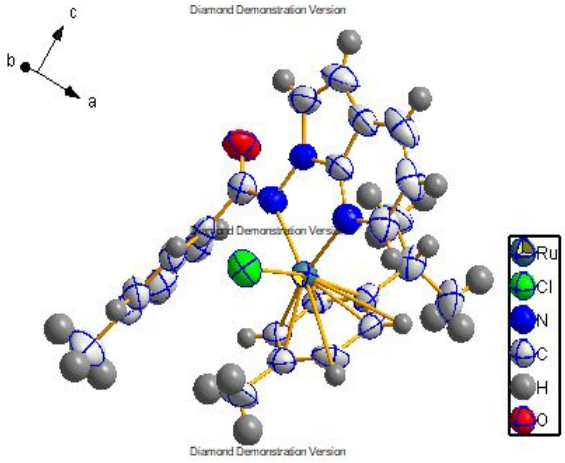

CCDC: 1913752

Table S4. Crystal data and structure refinement for SPS_04_348.

Identification code	SPS_04_348
Empirical formula	$C_{25}H_{26}ClN_3ORu$
Formula weight	521.01

Temperature/K	293(2)
Crystal system	orthorhombic
Space group	$Pca2_1$
a/Å	9.1000(4)
b/Å	14.3544(4)
c/Å	17.5769(7)
α/°	90.00
β/°	90.00
γ/°	90.00
Volume/Å^3	2295.99(15)
Z	4
ρ_{calc}g/cm^3	1.507
μ/mm^{-1}	6.764
F(000)	1064.0
Crystal size/mm^3	0.404 × 0.241 × 0.124
Radiation	CuKα (λ = 1.54184)
2Θ range for data collection/°	6.16 to 133.42
Index ranges	$-10 \leq h \leq 10$, $-14 \leq k \leq 17$, $-20 \leq l \leq 20$
Reflections collected	4575
Independent reflections	2616 [R_{int} = 0.0378, R_{sigma} = 0.0446]
Data/restraints/parameters	2616/1/284
Goodness-of-fit on F^2	1.064
Final R indexes [I>=2σ (I)]	R_1 = 0.0425, wR_2 = 0.1134
Final R indexes [all data]	R_1 = 0.0489, wR_2 = 0.1236
Largest diff. peak/hole / e Å^{-3}	0.40/-0.73
Flack parameter	-0.05(2)

Using Olex2[1], the structure was solved with the ShelXS[2] structure solution program using Direct Methods and refined with the ShelXL[2] refinement package using Least Squares minimisation.

1. Dolomanov, O. V; Bourhis, L. J.; Gildea, R. J.; Howard, J. A. K.; Puschmann, H. {\it OLEX2}: A Complete Structure Solution, Refinement and Analysis Program. *J. Appl. Crystallogr.* **2009**, *42* (2), 339–341.
2. Sheldrick, G. M. A Short History of {\it SHELX}. *Acta Crystallogr. Sect. A* **2008**, *64* (1), 112–122.